Model Equations for Surface Wave Propagation

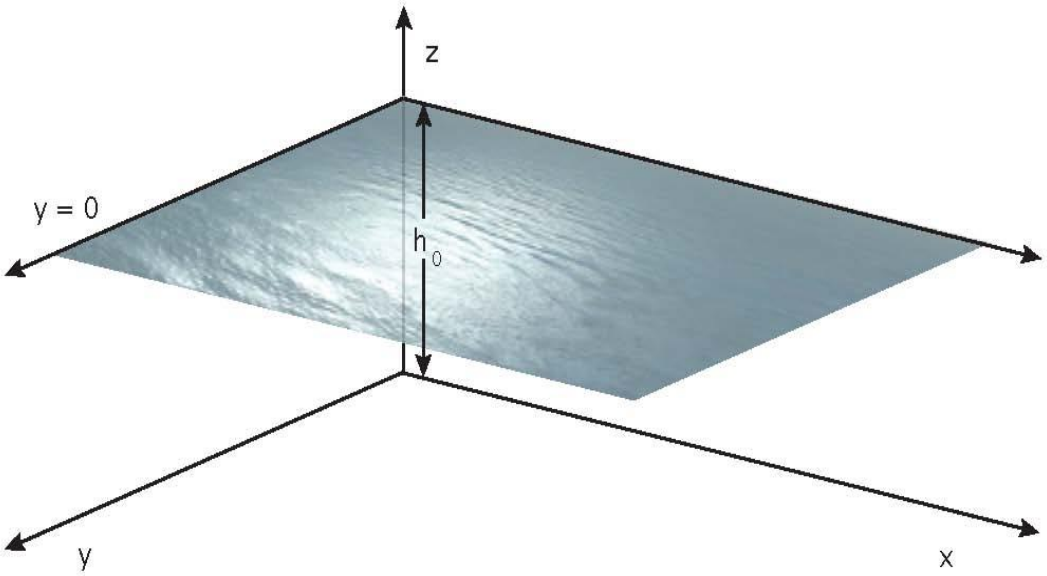

$$\alpha = \frac{a}{h_0} \qquad \beta = \left(\frac{h_0}{\lambda}\right)^2$$

$$S = \frac{\alpha}{\beta} = \frac{a\lambda^2}{h_0^3}$$

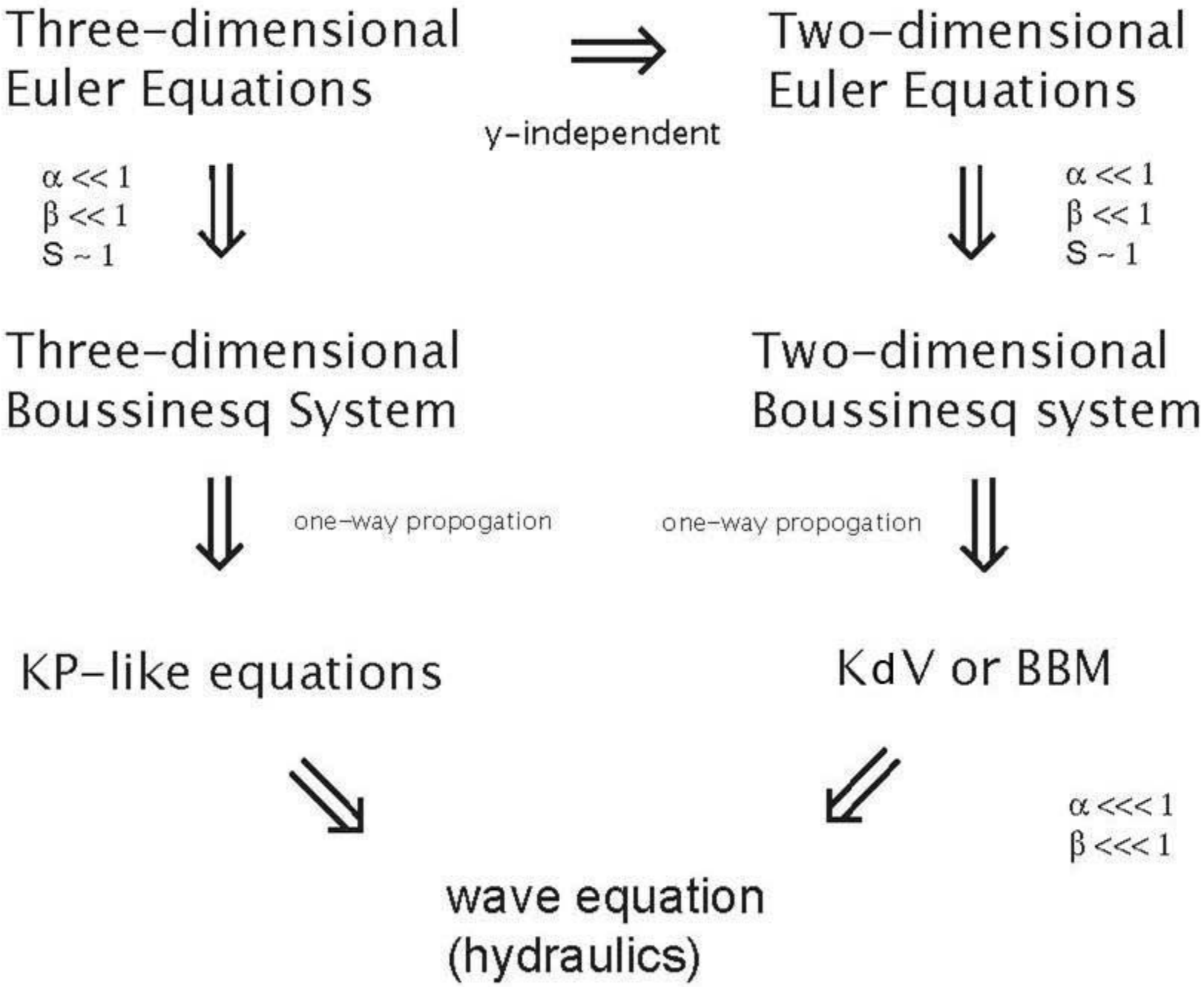
Three-dimensional
Euler Equations
y-independent
Two-dimensional
Euler Equations
α << 1
β << 1
S ~ 1
α << 1
β << 1
S ~ 1
Three-dimensional
Boussinesq System
Two-dimensional
Boussinesq system
one-way propogation
one-way propogation
KP-like equations
KdV or BBM
α <<< 1
β <<< 1
wave equation
(hydraulics)

Scaled Euler Equations

$$\beta\triangle\phi + \partial_z^2\phi = 0 \quad \text{where} \quad 0 < z < 1 + \alpha\eta(x,y,t)$$
$$\partial_z\phi = 0 \quad \text{at the bottom} \quad z = 0$$

$$\left.\begin{aligned} \partial_t\phi + \tfrac{1}{2}\left(\alpha|\nabla\phi|^2 + \tfrac{\alpha}{\beta}|\partial_z\phi|^2\right) + \eta = 0 \\ \partial_t\eta + \alpha\nabla\phi\cdot\nabla\eta - \tfrac{1}{\beta}\partial_z\phi = 0 \end{aligned}\right\}$$

on the free surface $z = 1 + \alpha\eta(x,y,t)$.

Scaling: x, y by λ

z by h_0

t by $\dfrac{\lambda}{\sqrt{gh_0}}$

η by a

ϕ by $a\lambda\sqrt{\dfrac{g}{h_0}}$

where g is the gravity constant

Two-dimensional Euler Equations

$$\beta\partial_x^2\phi + \partial_z^2\phi = 0 \quad \text{where} \quad 0 < z < 1 + \alpha\eta(x,t)$$
$$\partial_z\phi = 0 \quad \text{at the bottom} \quad z = 0$$

$$\left.\begin{aligned} &\partial_t\phi + \tfrac{1}{2}\left(\alpha|\partial_x\phi|^2 + \tfrac{\alpha}{\beta}|\partial_z\phi|^2\right) + \eta = 0 \\ &\partial_t\eta + \alpha\partial_x\phi\cdot\partial_x\eta - \tfrac{1}{\beta}\partial_z\phi = 0 \end{aligned}\right\}$$

on the free surface $z = 1 + \alpha\eta(x,t)$.

Scaling:

	x	by λ
	z	by h_0
	t	by $\dfrac{\lambda}{\sqrt{gh_0}}$
	η	by a
	ϕ	by $a\lambda\sqrt{\dfrac{g}{h_0}}$
where	g	is the gravity constant

Consider the Boussinesq régime where

$$S = \frac{\alpha}{\beta} = \frac{a\lambda^2}{h_0^3} \sim 1,$$

and for convenience, suppose $S = 1$. Let

$$\epsilon = \frac{a}{h_0} = \frac{h_0^2}{\lambda^2}.$$

Two-dimensional Euler Equations

$$\epsilon\partial_x^2\phi + \partial_z^2\phi = 0 \quad \text{where} \quad 0 < z < 1 + \epsilon\eta(x,t)$$
$$\partial_z\phi = 0 \quad \text{at the bottom} \quad z = 0$$

$$\left.\begin{aligned} \partial_t\phi + \tfrac{1}{2}\left(\epsilon|\partial_x\phi|^2 + |\partial_z\phi|^2\right) + \eta = 0 \\ \partial_t\eta + \epsilon\partial_x\phi\partial_x\eta - \tfrac{1}{\epsilon}\partial_z\phi = 0 \end{aligned}\right\}$$

on the free surface $z = 1 + \epsilon\eta(x,t)$.

Scaling:

	x	by λ
	z	by h_0
	t	by $\dfrac{\lambda}{\sqrt{gh_0}}$
	η	by a
	ϕ	by $a\lambda\sqrt{\dfrac{g}{h_0}}$
where	g	is the gravity constant

The two-dimensional Euler equations may be simplified by a formal expansion of the velocity potential, *viz.*

$$\phi(x,z,t) = \sum_{m=0}^{\infty} \phi_m(x,t) z^m.$$

Demanding Laplace's equation holds in the flow domain, and that there is no flow through the bottom yields the much simpler expression

$$\phi(x,z,t) = \sum_{m=0}^{\infty} (-1)^m \partial_x^{2m} \phi_0(x,t) \epsilon^m \frac{z^{2m}}{(2m)!}.$$

Putting this relation into the free-surface conditions and truncating at first order in ϵ yields the system

$$\partial_t u + \partial_x \eta + \epsilon u \partial_x u = O(\epsilon^2)$$

$$\partial_t \eta + \partial_x u + \epsilon \left(\partial_x (\eta u) + \frac{1}{3} \partial_x^3 u \right) = O(\epsilon^2)$$

where $u = u(x,t)$ is the horizontal velocity field at the bottom, $u = \partial_x \phi(x, 0, t)$.

In the terms of u_θ, the Boussinesq system becomes, to order ϵ,

$$\partial_t u_\theta + \partial_x \eta + \epsilon \left(u_\theta \partial_x u_\theta - (1-\theta^2)\partial_x^2 \partial_t u_\theta \right) = O(\epsilon^2),$$

$$\partial_t \eta + \partial_x u_\theta + \epsilon \left(\partial_x (\eta u_\theta) + \left(\frac{\theta^2}{2} - \frac{1}{6} \right) \partial_x^3 u_\theta \right) = O(\epsilon^2).$$

One may use the lowest-order relations

$$\begin{aligned} \partial_t u_\theta &= -\partial_x \eta + O(\epsilon) \\ \partial_t \eta &= -\partial_x u_\theta + O(\epsilon) \end{aligned}$$

to systematically alter the dispersive terms, thereby reaching the even more complicated looking system

$$\begin{aligned} \partial_t u_\theta + \partial_x \eta &+ \epsilon \left(\frac{1}{2} \partial_x |u_\theta|^2 - (1-\mu) \frac{1-\theta^2}{2} \partial_t \partial_x^2 u_\theta + \right. \\ &+ \left. \mu \frac{1-\theta^2}{2} \partial_x^3 \eta \right) = O(\epsilon^2) \\ \partial_t \eta + \partial_x u_\theta &+ \epsilon \left(\partial_x (\eta u_\theta) + \lambda \left(\frac{\theta^2}{2} - \frac{1}{2} \right) \partial_x^3 u_\theta + \right. \\ &+ \left. (1-\lambda) \left(\frac{1}{6} - \frac{\theta^2}{2} \right) \partial_x^2 \partial_t \eta \right) = O(\epsilon^2) \end{aligned}$$

Two-dimensional Boussinesq Systems
(negligable variation in the y-direction)

$$\begin{aligned} \eta_t + u_x + \epsilon(u\eta)_x + \epsilon(au_{xxx} - b\eta_{xxt}) &= 0 \\ u_t + \eta_x + \epsilon u u_x + \epsilon(c\eta_{xxx} - du_{xxt}) &= 0 \end{aligned}$$

where
$$\begin{aligned} a &= \frac{1}{2}\left(\theta^2 - \frac{1}{3}\right)\lambda \\ b &= \frac{1}{2}\left(\theta^2 - \frac{1}{3}\right)(1-\lambda) \\ c &= \frac{1}{2}(1-\theta^2)\mu \\ d &= \frac{1}{2}(1-\theta^2)(1-\mu) \end{aligned}$$

$$0 \le \theta \le 1, \lambda, \mu \in \mathcal{R}$$

$$a + b + c + d = \frac{1}{3}$$

The fully three-dimensional version of these systems have the form

$$V_t + \nabla\eta + \epsilon\left(\frac{1}{2}\nabla|V|^2 + a\nabla\triangle\eta - b\triangle V_t\right) = 0$$
$$\eta_t + \nabla\cdot V + \epsilon\left(\nabla\cdot(\eta V) + c\triangle\nabla V - d\triangle\eta_t\right) = 0$$

where $a = \dfrac{1-\theta^2}{2}\mu$ $\qquad b = \dfrac{1-\theta^2}{2}(1-\mu)$

$c = \dfrac{\theta^2 - \frac{1}{3}}{2}\lambda$ $\qquad d = \dfrac{\theta^2 - \frac{1}{3}}{2}(1-\lambda)$

and $\theta \in [0,1], \lambda, \mu \in \mathcal{R}$ and $V(x,y,t) = (u(x,y,t), v(x,y,t))$ is the horizontal velocity field at the depth θ.

coupled KdV system:

$$\eta_t + u_x + (u\eta)_x + \frac{1}{6}u_{xxx} = 0$$

$$u_t + \eta_x + uu_x + \frac{1}{6}\eta_{xxx} = 0$$

---

regularized Boussinesq system:

(coupled BBM system):

$$\eta_t + u_x + (u\eta)_x - \frac{1}{6}\eta_{xxt} = 0$$

$$u_t + \eta_x + uu_x - \frac{1}{6}u_{xxt} = 0$$

Boussinesq's 'original' system:

$$\begin{aligned} \eta_t + u_x + (u\eta)_x &= 0 \\ u_t + \eta_x + uu_x - u_{xxt} &= 0 \end{aligned}$$

Kaup system:

$$\begin{aligned} \eta_t + u_x + (u\eta)_x + \frac{1}{3}u_{xxx} &= 0 \\ u_t + \eta_x + uu_x &= 0 \end{aligned}$$

Mathematical & Physical Criteria

1. Well-posed

   linearly, nonlinearly locally, globally
2. Preserves ‘Energy’
3. Has Solitary Waves

   existence, stability and resolution into solitary waves
4. Comparison with the Euler equation

   on Boussinesq time scale
5. Qualitative & Quantitative agreement with Experiments

   in the laboratory and with field observations

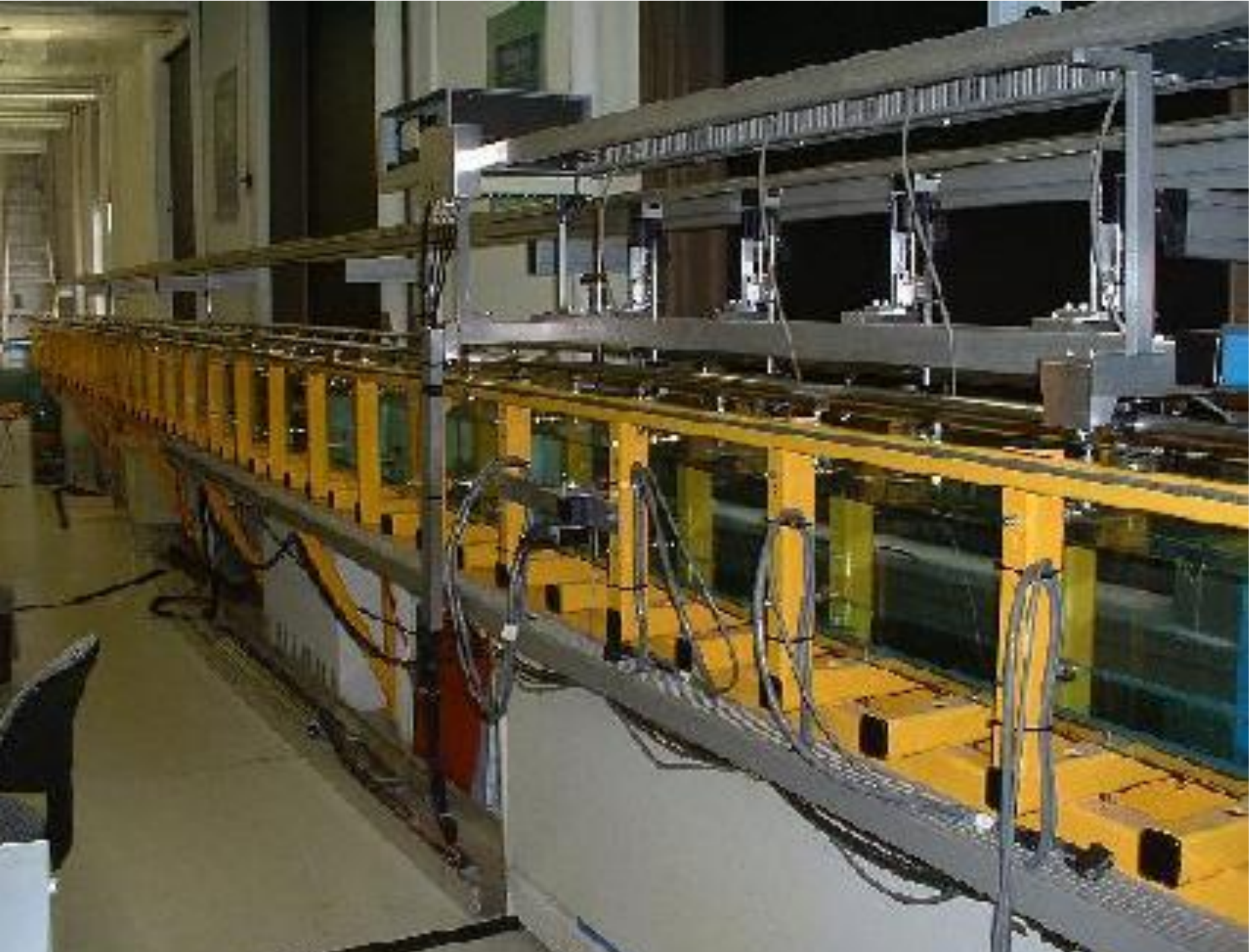

Comparisons Between Models

John Albert
Min Chen
Thierry Colin
David Lannes
Jean-Claude Saut
Jiahong Wu

Comparison Time Scales

Over what time scales can we possibly expect the Boussinesq equations to faithfully approximate solutions of the Euler equations? Example:

$$\begin{aligned} u_t + u_x &= 0, \\ v_t + v_x + \epsilon &= 0, \\ u(x,0) = v(x,0) &= \phi(x). \end{aligned}$$

The solutions of these problems are, respectively,

$$\begin{aligned} u(x,t) &= \phi(x-t), \\ v(x,t) &= \phi(x-t) + t\epsilon. \end{aligned}$$

The difference between the two solutions is exactly

$$\|u(\cdot,t) - v(\cdot,t)\| = \epsilon t.$$

So, on the time scale

$$T_0 = O(1),$$

u is a good approximation of v, whereas on the time scale

$$T_1 = O\left(\frac{1}{\epsilon}\right),$$

u no longer approximates v.

The time-scale T_0 is the time scale over which one might as well use the linear wave equation.

Whereas the much longer time scale T_1, called the *Boussinesq* time scale, is the temporal interval over which nonlinear and dispersive effects cannot be ignored if one wants to maintain approximation to order ϵ.

By formal analogy, we might expect that the Boussines system can provide a good approximation of solutions of the full Euler equations on the Boussinesq time scale

$$T_1 = O\left(\frac{1}{\epsilon}\right).$$

But, on the yet longer time scale

$$T_2 = O\left(\frac{1}{\epsilon^2}\right),$$

this would no longer be guaranteed..

Linear Euler Equations

$$\epsilon \triangle \phi + \partial_z^2 \phi = 0 \quad \text{where} \quad 0 < z < 1$$

$$\partial_z \phi = 0 \quad \text{at the bottom} \quad z = 0$$

$$\left.\begin{array}{l} \partial_t \phi + \eta = 0 \\ \partial_t \eta - \frac{1}{\epsilon} \partial_z \phi = 0 \end{array}\right\} \text{on the surface} \quad z = 1$$

Cross differentiating, it is seen that

$$\phi_{tt} + \frac{1}{\epsilon} \phi_z = 0$$

at $z = 1$. The variable η has been eliminated.

The outcome of simple estimates in Fourier transformed variables is the following inequality, which is sharp in its dependence upon t and the parameter ϵ.

Let $(\eta_0, U_0) \in H^s(R^n)$ be given initial data for the linear Euler equation, $n = 1, 2$. Let $\{(\eta_\epsilon, U_\epsilon)\}_{0<\epsilon\leq\epsilon_0}$ be the solution of the linear Euler equations with (η_0, U_0) as initial data. Let $\Sigma(\eta_0, U_0)$ be the associated inital data for one of the well-posed linear Boussinesq systems and let $\{(\mu_\epsilon, V_\epsilon)\}_{0<\epsilon\leq\epsilon_0}$ be the associated solutions of the Boussinesq system.

If we define $(\bar{\eta}_\epsilon, \bar{U}_\epsilon)$ by

$$(\bar{\eta}_\epsilon, \bar{U}_\epsilon) = \Sigma^{-1}(\mu_\epsilon, V_\epsilon),$$

then for any $t \in [0, \frac{1}{\epsilon}]$,

$$sup_{0 \leq s \leq t} \|\eta_\epsilon(\cdot, s) - \bar{\eta}_\epsilon(\cdot, s)\| = C_1 \epsilon^2 t$$

and similarly,

$$sup_{0 \leq s \leq t} \|U_\epsilon(\cdot, s) - \bar{U}_\epsilon(\cdot, s)\| \quad = \quad C_2 \epsilon^2 t,$$

where C_1 and C_2 depend only the inital data and are bounded on bounded subsets of the initial data.

Scaled Euler Equations

$$\epsilon \triangle \phi + \partial_z^2 \phi = 0 \qquad \text{where} \quad 0 < z < 1 + \epsilon\eta(x, y, t)$$
$$\partial_z \phi = 0 \qquad \text{at the bottom} \quad z = 0$$

$$\left.\begin{array}{l} \partial_t \phi + \frac{1}{2}\left(\epsilon|\nabla\phi|^2 + |\partial_z\phi|^2\right) + \eta = 0 \\ \partial_t \eta + \epsilon \nabla\phi \cdot \nabla\eta - \frac{1}{\epsilon}\partial_z \phi = 0 \end{array}\right\} \text{on } z = 1 + \epsilon\eta(x, y, t)$$

where $\epsilon = \frac{a}{h_0}$ and $S = \frac{a\lambda^2}{h_0^3} = 1$.

Theorem (Alazman, Albert, Alvarez, Chen, Chen, Colin, Lannes, Saut, Wu) Let $\{(\eta_\epsilon, U_\epsilon)\}_{0<\epsilon\leq 1}$ be a one parameter familiy of solutions of the scaled Euler equations, corresponding to given initial data (η_0, U_0) lying in $H^s(\mathbf{R}^n)^{n+1}, n = 1, 2$.

Let Σ connote the mapping that takes Euler data into the associated data for one of the well-posed Boussinesq systems and let $\{(\mu_\epsilon, V_\epsilon)\}_{0<\epsilon\leq 1}$ be the solution of the associated Boussinesq system with initial data $\Sigma(\eta_0, U_0)$.

Then, these solutions exist over the time scale

$$T_1 = O\left(\frac{1}{\epsilon}\right),$$

uniformly for $\epsilon \in (0, 1]$. Moreover, if

$$(\bar{\eta}_\epsilon, \bar{U}_\epsilon) = \Sigma^{-1}(\mu_\epsilon, V_\epsilon),$$

then for $0 \leq t \leq \frac{1}{\epsilon}$,

$$\begin{aligned} sup_{0 \leq s \leq t}\{\|\eta_\epsilon(\cdot, s) - \bar{\eta}_\epsilon(\cdot, s)\| + \\ \|U_\epsilon(\cdot, s) - \bar{U}_\epsilon(\cdot, s)\|\} \quad &\leq \quad C\epsilon^2 t, \end{aligned}$$

where C depends only upon the norm of the inital data.

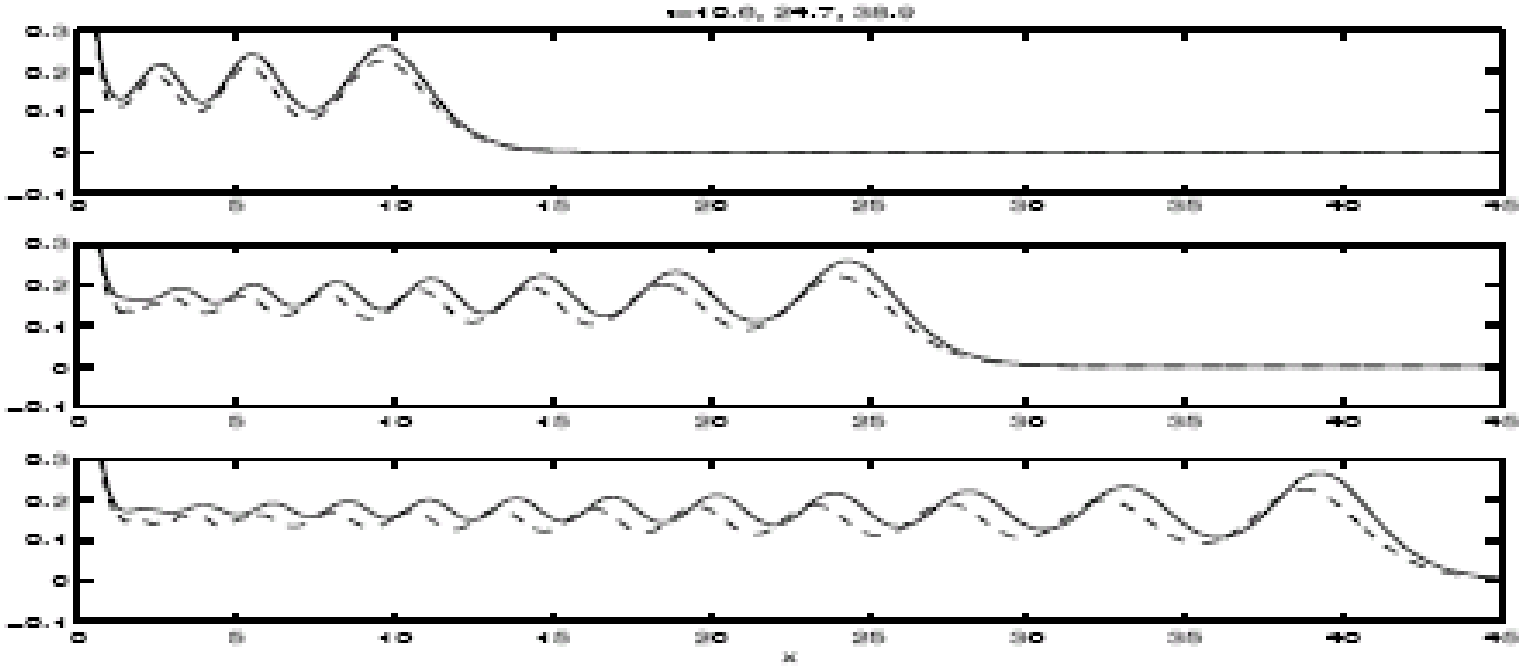

FIGURE 12. Comparison with $\epsilon = 0.5$.

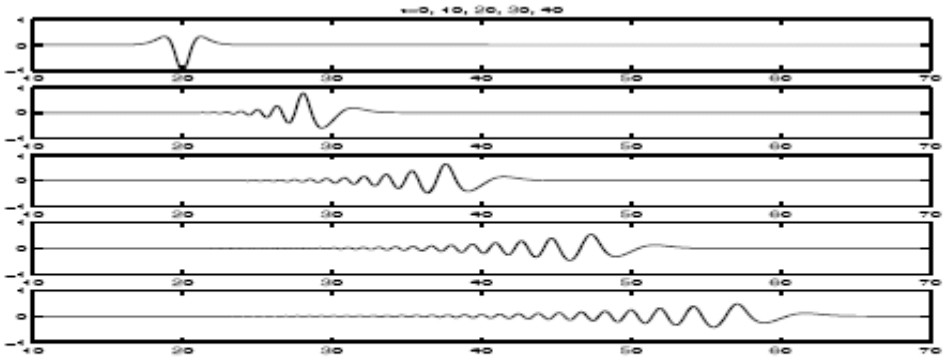

FIGURE 6. Solution of Boussinesq system with $\epsilon = 0.05$.

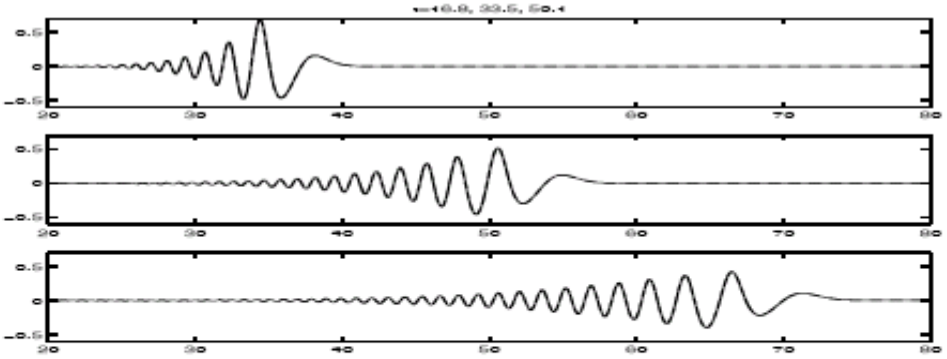

FIGURE 7. Comparison between solutions of BBM equation (solid line) and Boussinesq system (dashed line) with $\epsilon = 0.05$. The difference between the two solutions is not visible.

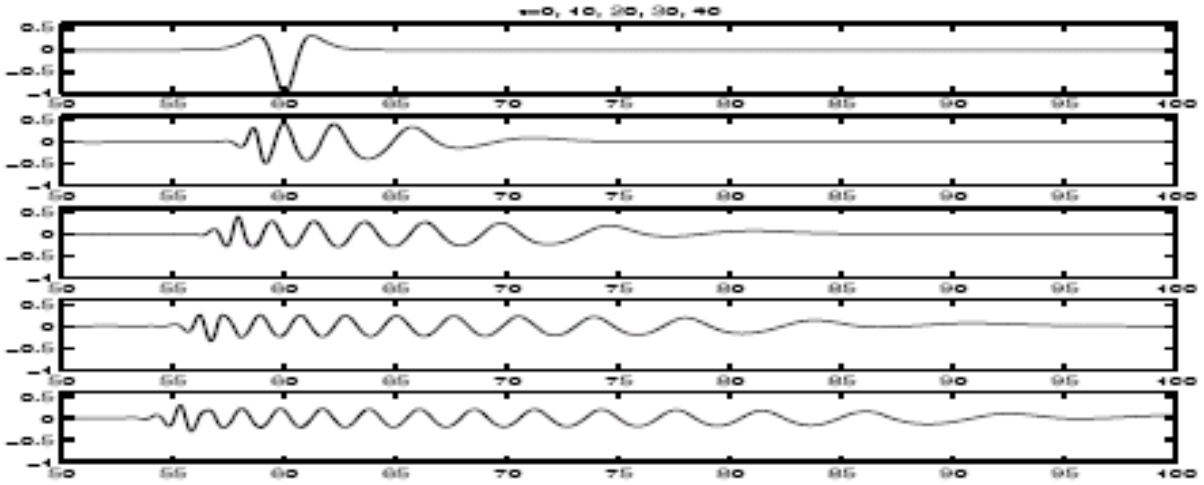

FIGURE 3. Solution of Boussinesq system with $\epsilon = 0.5$.

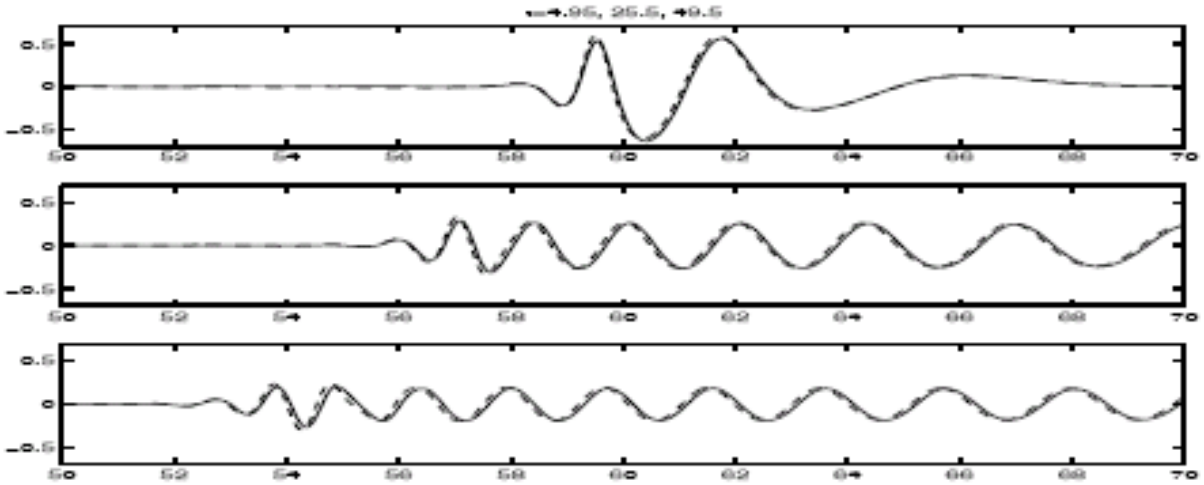

FIGURE 4. Comparison between solutions of BBM equation (solid line) and Boussinesq system (dashed line) with $\epsilon = 0.5$.

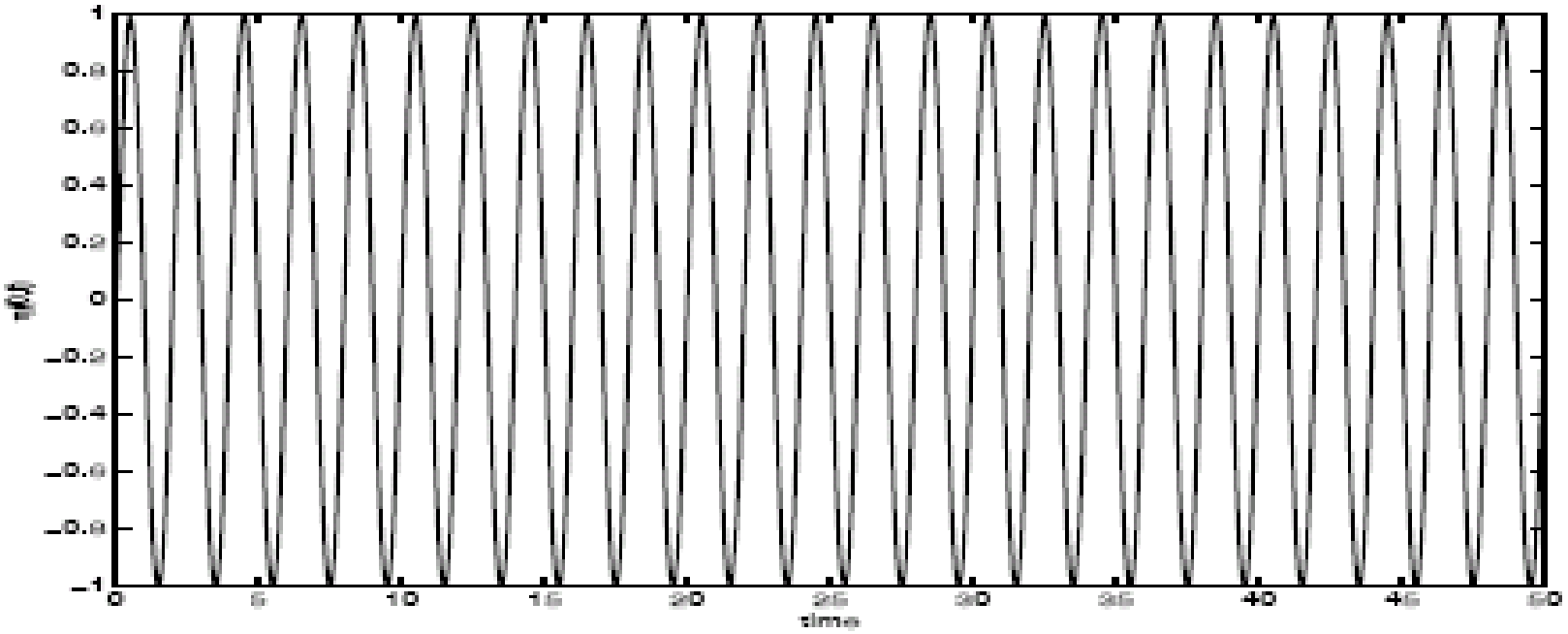

FIGURE 10. Water surface level at the wave maker.

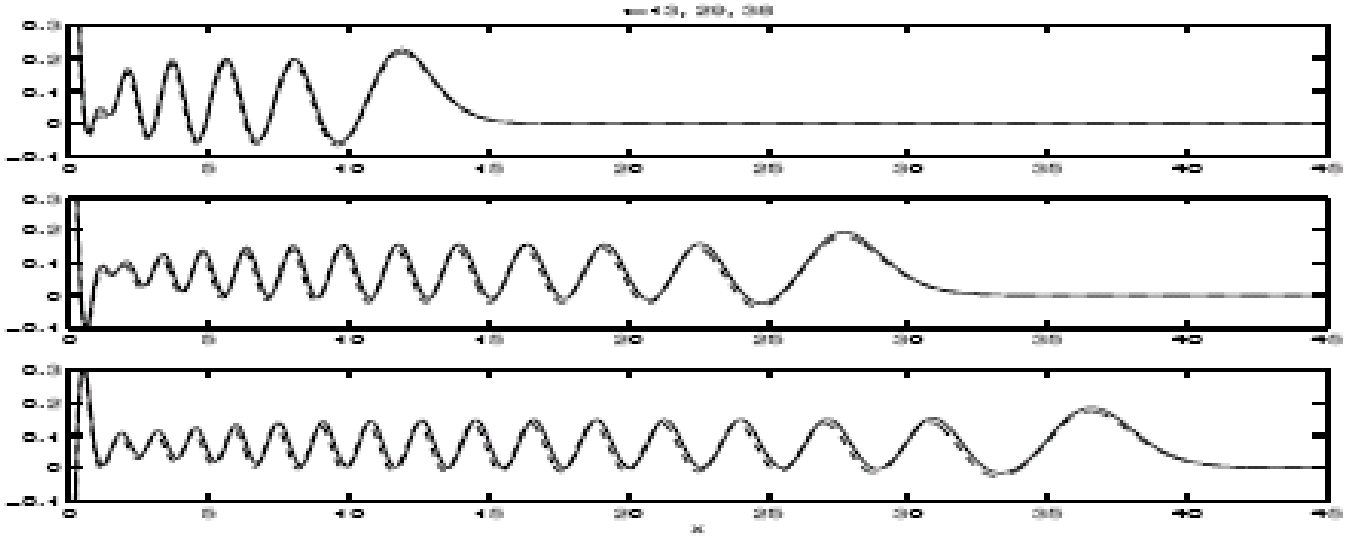

FIGURE 11. Comparison with $\epsilon = 0.2$.

Rogue Waves

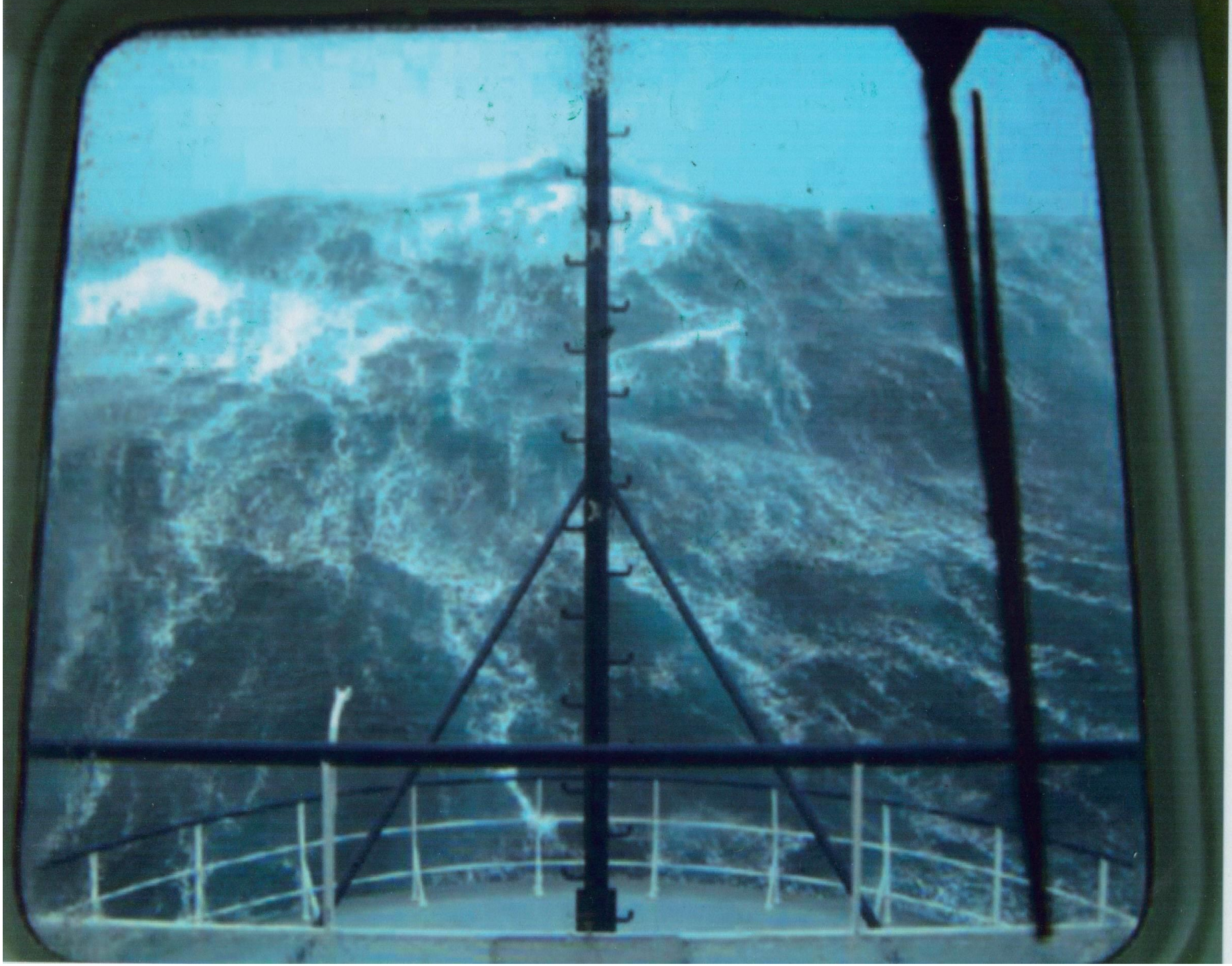

- Concurrence
- Statistical theory for wave amplitude
- Wave – current interaction
- Topographical forcing

- Gustavo Ponce
- Jean-Claude Saut
- Christof Sparber

Sand Bar Formation and Soft Beach Protection

Jerry Bona

University of Illinois at Chicago

Collaborators

- B. Boczar-Karakiewicz
- Bill Pritchard
- Wojtek Romanczyk
- Ed Thornton
- Angus Jackson
- Ridgway Scott
- Thierry Colin
- Hongqiu Chen
- Min Chen
- David Lannes
- Jean-Claude Saut
- Juan Restrepo

Examples of Sand Bars

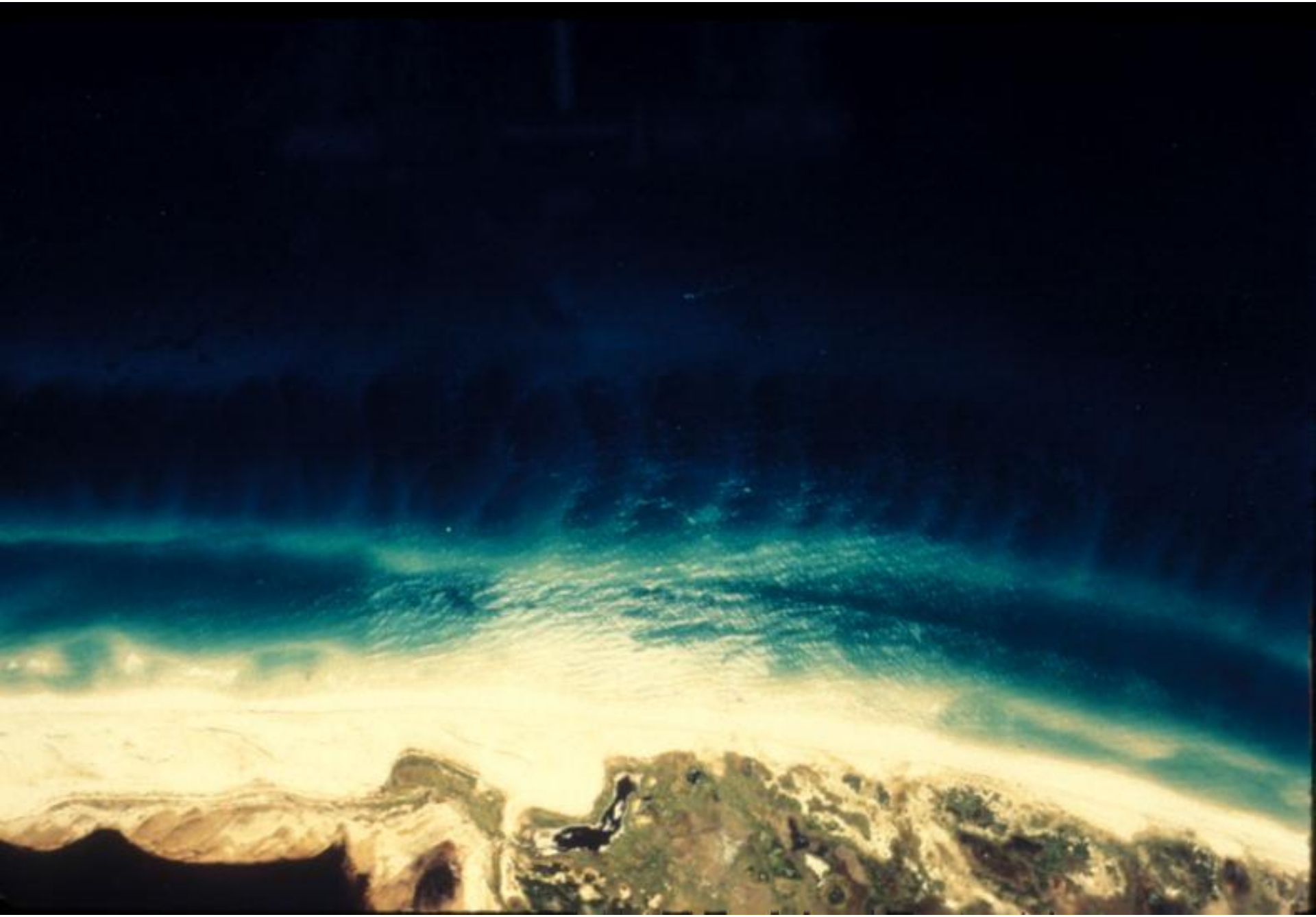

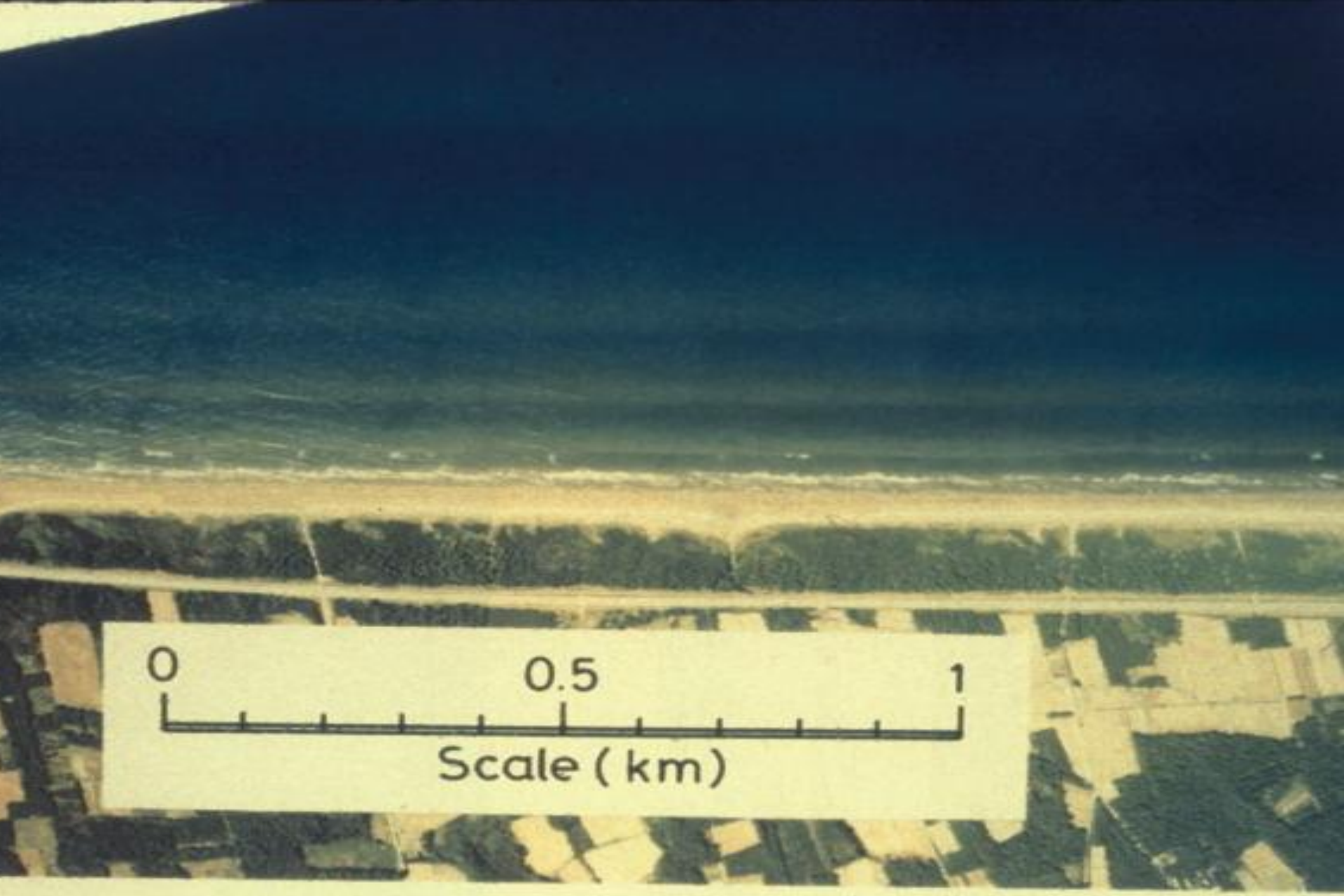

(a) Sept. 6, 1975 (11h. 29m.). Reference point No.42 to No.54.

otograph 1 Multiple longshore bars at Hakui Beach, Japan taken by the Geographical Survey Institute, Ministry of Construction. Number of reference points

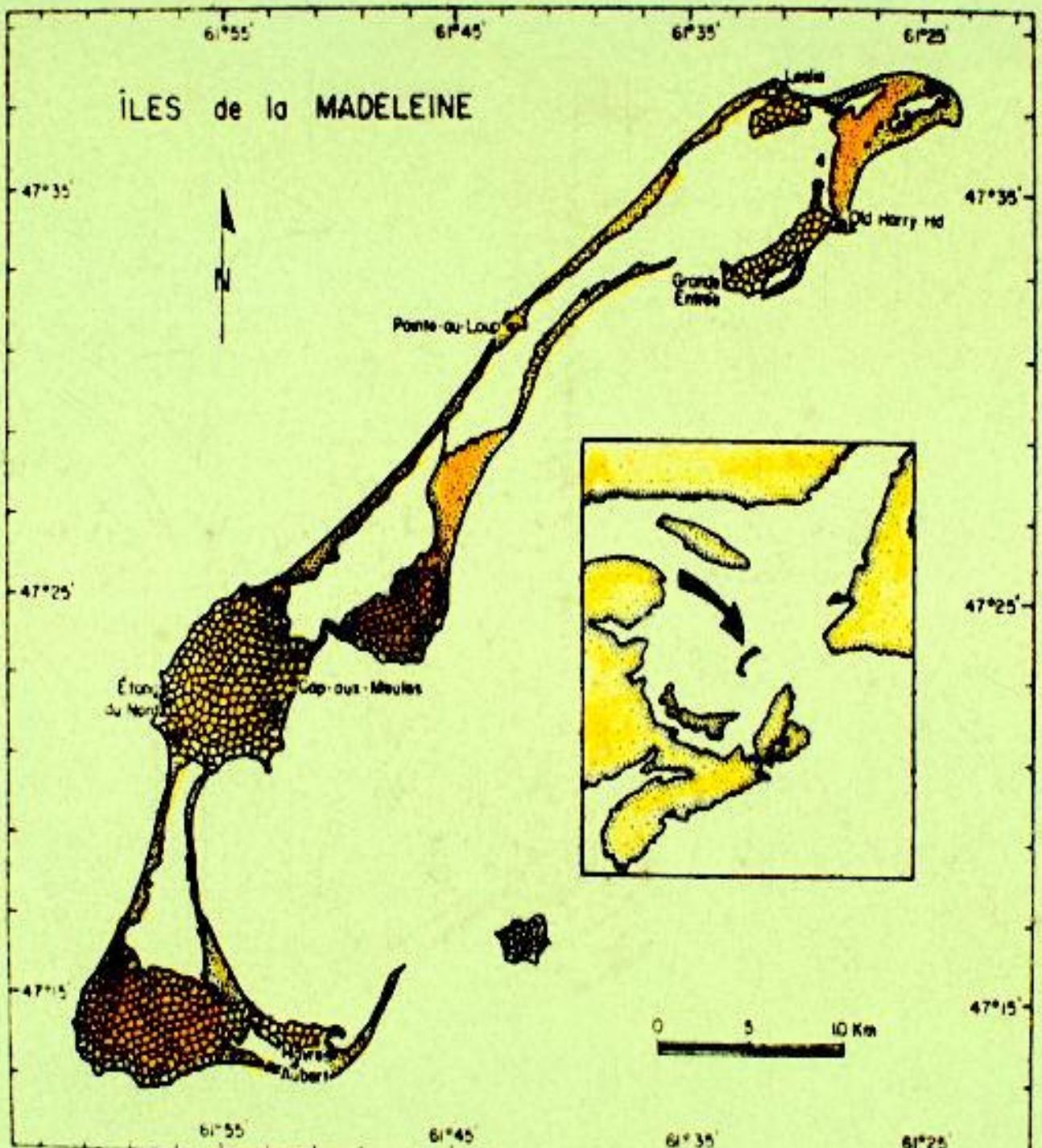
ÎLES de la MADELEINE
61°55'
61°45'
61°35'
61°25'
47°35'
47°25'
47°15'
N
Old Harry Hd
Grande Entrée
Pointe-au-Loup
Cap-aux-Meules
0
5
10 Km

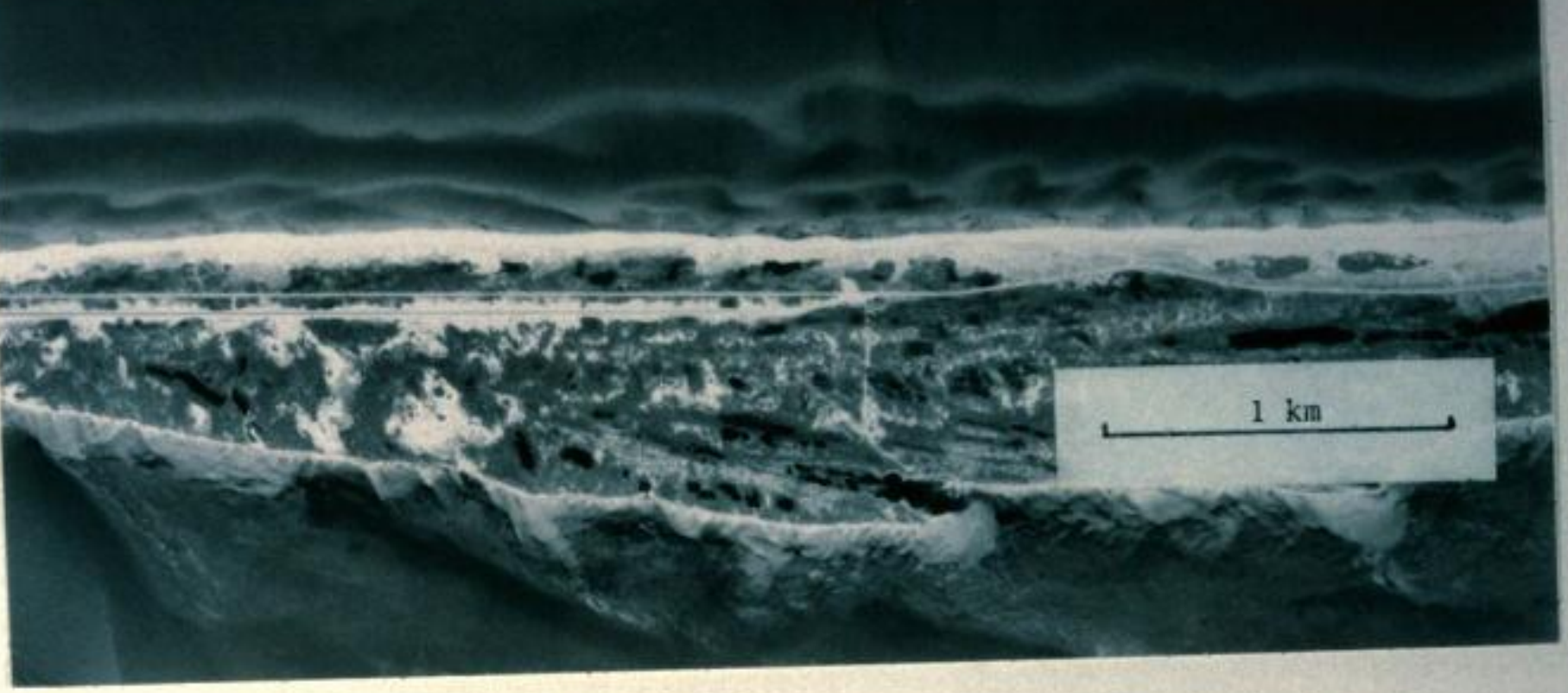
1 km

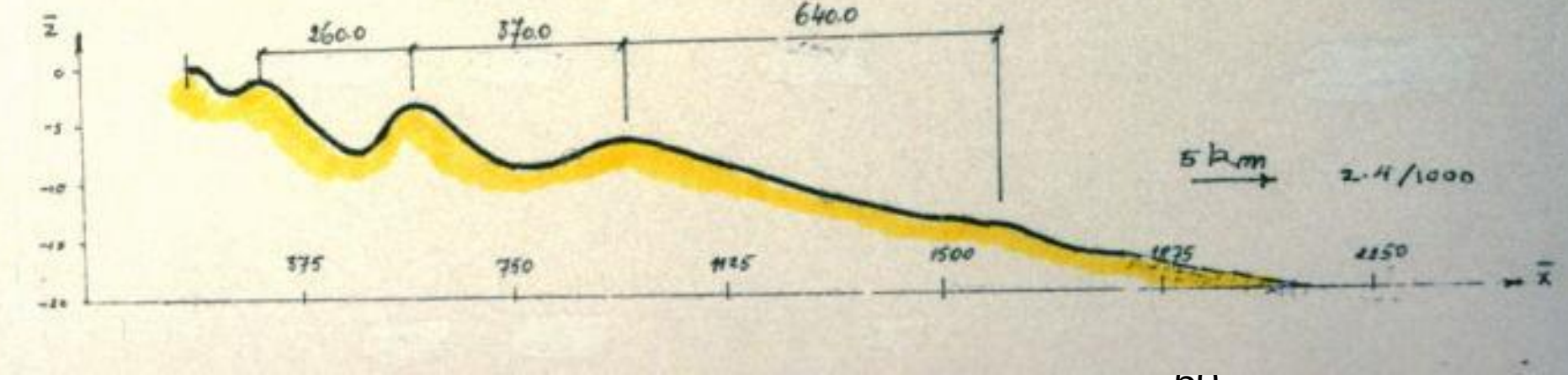
260.0
370.0
640.0
5 km
2.4 /1000
375
750
1125
1500
1875
2250

Laboratory Experiments (sand bar formation)

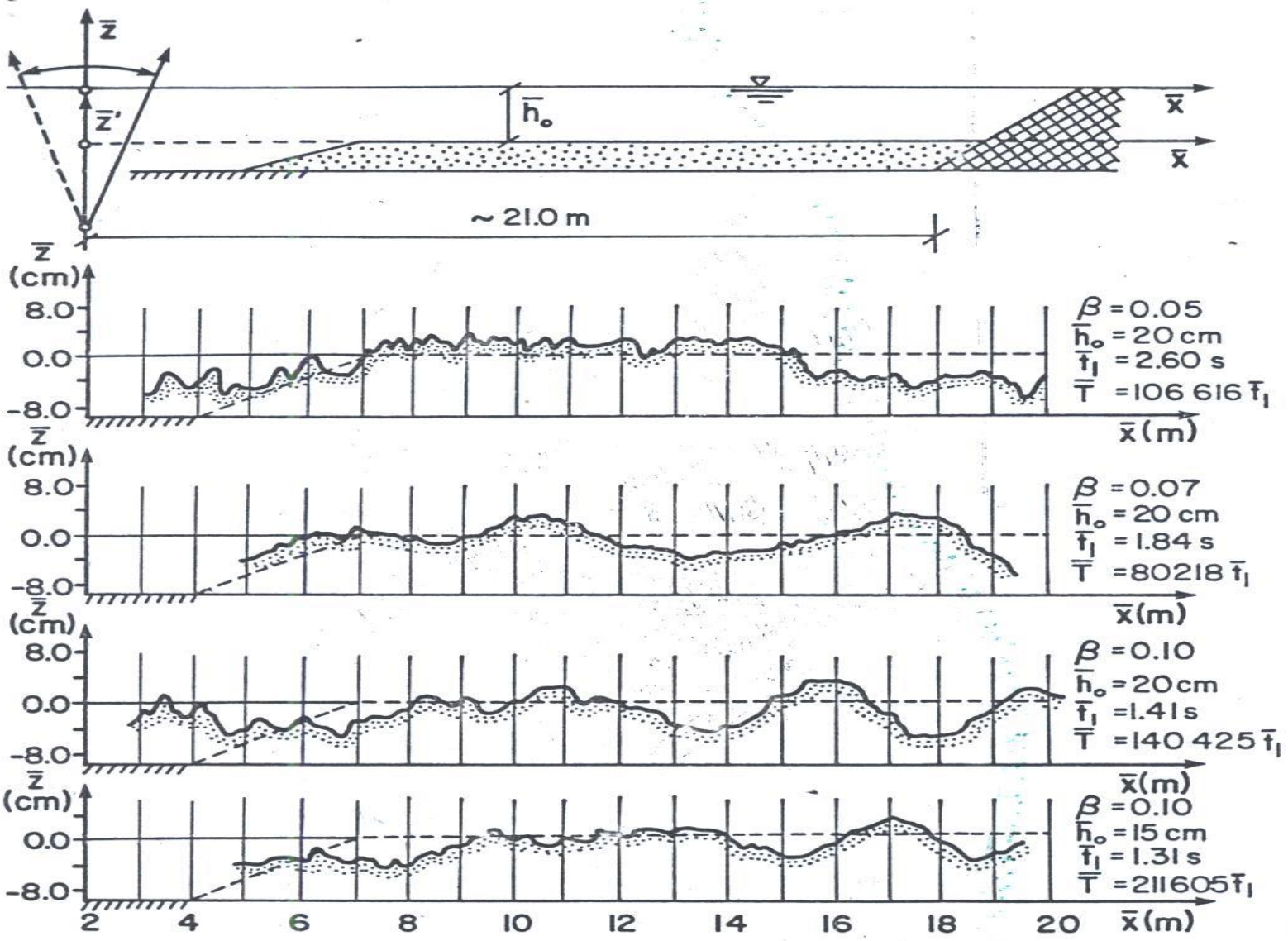
z̄
z̄'
h̄o
x̄
x̄
~ 21.0 m
z̄ (cm)
8.0
0.0
-8.0
x̄ (m)
β = 0.05
h̄o = 20 cm
f̄l = 2.60 s
T̄ = 106 616 f̄l
β = 0.07
h̄o = 20 cm
f̄l = 1.84 s
T̄ = 80218 f̄l
β = 0.10
h̄o = 20 cm
f̄l = 1.41 s
T̄ = 140 425 f̄l
β = 0.10
h̄o = 15 cm
f̄l = 1.31 s
T̄ = 211605 f̄l
2
4
6
8
10
12
14
16
18
20

Wave amplitude ↗

bar spacing ↘

wavelength ↗

bar spacing ↗

slope ↗

bar spacing ↘

The Model

1. Waves entering the near-shore zone from deep water – assumed known

2. Boussinesq systems of equations for variable depth is used to compute the evolution of deep water waves into the very near-shore zone.

3. Calculation of the velocity field from the evolution of the free surface (and the average horizontal velocity).

4. Assume a vertical distribution of sediment (or predict it using the velocity field) and assume this is driven by the calculated velocity field.

5. Average the velocity over the fundamental period of the incoming waves and over the depth to obtain the mass transport

$$Q = \lambda \int_{\text{bottom}}^{\text{top}} \int_{0}^{P} u(x,y,t+s)\rho(y)\,d$$

($P = 2\pi/\omega$ fundamental period)

III. Bottom change rate.

$$\frac{\partial h}{\partial t} = \frac{\partial Q}{\partial x} \qquad [3]$$

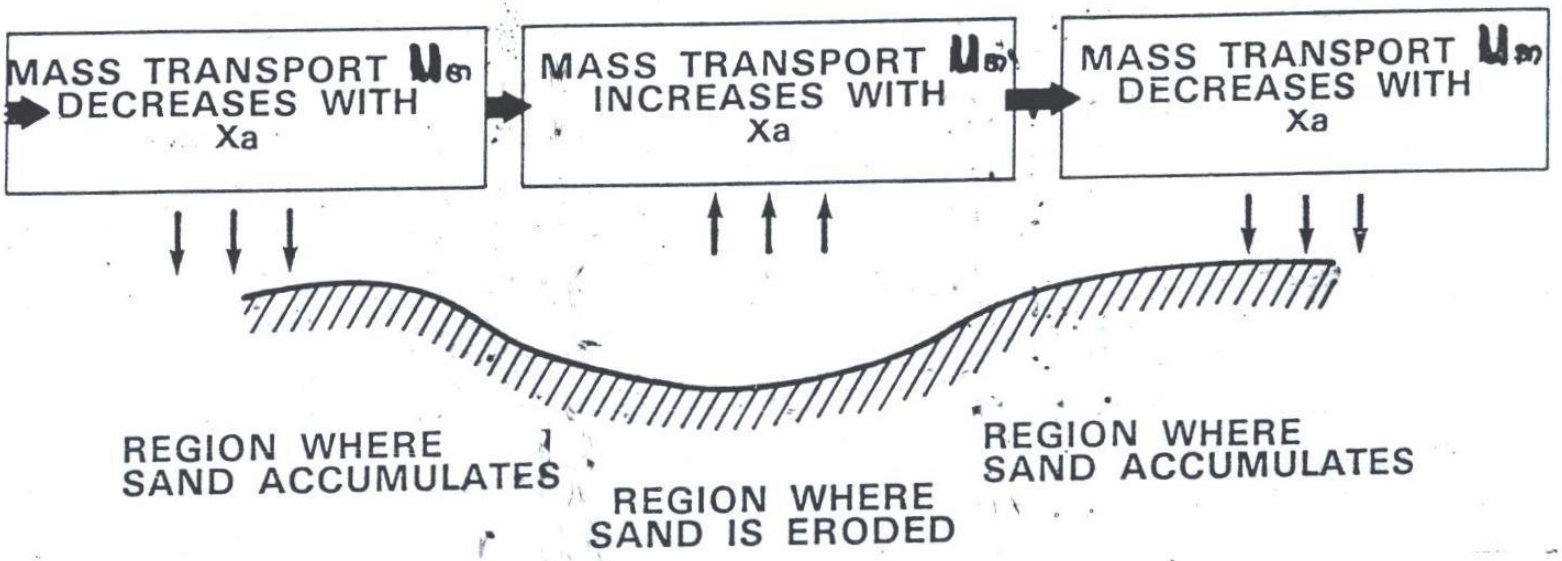

Flow chart for the integration of the mathematical model

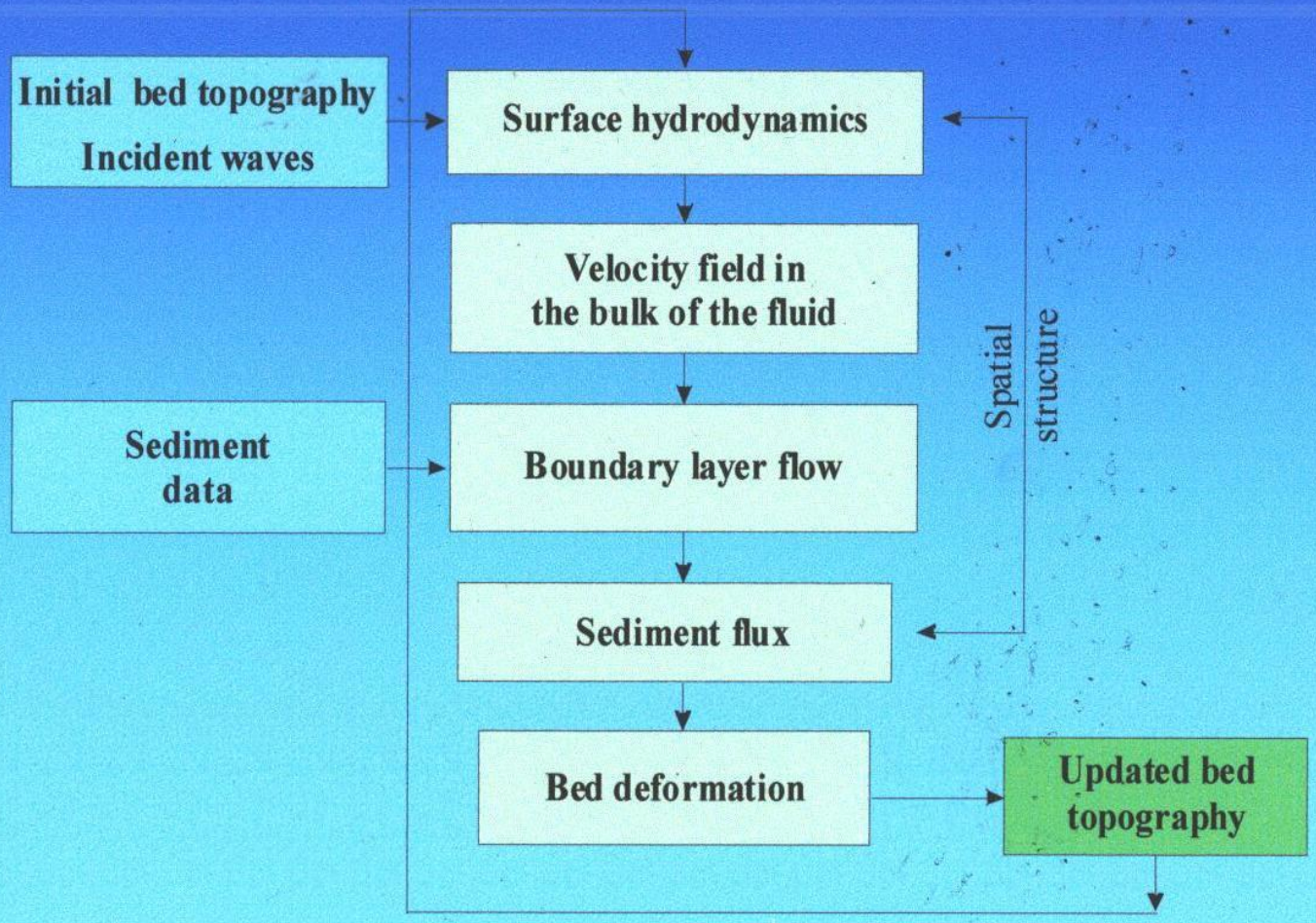

Fig 12 (1)

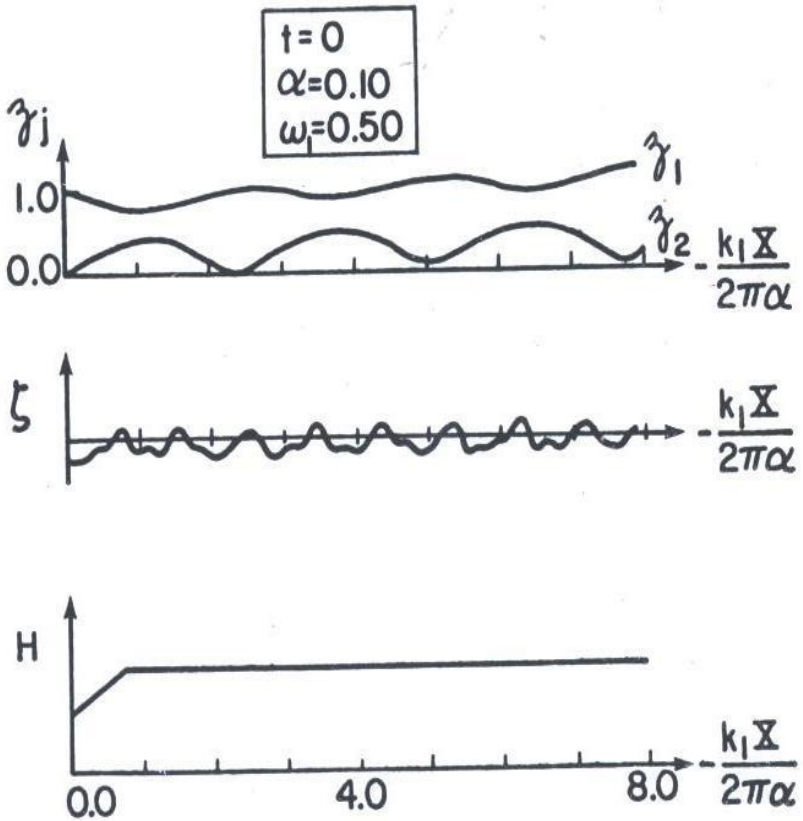
t=0
α=0.10
ω_I=0.50
γ_j
1.0
0.0
γ_1
γ_2
k_1X / 2πα
ζ
k_1X / 2πα
H
0.0
4.0
8.0
k_1X / 2πα

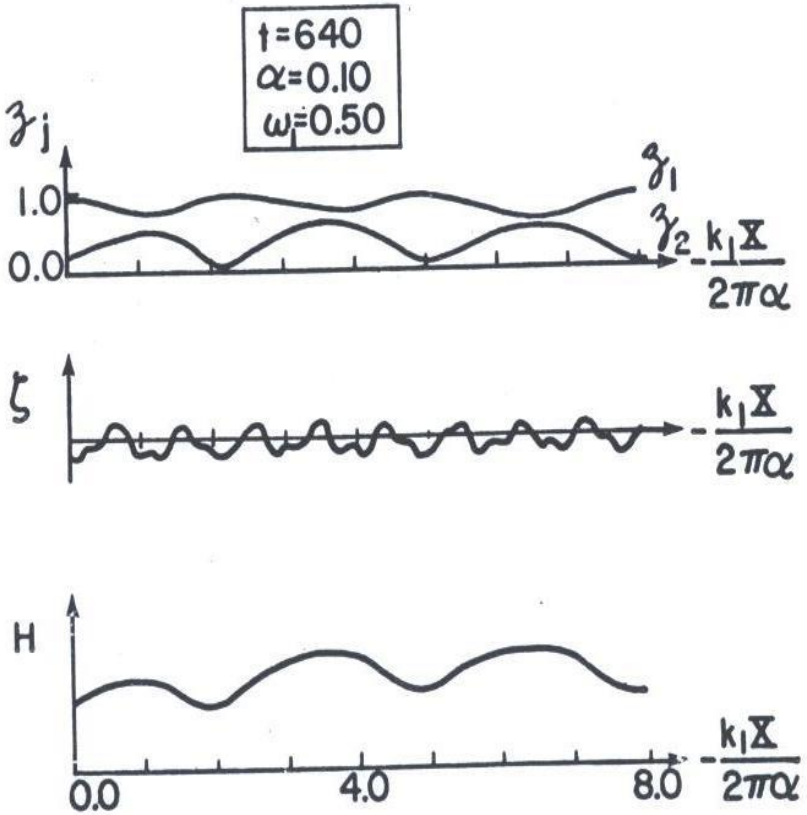
t=640
α=0.10
ω_I=0.50
γ_j
1.0
0.0
γ_1
γ_2
k_1X / 2πα
ζ
k_1X / 2πα
H
0.0
4.0
8.0
k_1X / 2πα

Fig 12 (a)

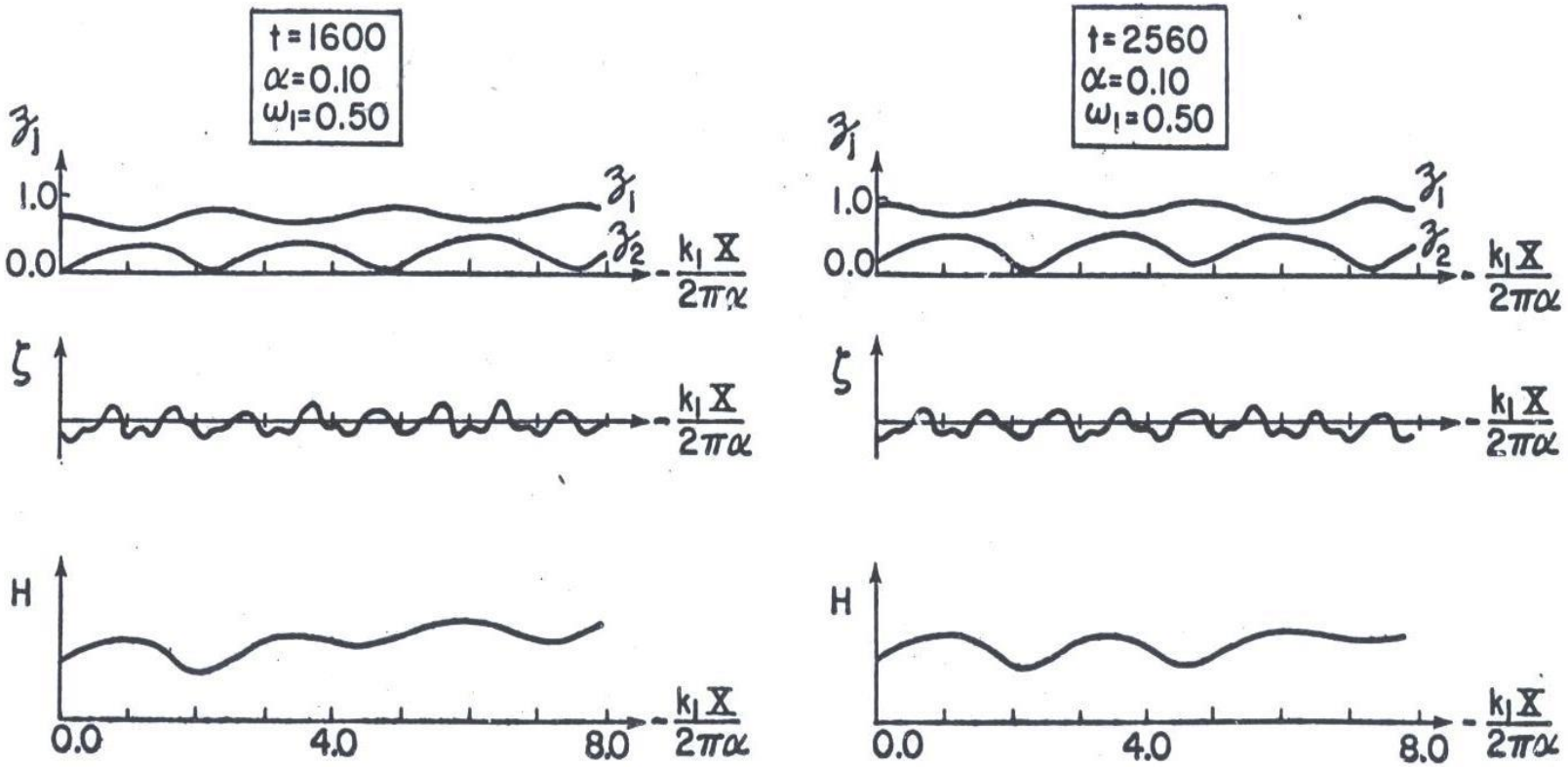
t = 1600
α = 0.10
ω1 = 0.50
z1
1.0
0.0
z1
z2
k1 X / 2πα
ζ
k1 X / 2πα
H
0.0
4.0
8.0
k1 X / 2πα
t = 2560
α = 0.10
ω1 = 0.50
z1
1.0
0.0
z1
z2
k1 X / 2πα
ζ
k1 X / 2πα
H
0.0
4.0
8.0
k1 X / 2πα

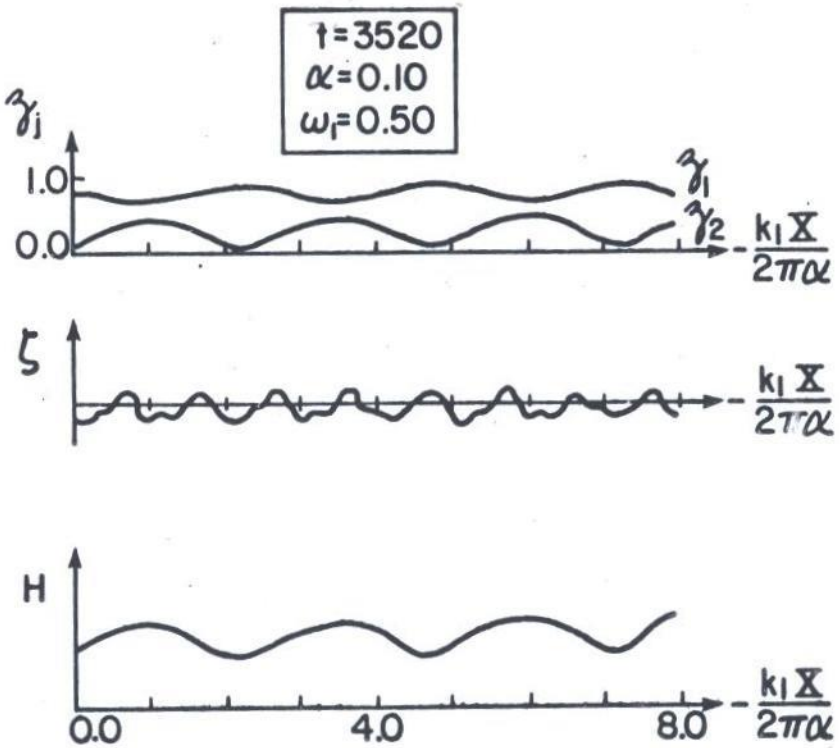
t=3520
α=0.10
ω1=0.50
γj
1.0
0.0
γ1
γ2
k1 X / 2πα
ζ
k1 X / 2πα
H
0.0
4.0
8.0
k1 X / 2πα

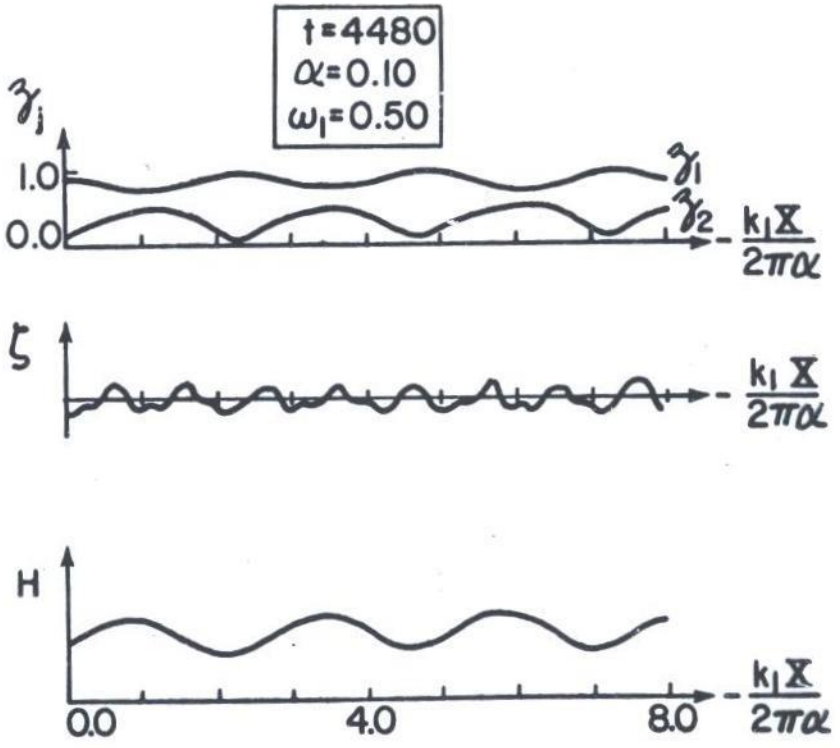
t=4480
α=0.10
ω1=0.50
γj
1.0
0.0
γ1
γ2
k1 X / 2πα
ζ
k1 X / 2πα
H
0.0
4.0
8.0
k1 X / 2πα

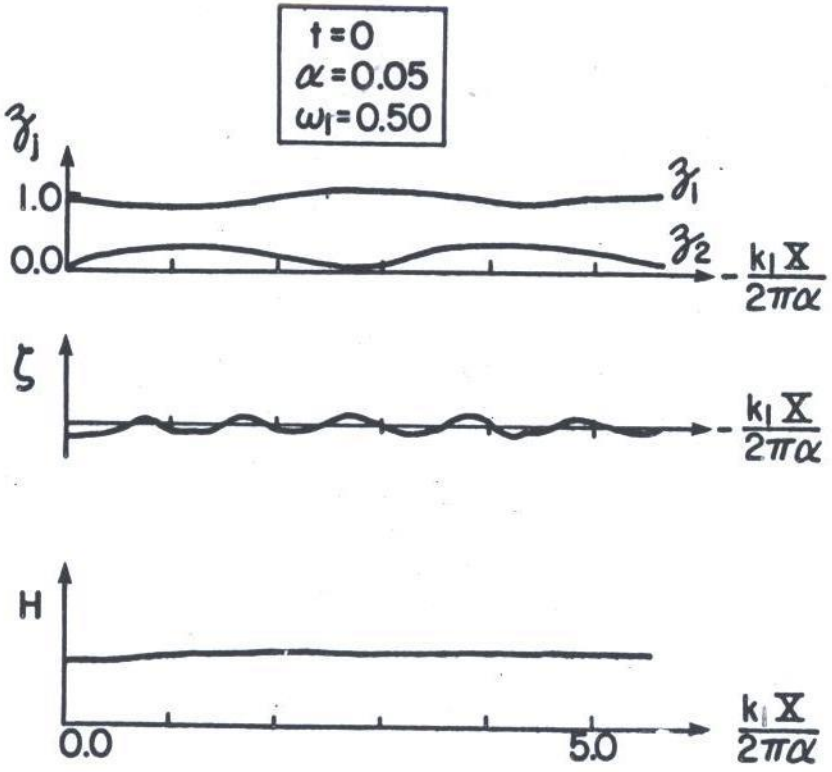
t=0
α=0.05
ω1=0.50
zj
1.0
0.0
z1
z2
k1X/2πα
ζ
k1X/2πα
H
0.0
5.0
k1X/2πα

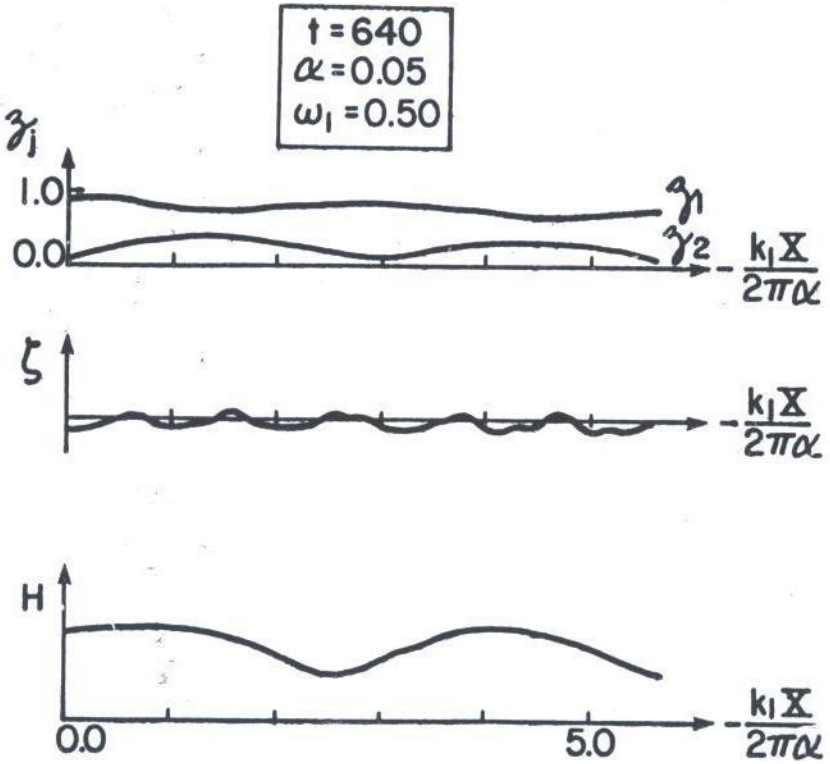
t=640
α=0.05
ω1=0.50
zj
1.0
0.0
z1
z2
k1X/2πα
ζ
k1X/2πα
H
0.0
5.0
k1X/2πα

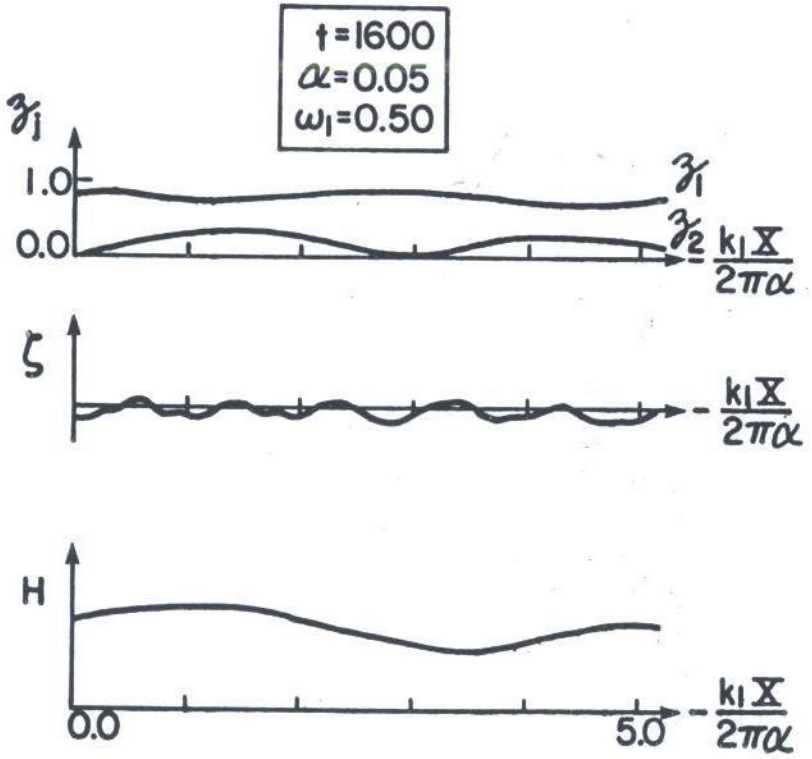
t=1600
α=0.05
ω1=0.50
zj
1.0
0.0
z1
z2
k1X/2πα
ζ
k1X/2πα
H
0.0
5.0
k1X/2πα

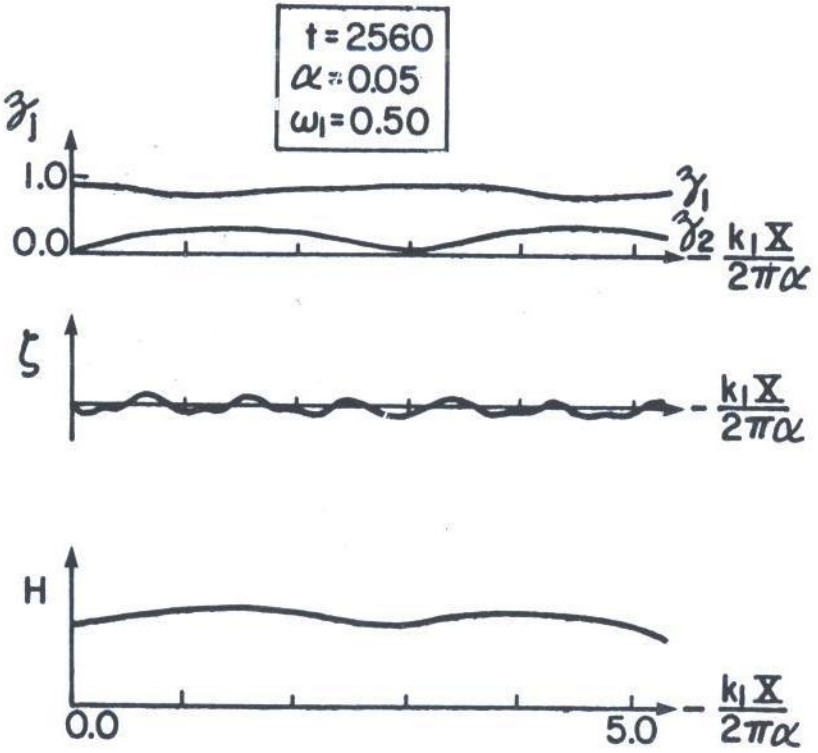
t=2560
α=0.05
ω1=0.50
zj
1.0
0.0
z1
z2
k1X/2πα
ζ
k1X/2πα
H
0.0
5.0
k1X/2πα

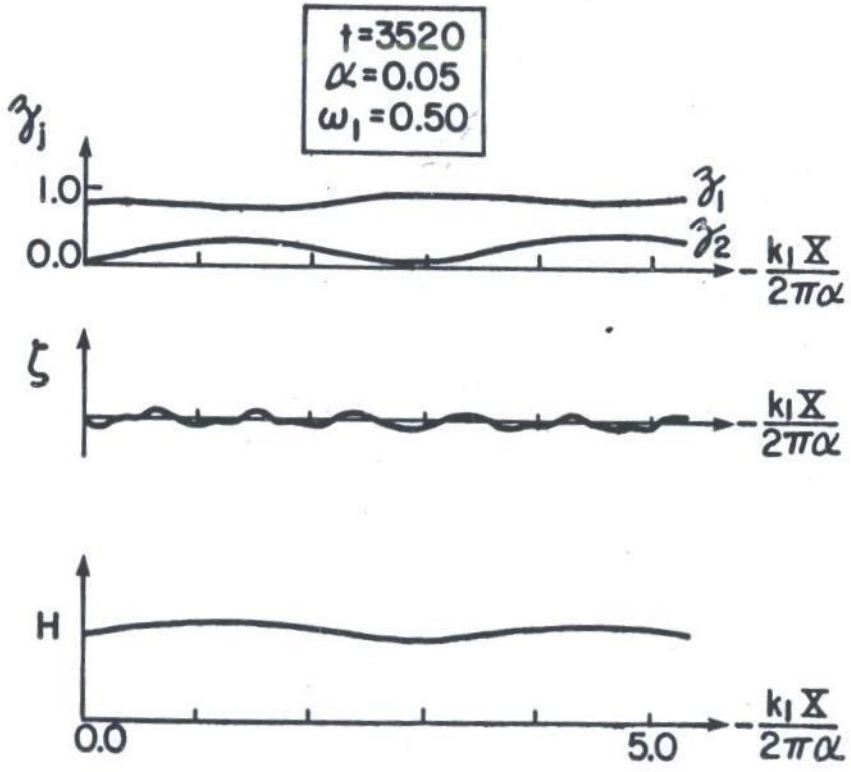
t=3520
α=0.05
ω1=0.50
zj
1.0
0.0
z1
z2
k1X/2πα
ζ
k1X/2πα
H
0.0
5.0
k1X/2πα

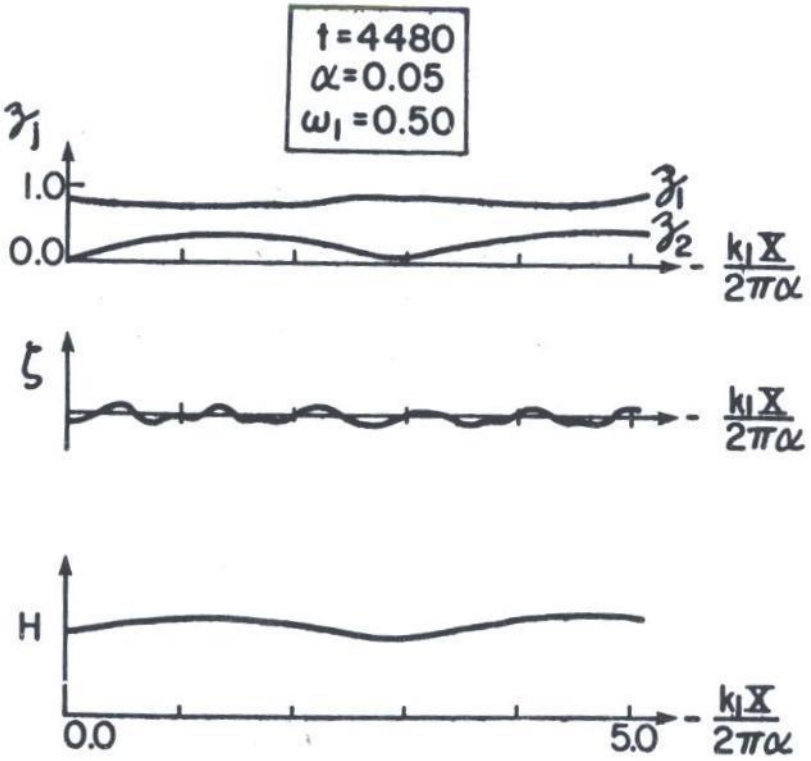
t=4480
α=0.05
ω1=0.50
zj
1.0
0.0
z1
z2
k1X/2πα
ζ
k1X/2πα
H
0.0
5.0
k1X/2πα

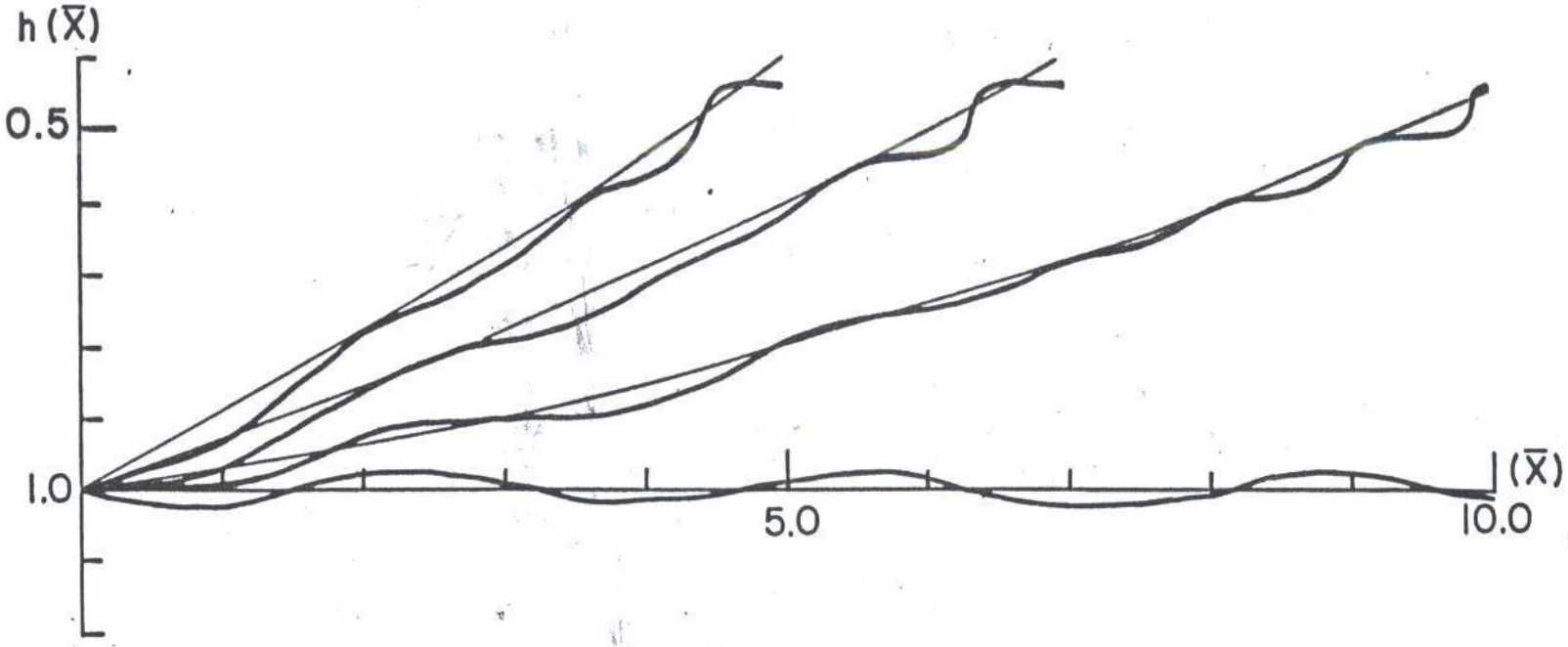
h (X̄)
0.5
1.0
5.0
10.0
(X̄)

Localization of the FRF at Duck

Aerial view of the local coordinates

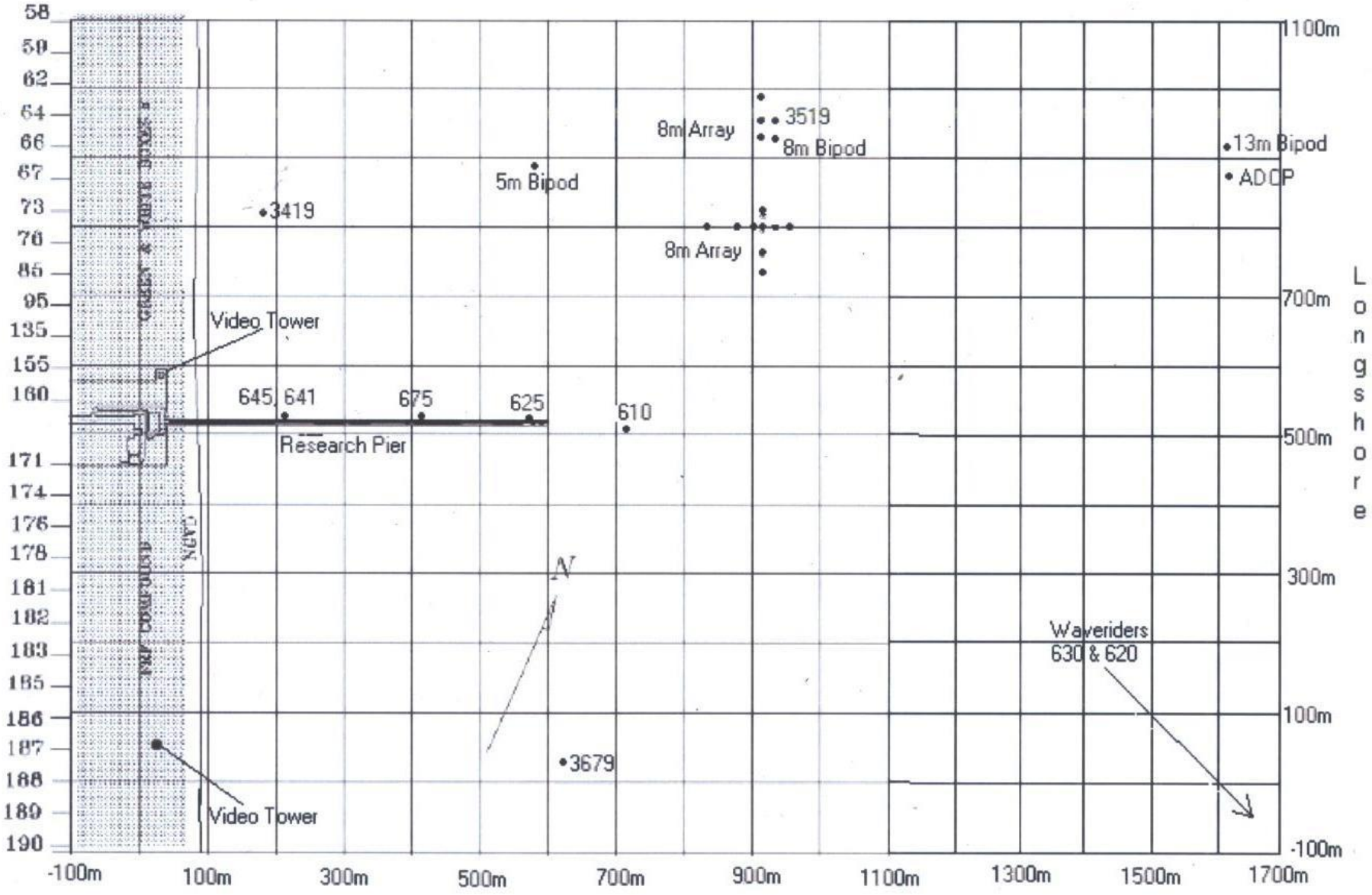

Location of profile #62

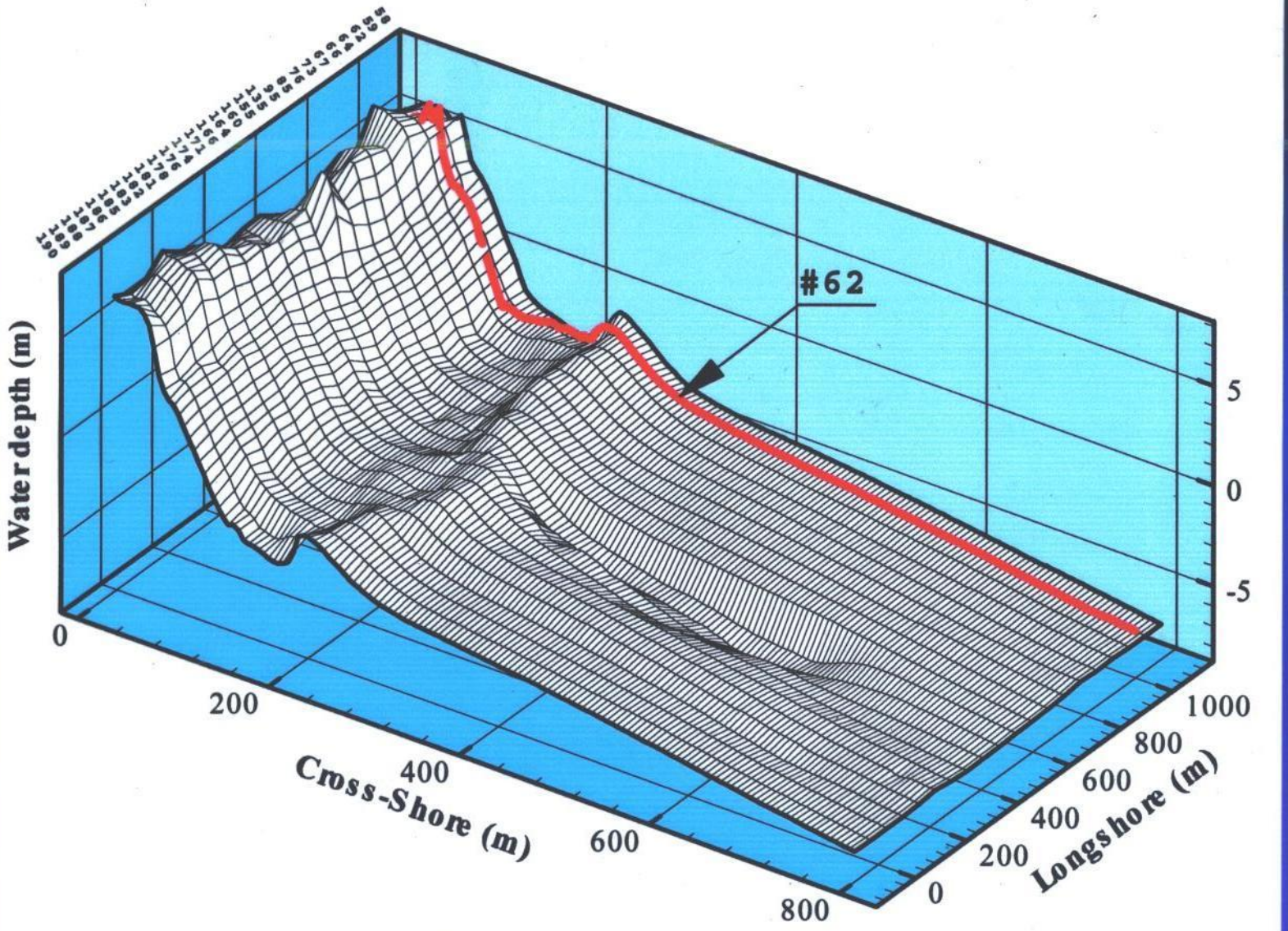

Topography data - profile 62

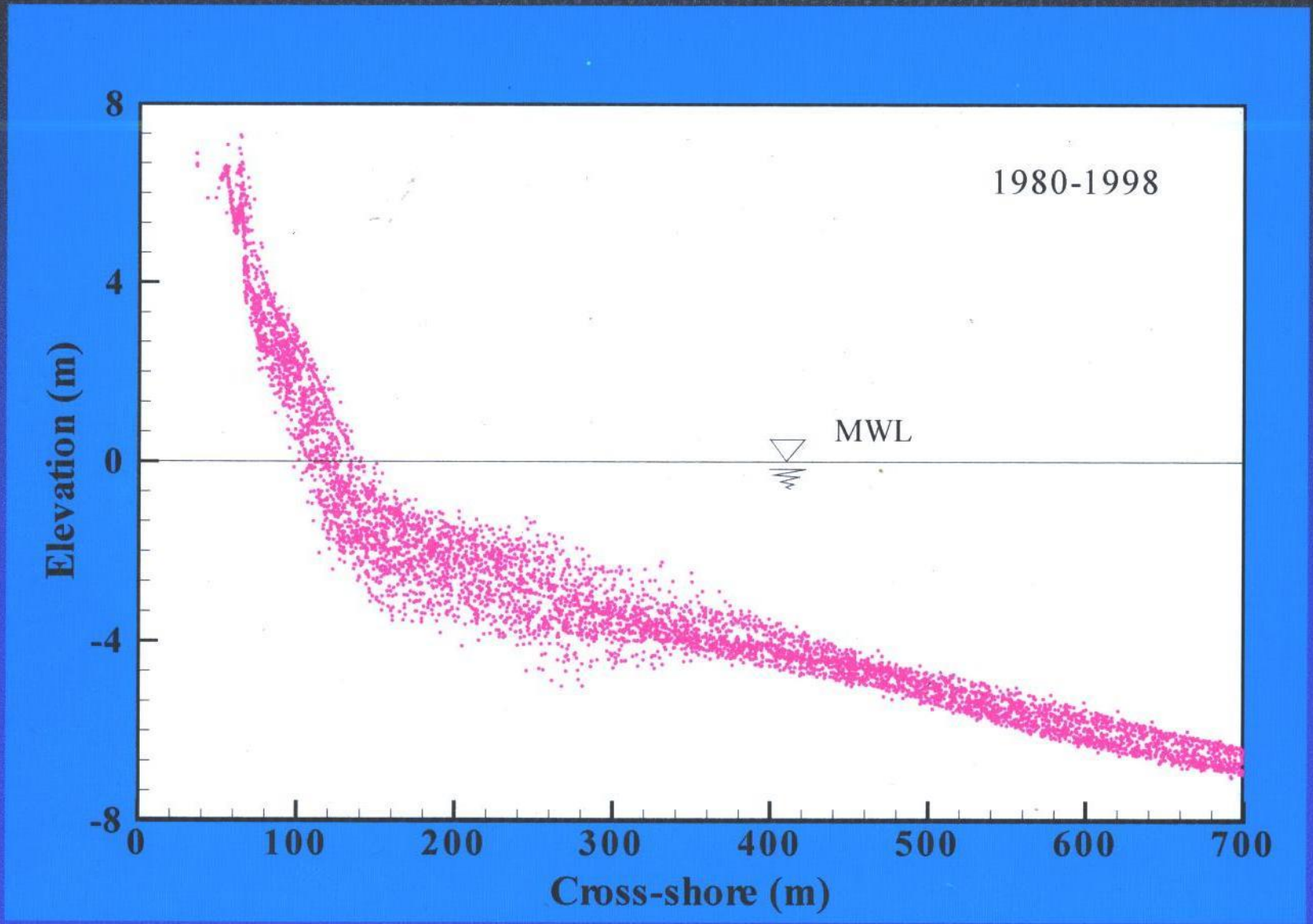

Measurements and futureless bed profile

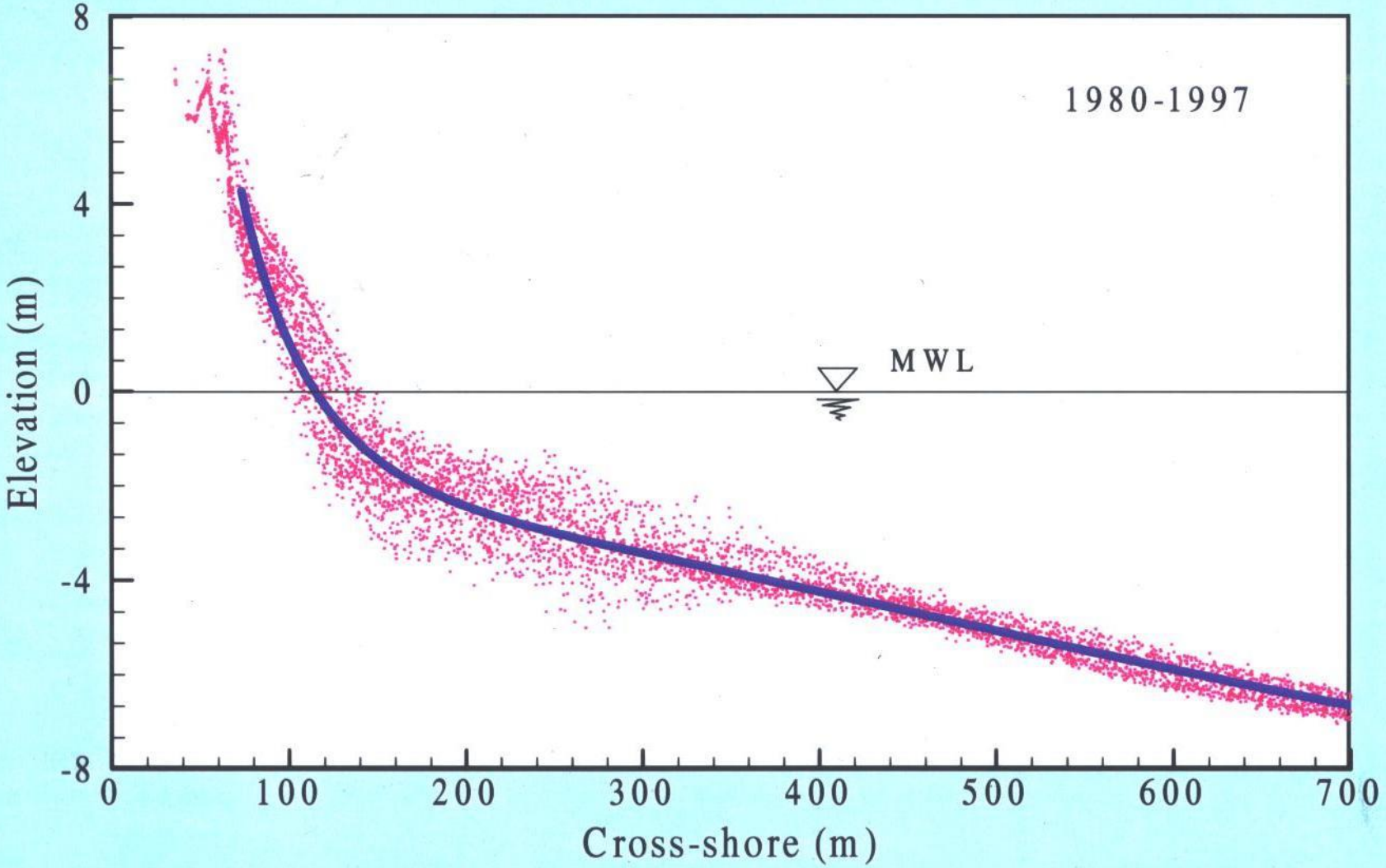

Duck

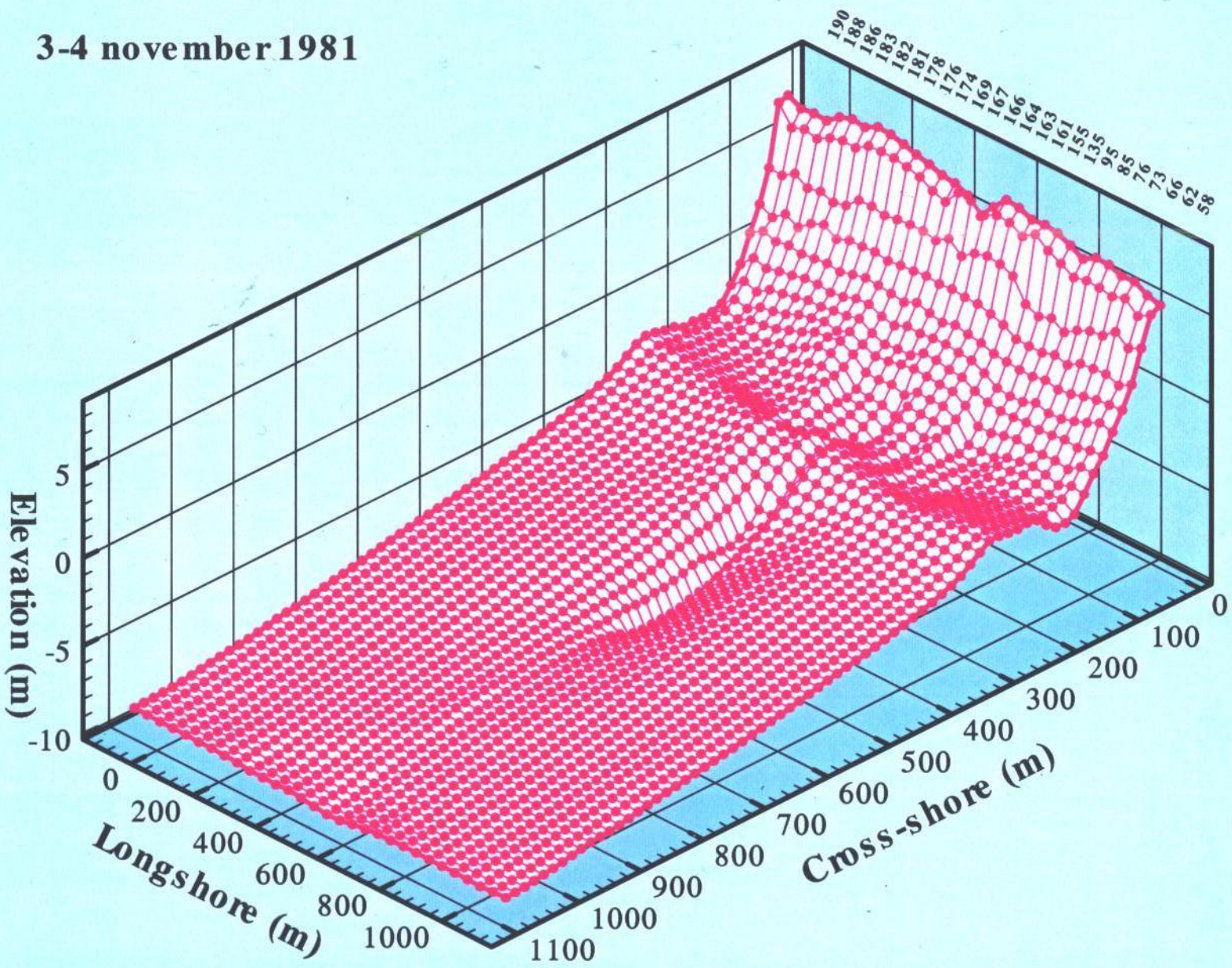
3-4 november 1981
190
188
186
183
182
181
178
176
174
169
167
166
164
163
161
155
135
95
85
76
73
66
62
58
Elevation (m)
5
0
-5
-10
0
200
400
600
800
1000
Longshore (m)
0
100
200
300
400
500
600
700
800
900
1000
1100
Cross-shore (m)

Duck

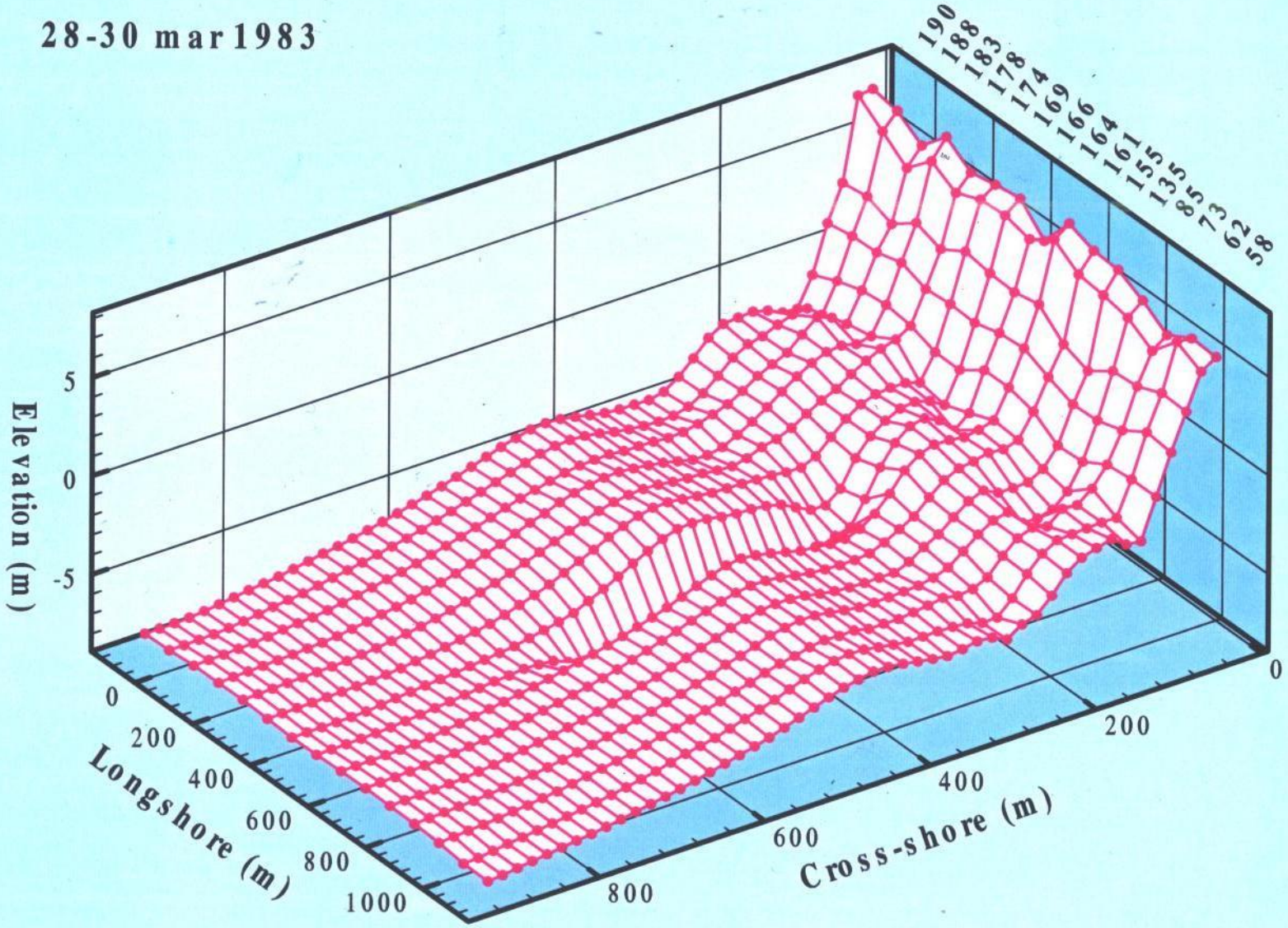
28-30 mar 1983
190
188
183
178
174
169
166
164
161
155
135
85
73
62
58
Elevation (m)
5
0
-5
0
200
400
600
800
1000
Longshore (m)
0
200
400
600
800
Cross-shore (m)

'Anomalies' in nearshore morphology

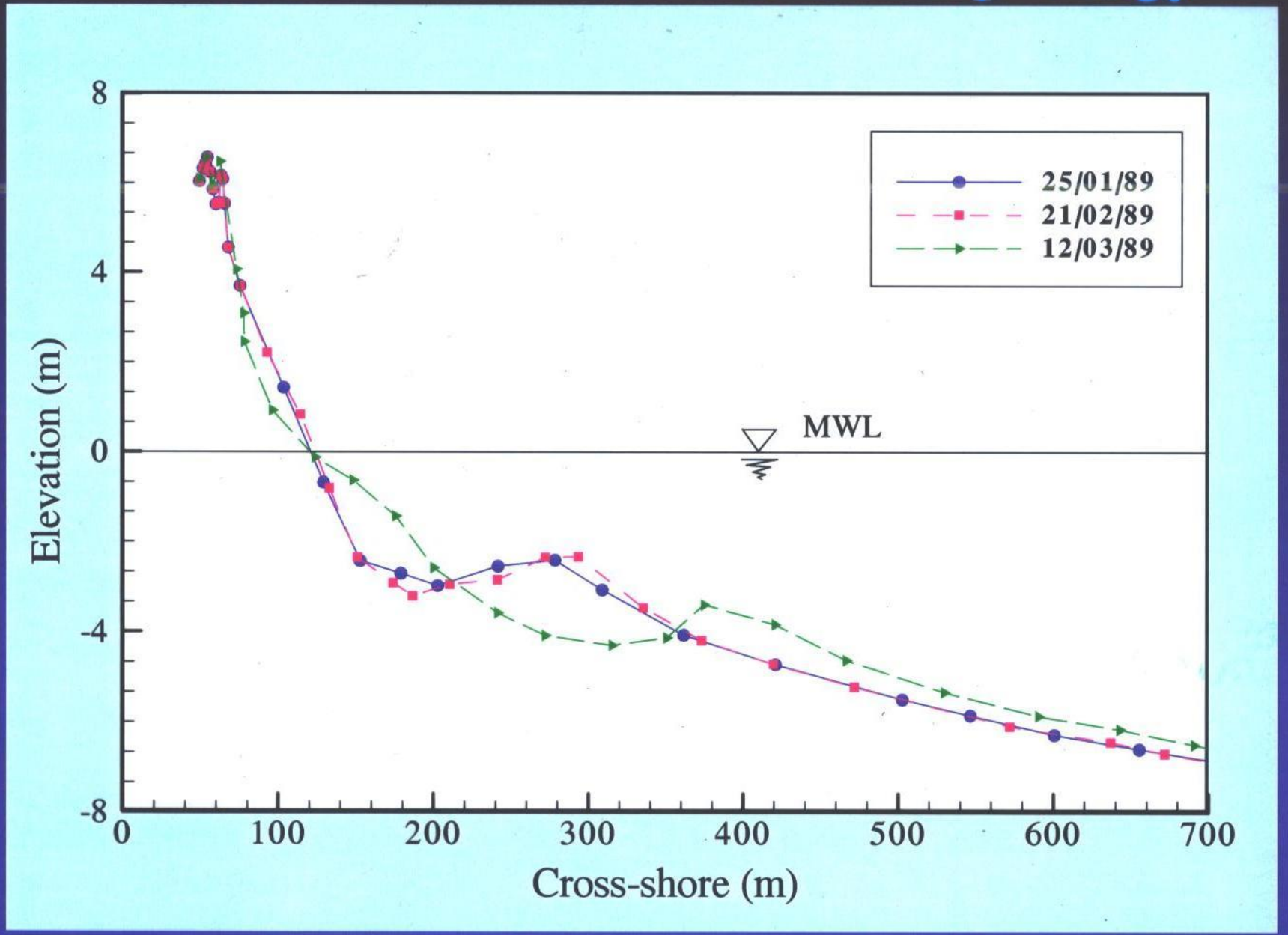

Annual wave data dynamics

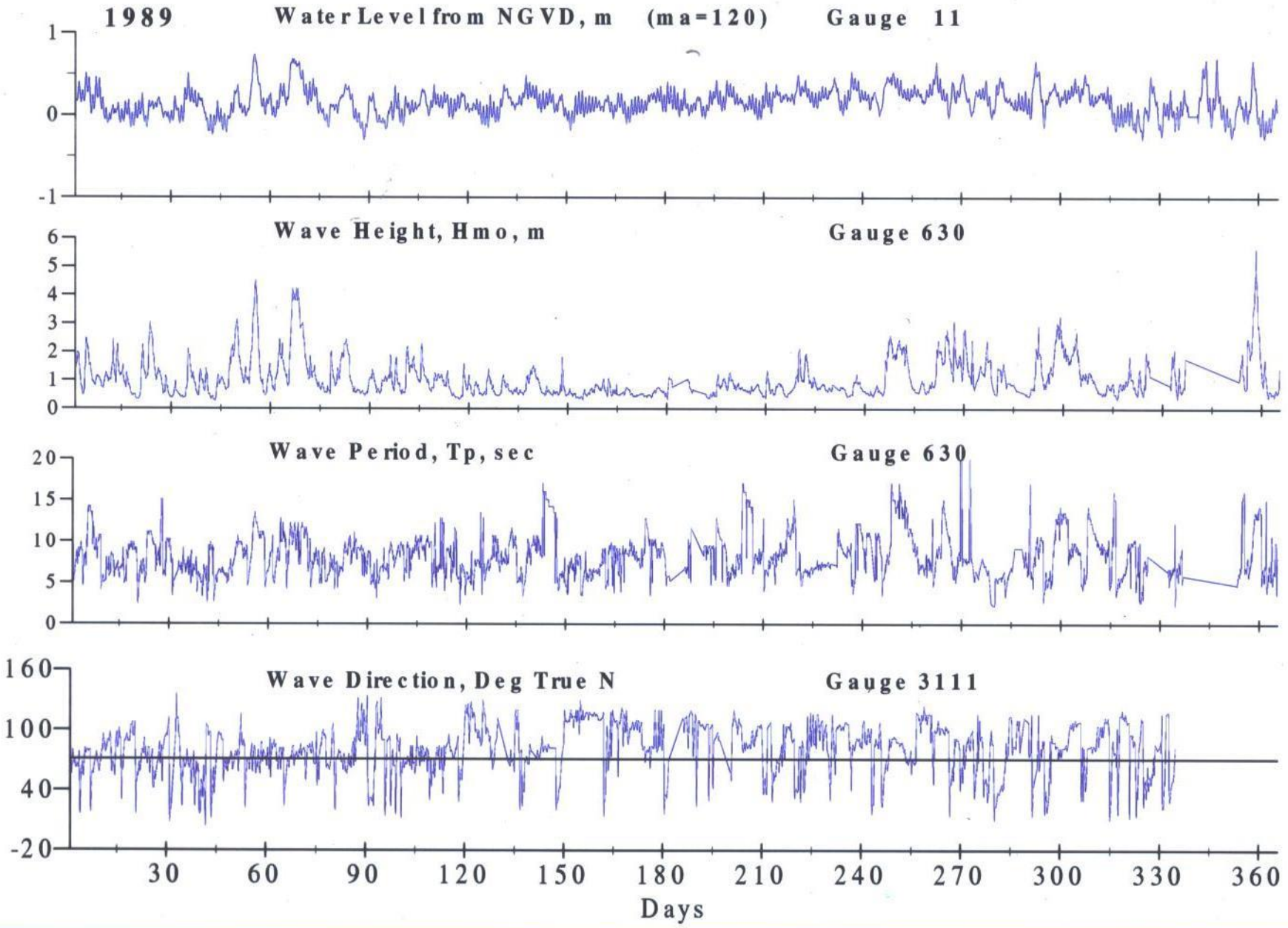

FEBRUARY, 1989

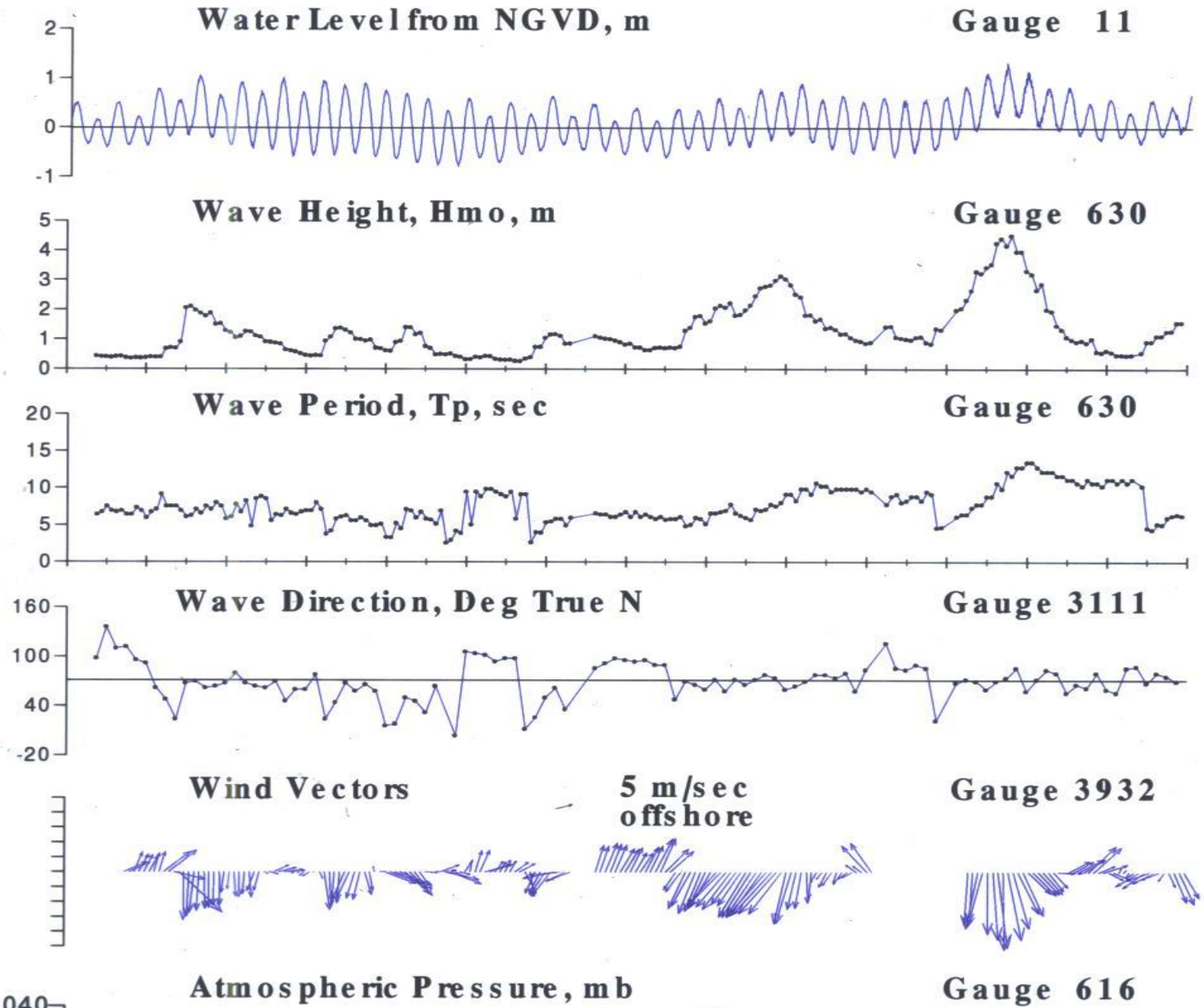

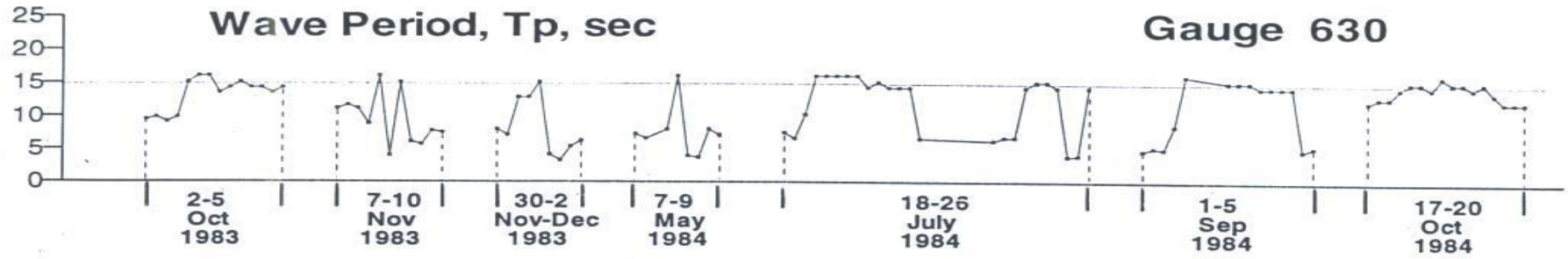

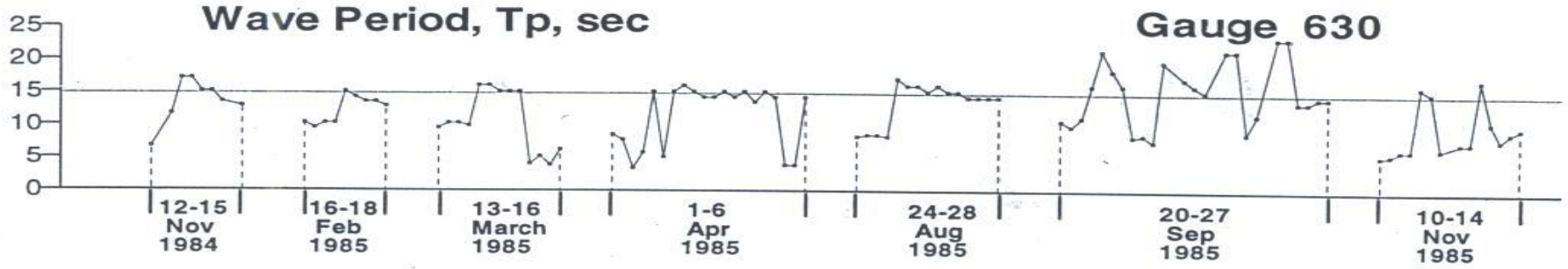

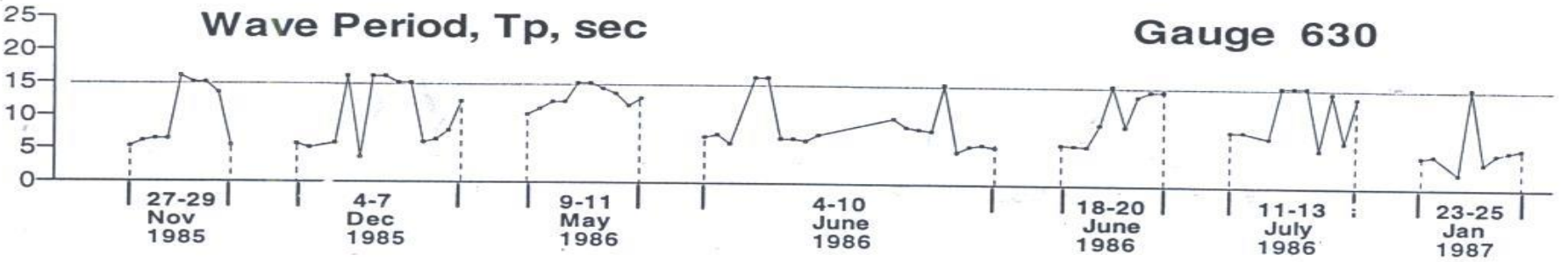

g630wp6.lay

g630wp2.lay,g630wp3.lay,g630wp4.lay)

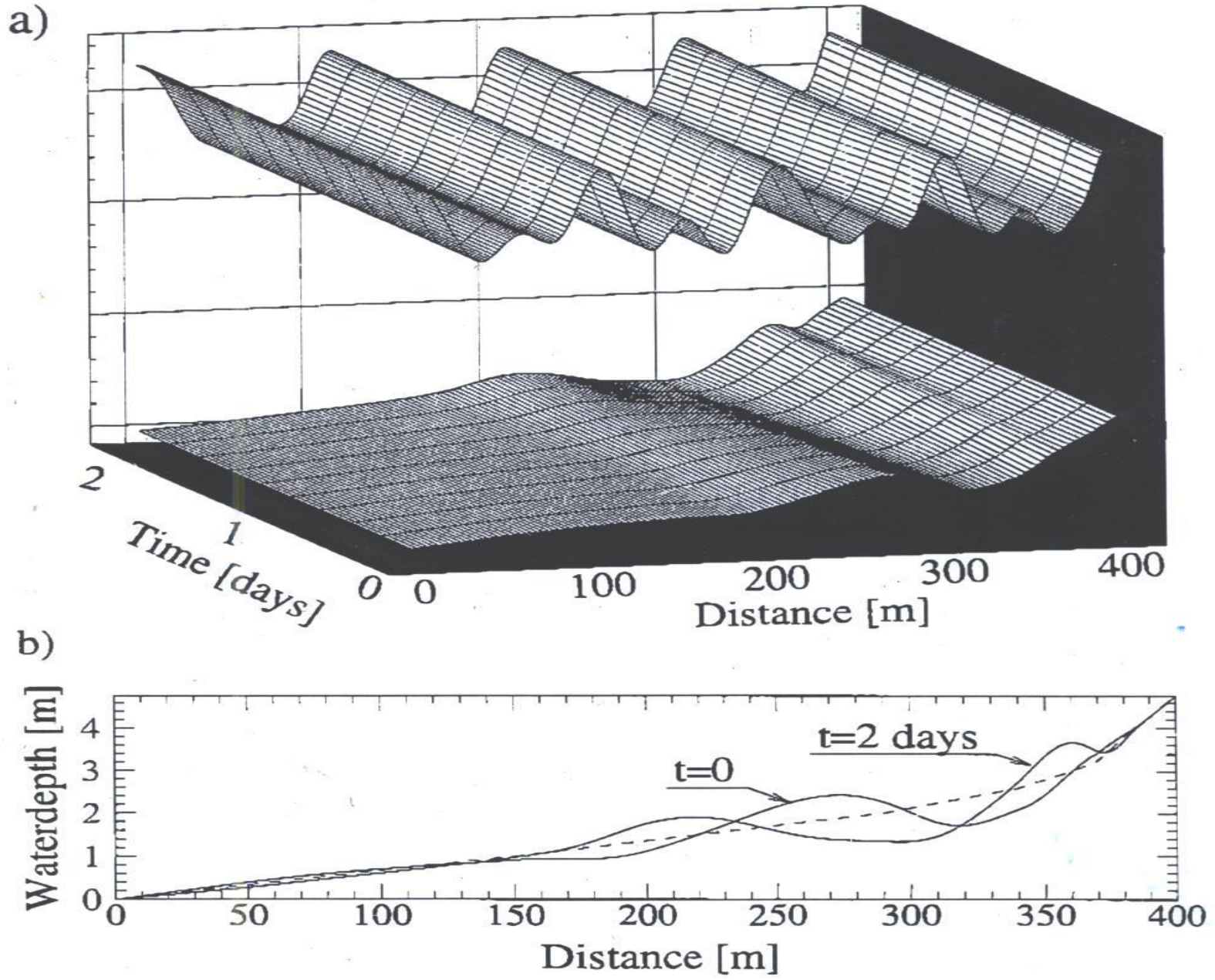
a)
2
1
0
Time [days]
0
100
200
300
400
Distance [m]
b)
Waterdepth [m]
0
1
2
3
4
t=0
t=2 days
0
50
100
150
200
250
300
350
400
Distance [m]

Temporal variability of the localization of bar crests

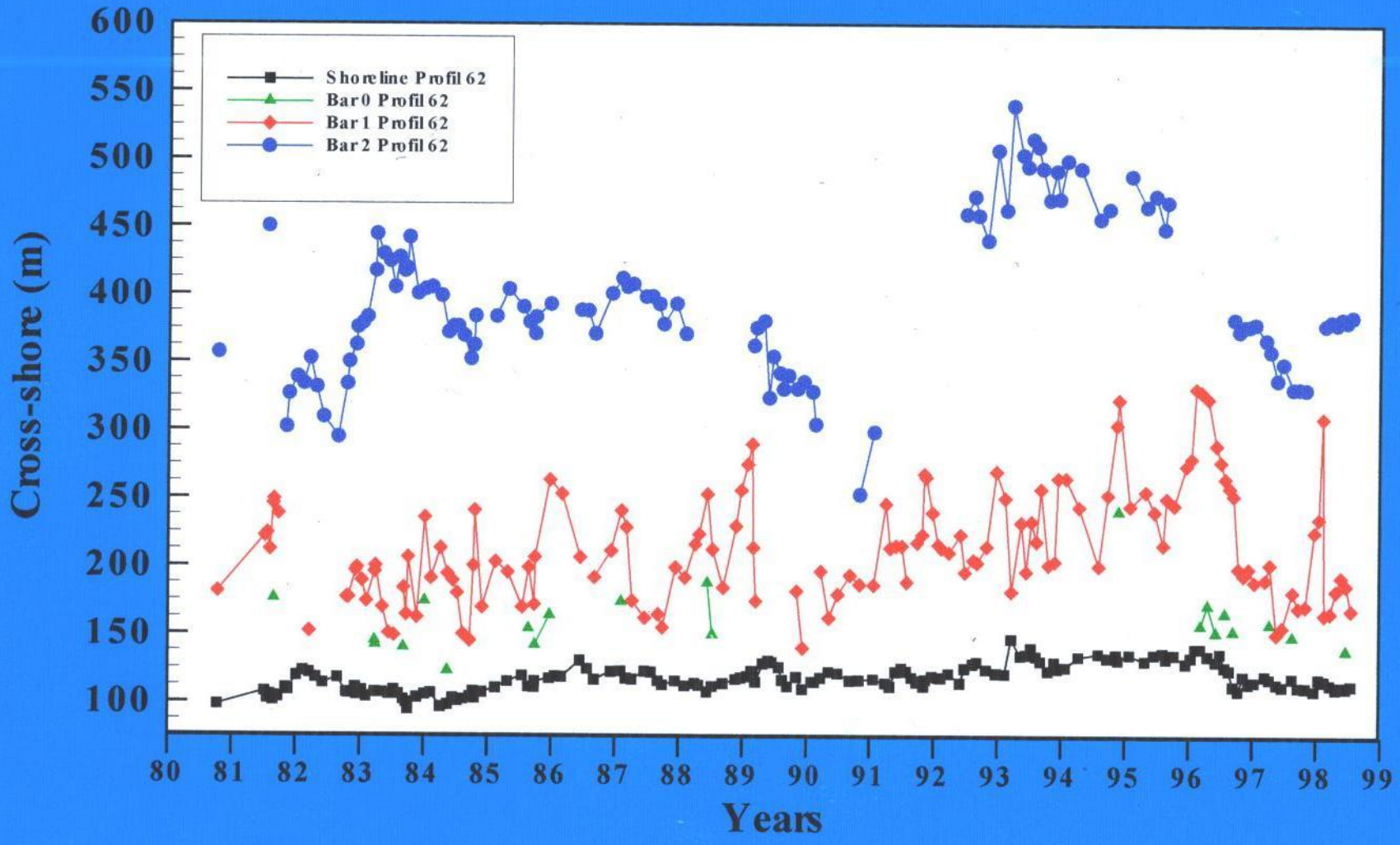

Temporal variability of bar crests localization

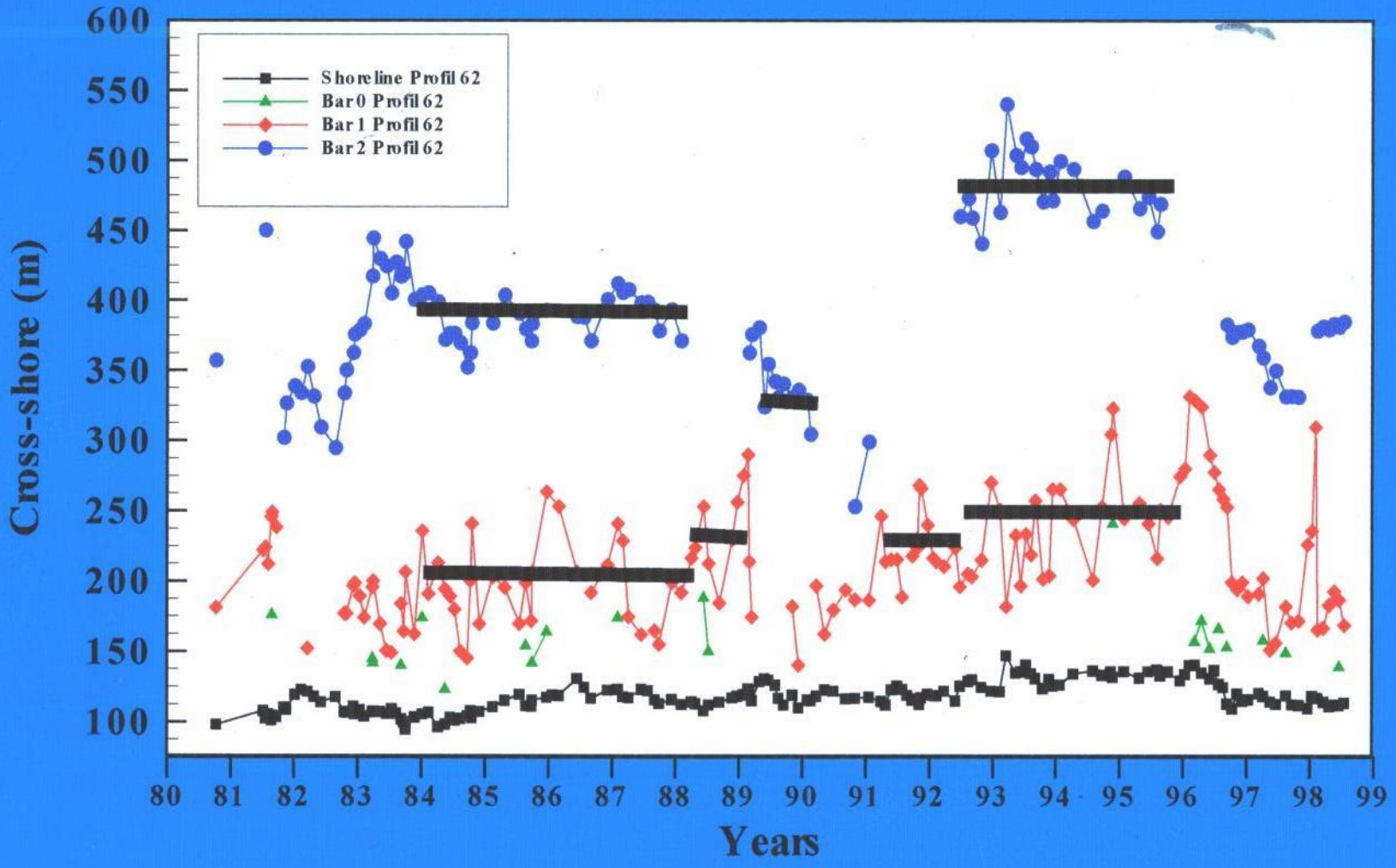

Simulation of bar formation by storm waves starting from the equilibrium profile

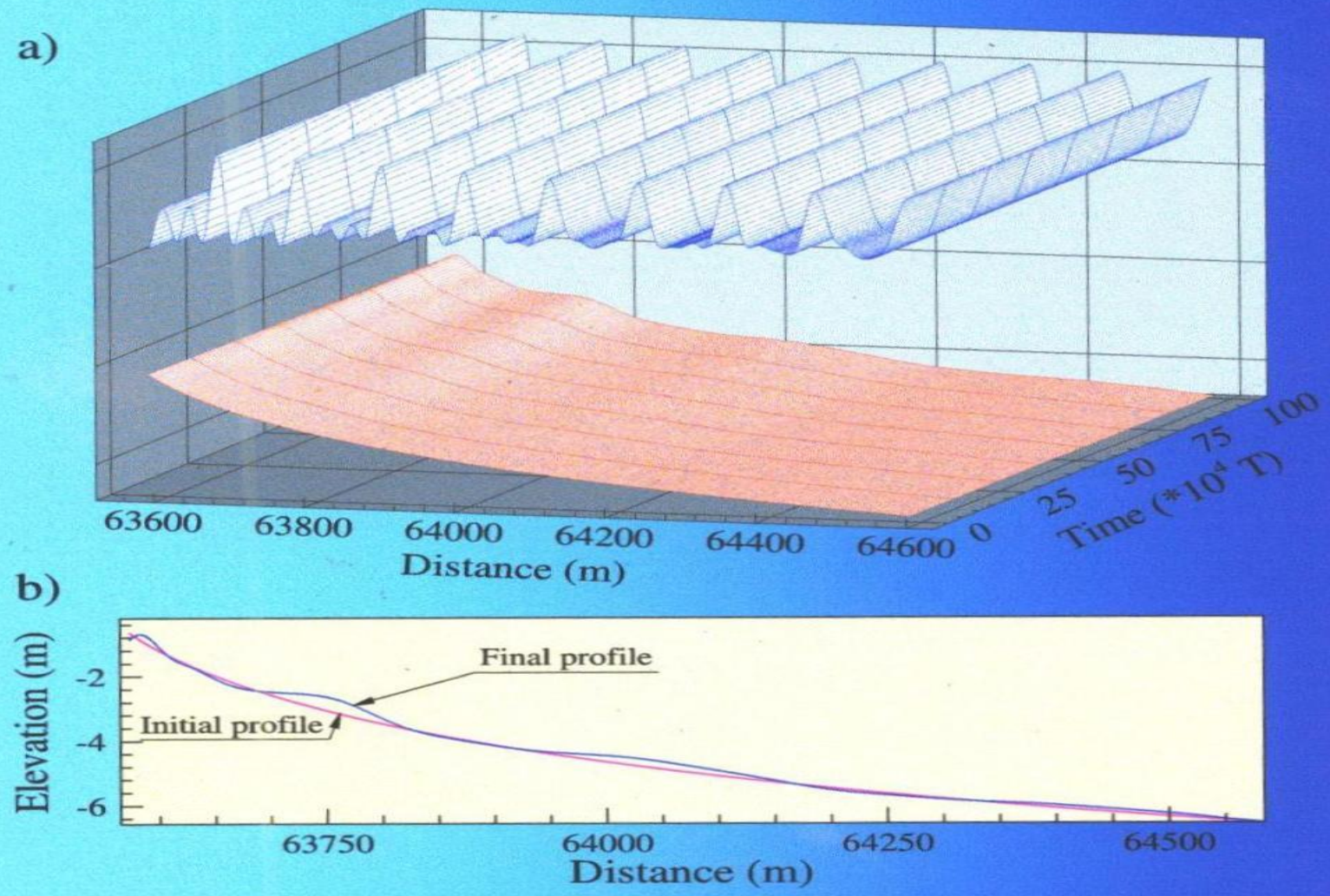

Formation of 200\400 bar system by typical T_p=15s storms

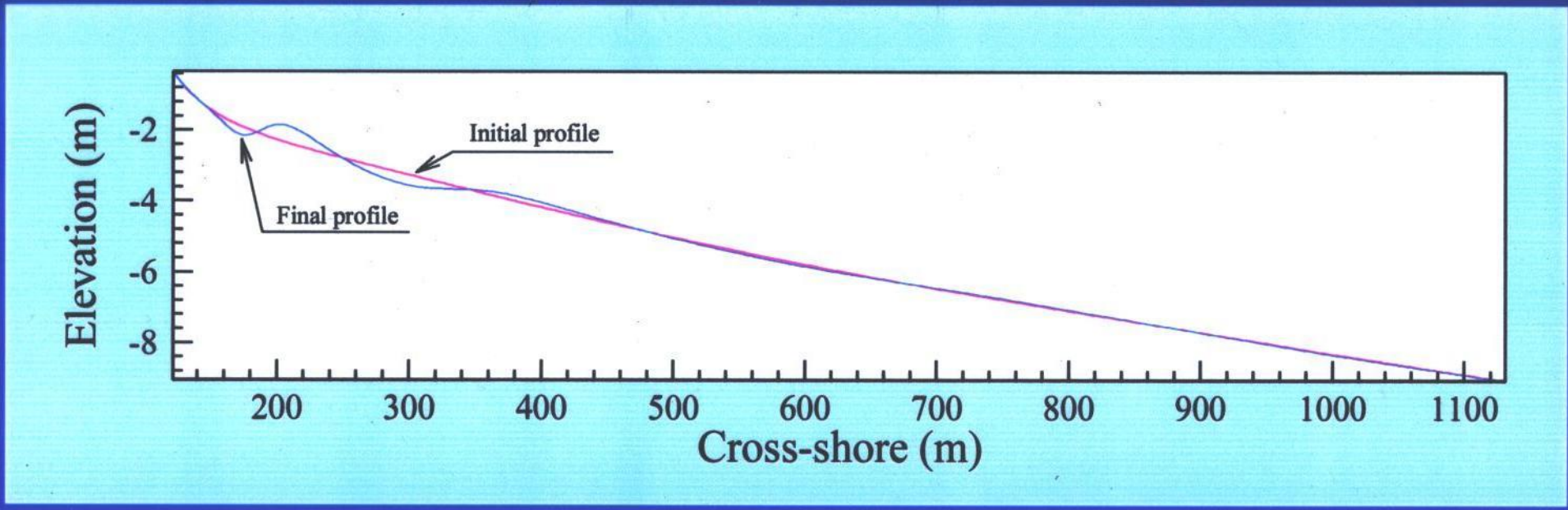

Formation of 200\400 bar system by typical Tp=15s storms

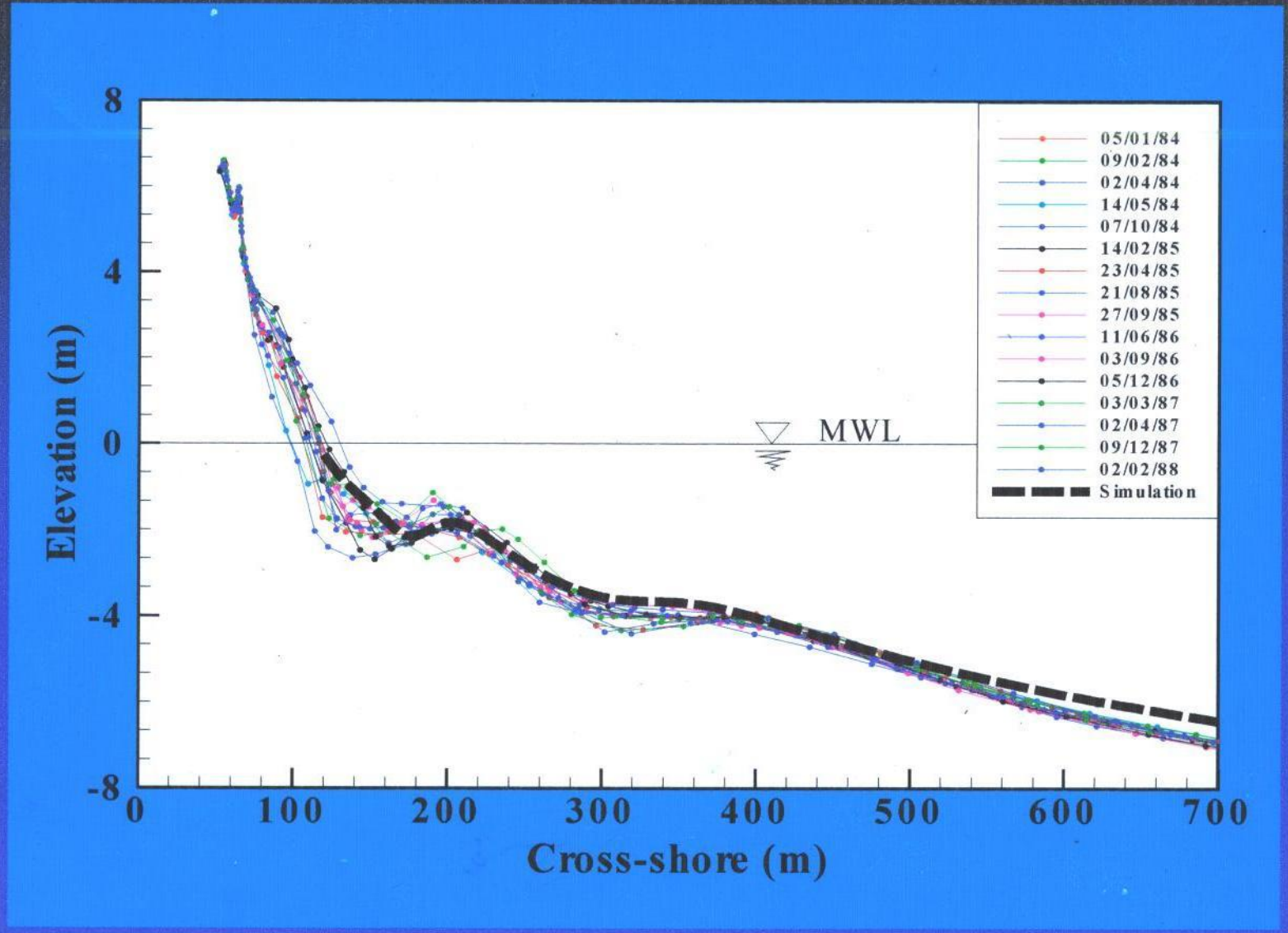

Formation of 220 bar system by moderate-amplitude waves T_p=10 s

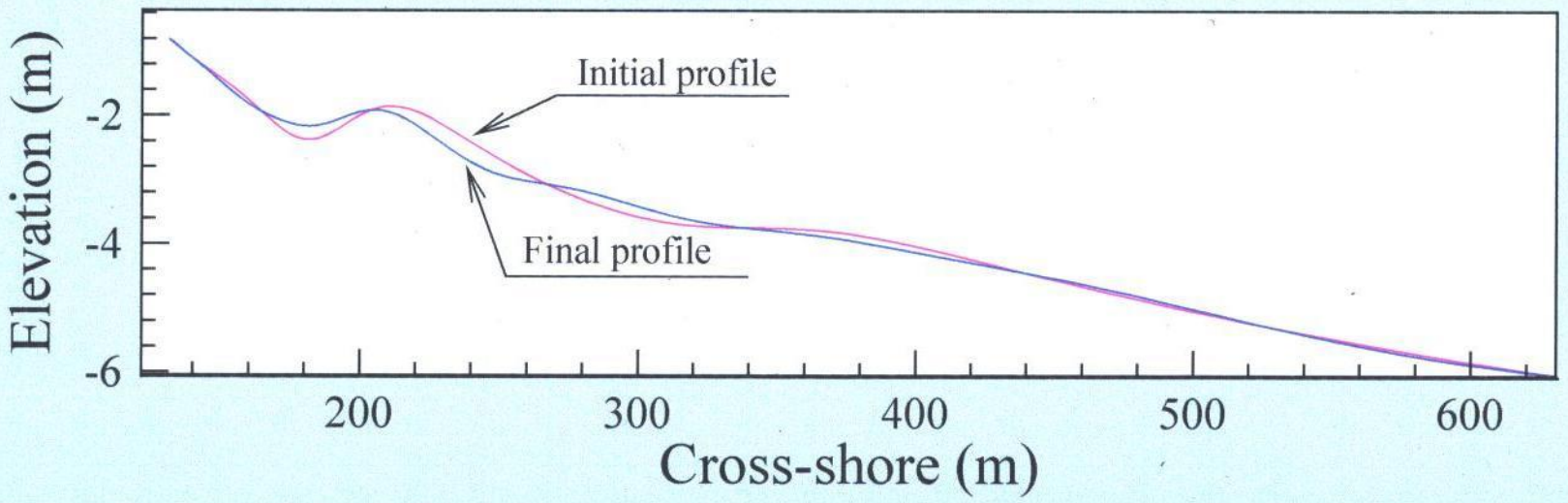

Formation of 220 bar system by moderate-amplitude waves T_p=10 s

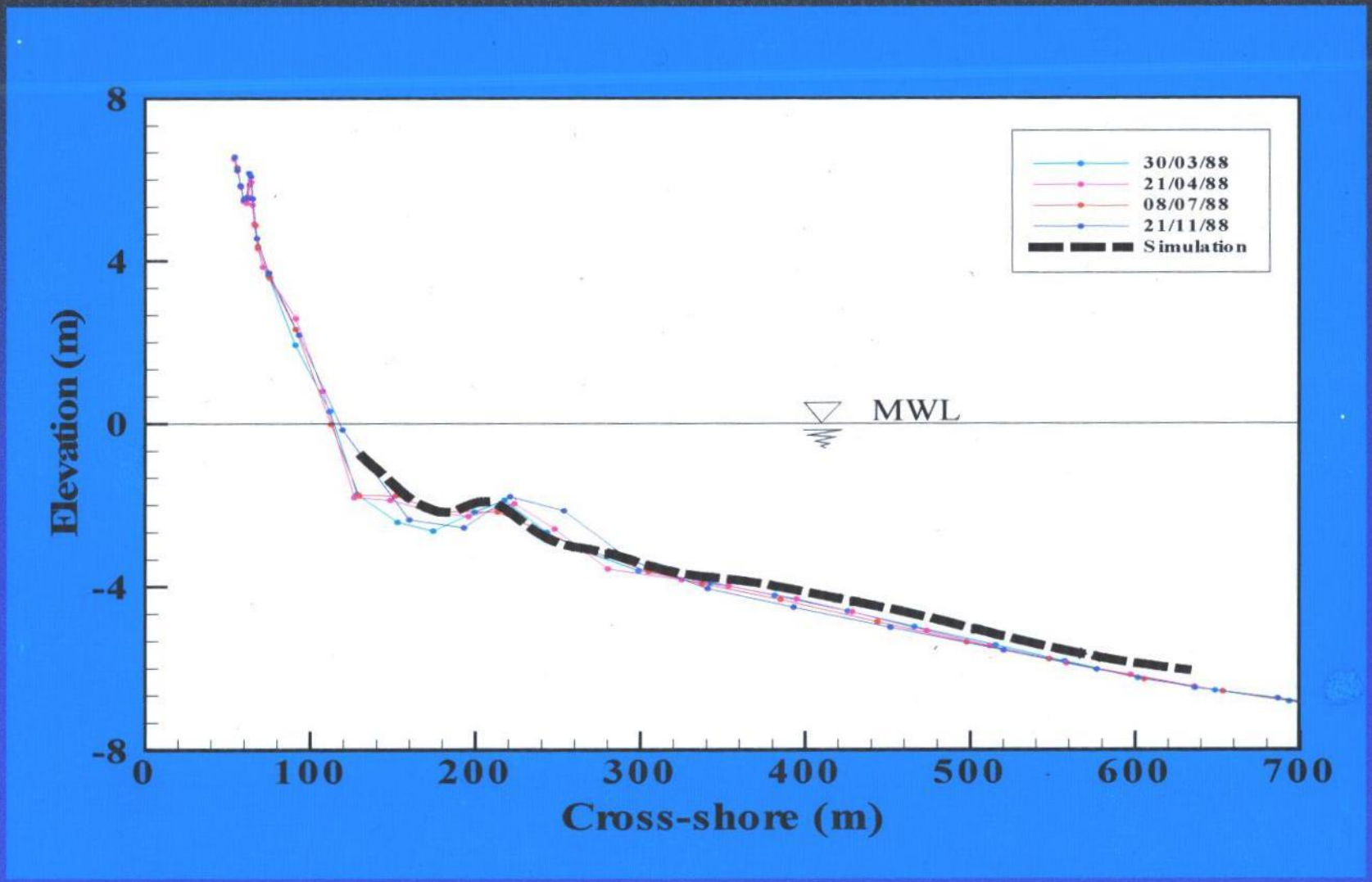

Temporal variability of bar crests localization

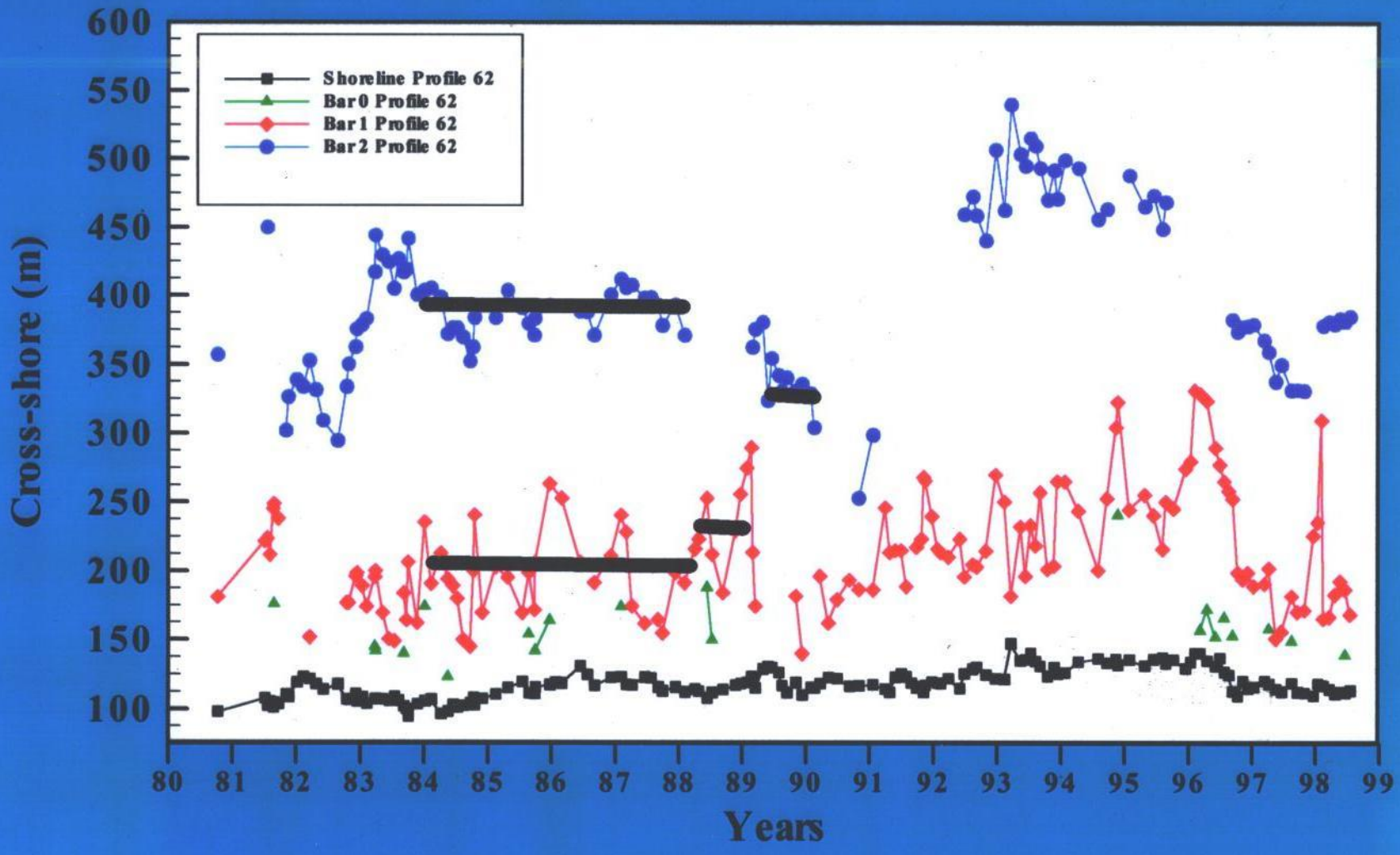

Formation of 320 one-bar system by extreme hurricane waves T_P= 20 s and MWL + 1 m

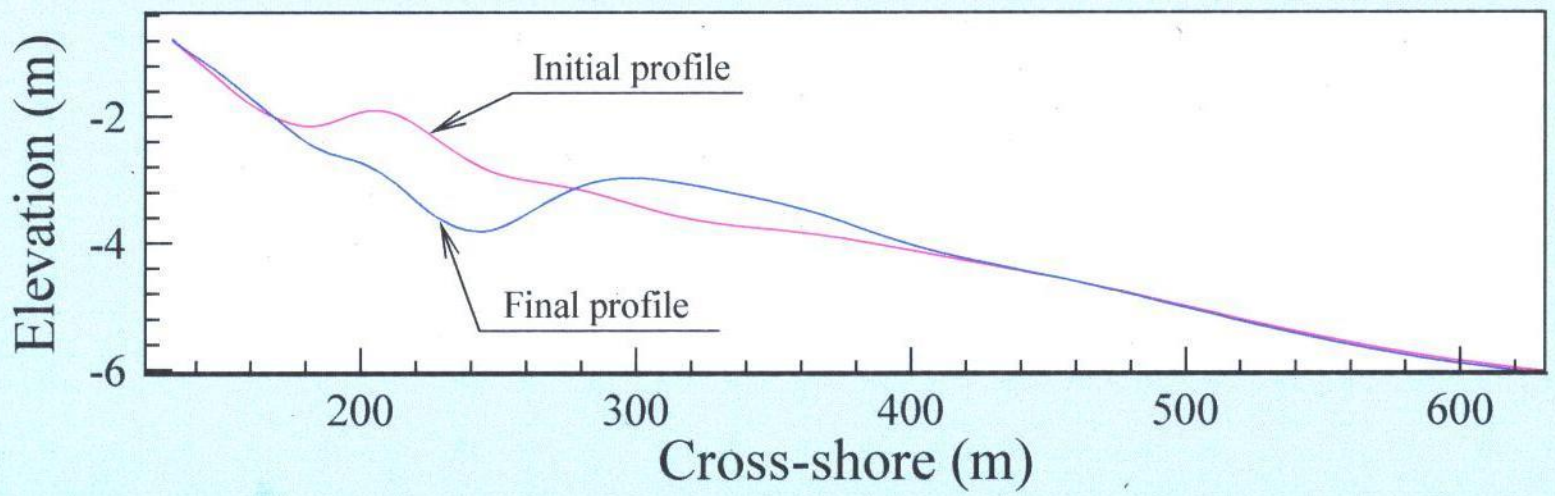

Formation of 320 one-bar system by extreme hurricane waves T_p=20 s and MWL + 1 m

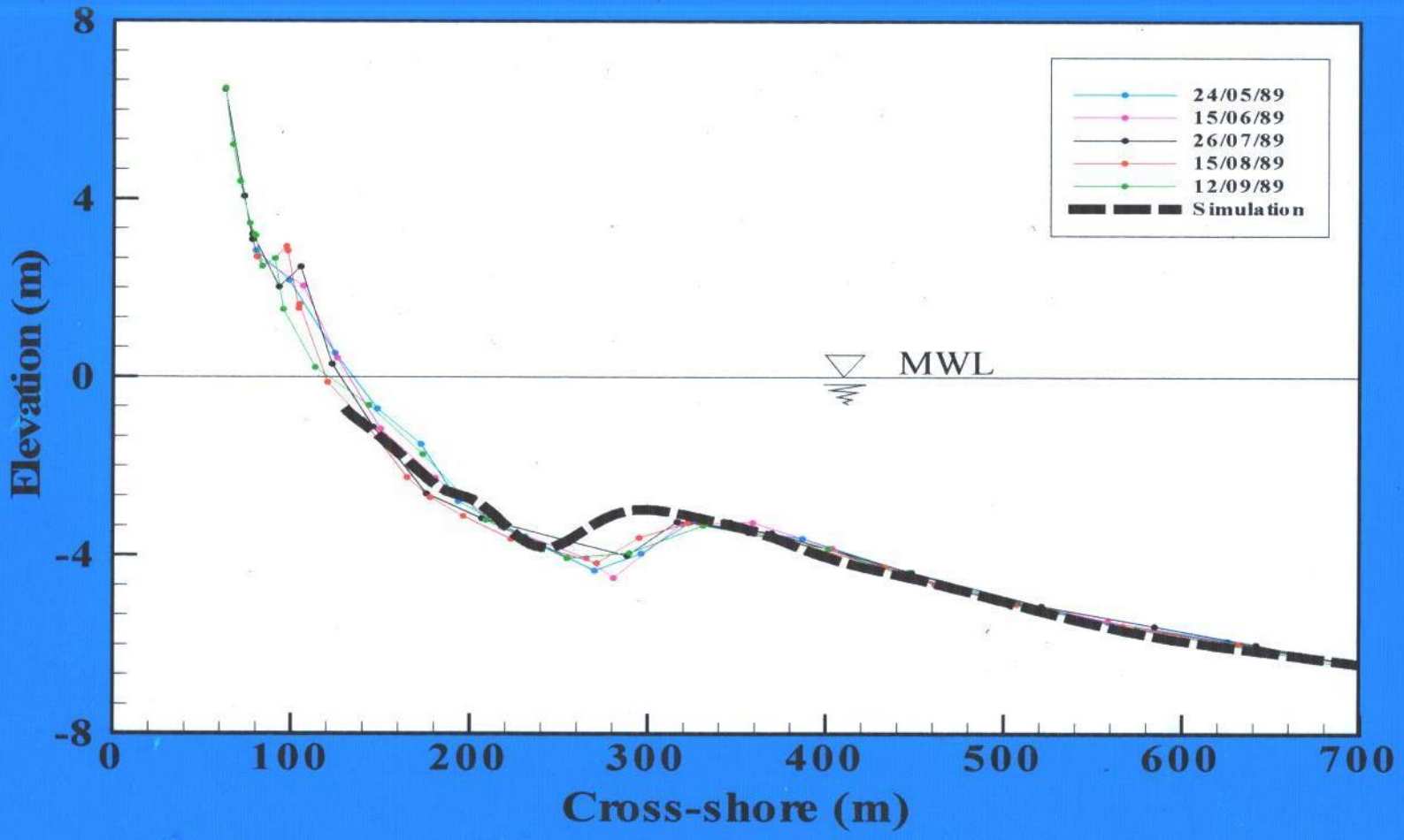

Sand Bars and Beach Protection


1/2/88


89

Sand Ridge Formation

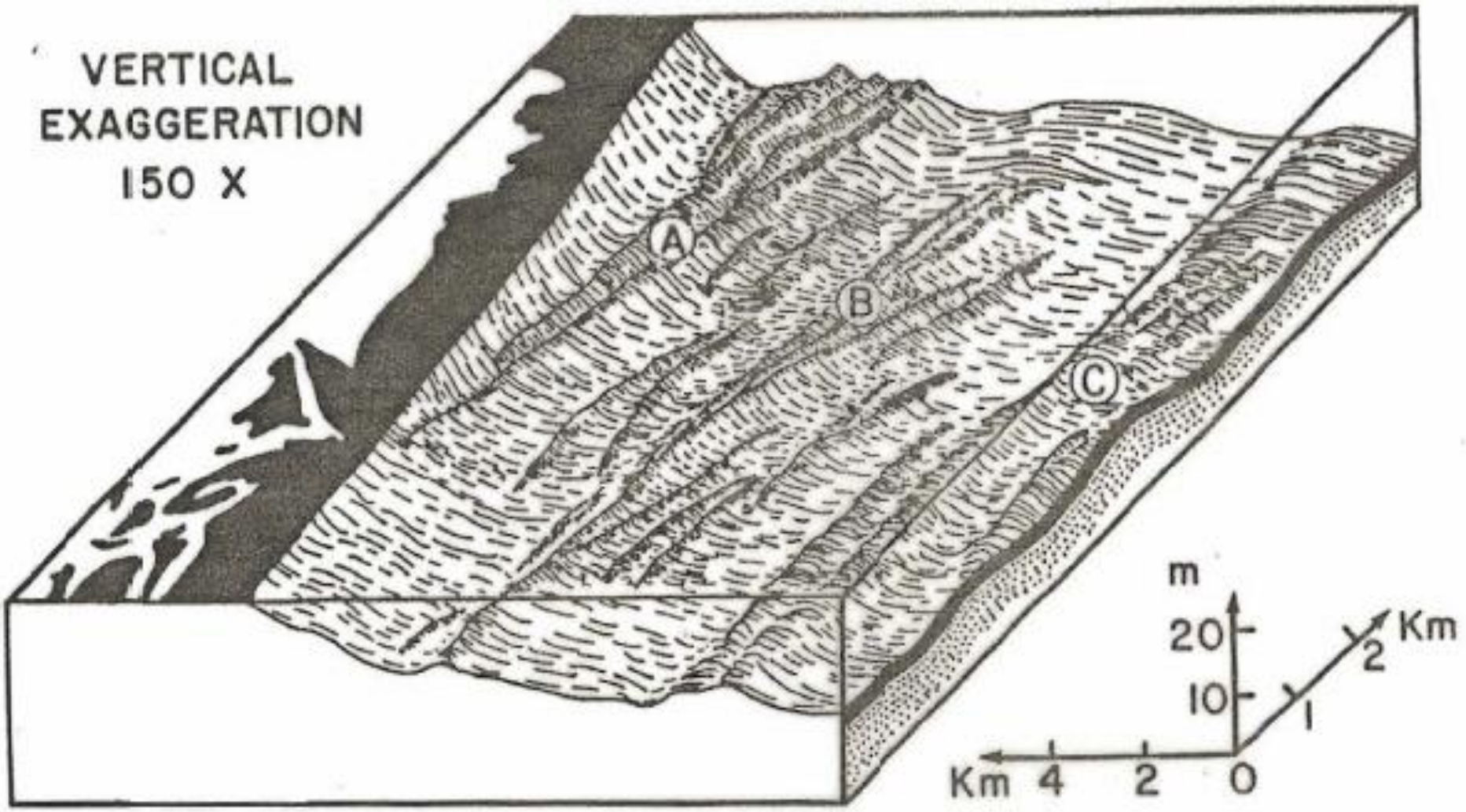
VERTICAL
EXAGGERATION
150 X
A
B
C
m
20
10
Km
2
1
Km 4
2
0

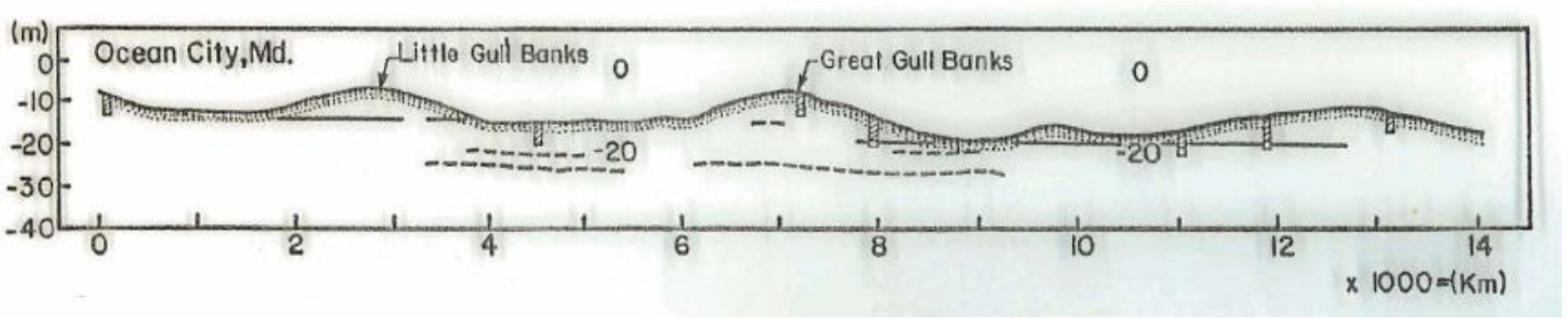
(m)
0
-10
-20
-30
-40
Ocean City,Md.
Little Gull Banks
0
Great Gull Banks
0
-20
-20
0
2
4
6
8
10
12
14
x 1000=(Km)

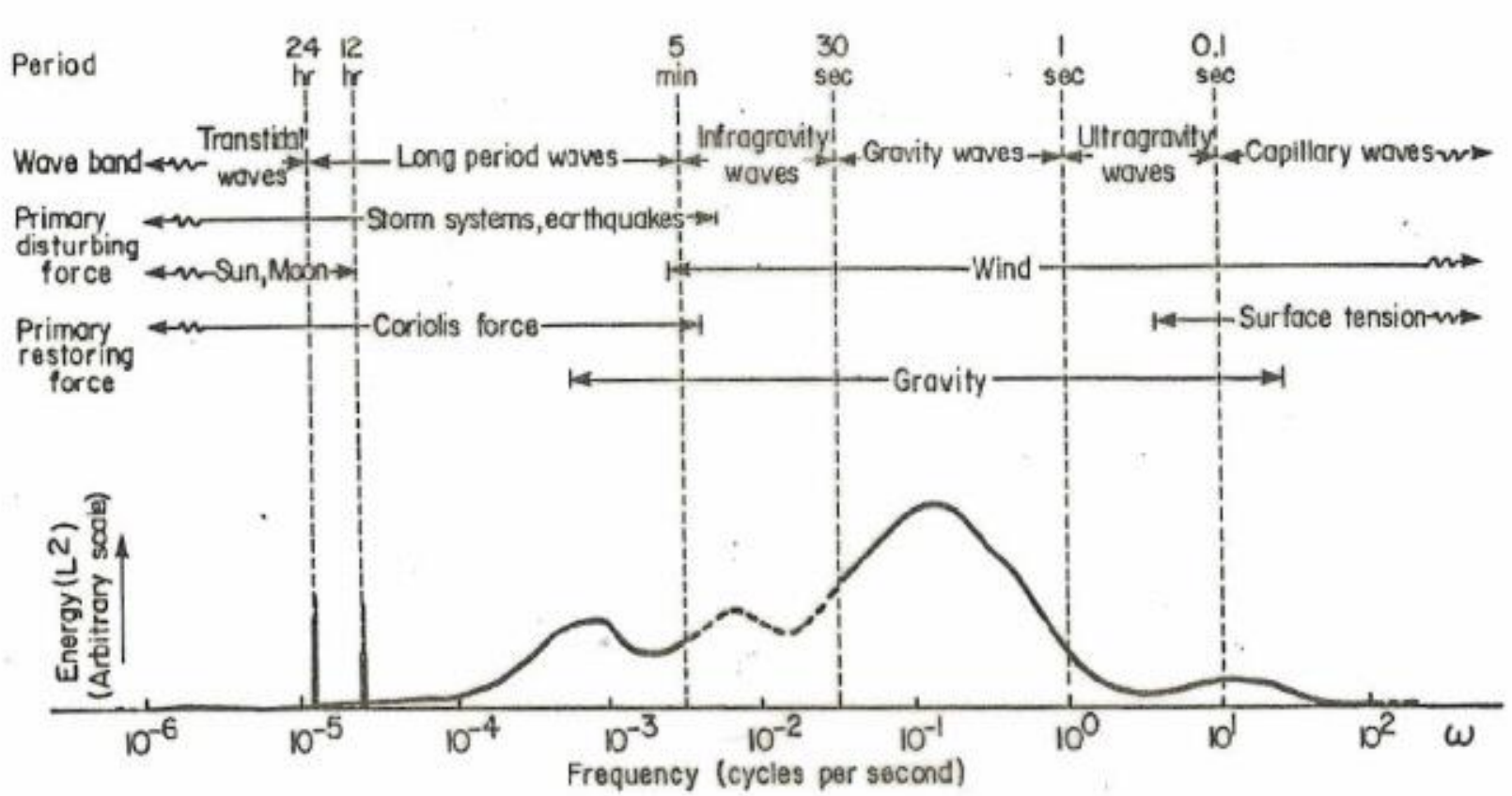
Period
24 hr
12 hr
5 min
30 sec
1 sec
0.1 sec
Wave band
Transtidal waves
Long period waves
Infragravity waves
Gravity waves
Ultragravity waves
Capillary waves
Primary disturbing force
Storm systems, earthquakes
Sun, Moon
Wind
Primary restoring force
Coriolis force
Surface tension
Gravity
Energy (L2) (Arbitrary scale)
10^{-6}
10^{-5}
10^{-4}
10^{-3}
10^{-2}
10^{-1}
10^{0}
10^{1}
10^{2}
ω
Frequency (cycles per second)

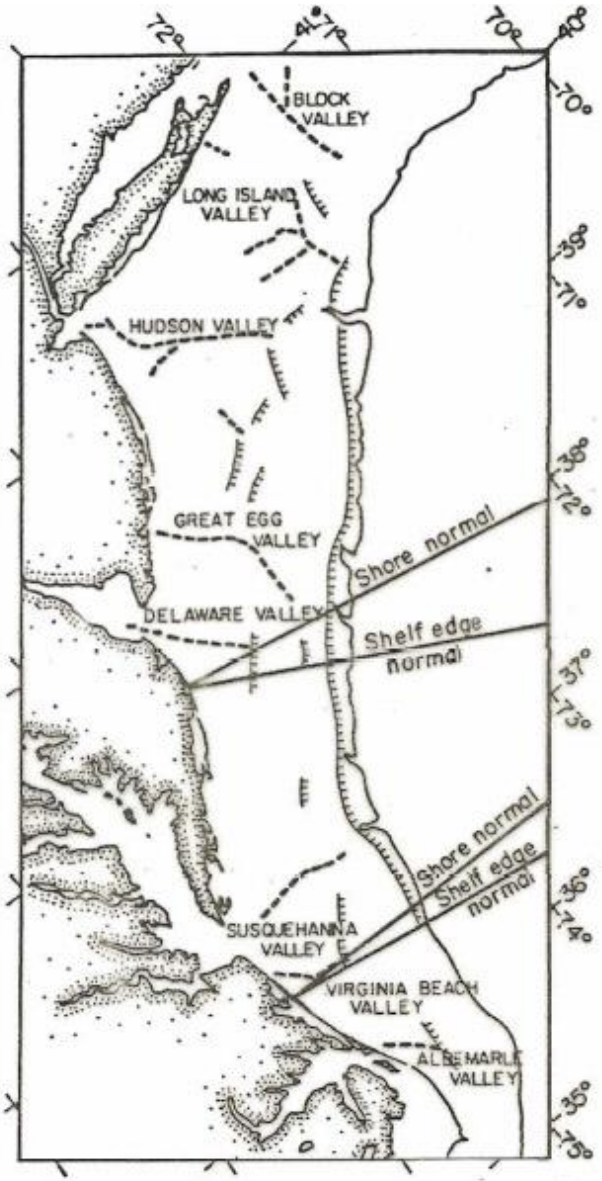
72°
41°
70°
BLOCK VALLEY
LONG ISLAND VALLEY
HUDSON VALLEY
GREAT EGG VALLEY
DELAWARE VALLEY
Shore normal
Shelf edge normal
SUSQUEHANNA VALLEY
Shore normal
Shelf edge normal
VIRGINIA BEACH VALLEY
ALBEMARLE VALLEY
40°
39°
38°
37°
36°
35°
70°
71°
72°
73°
74°
75°

FALSE CAPE. 007

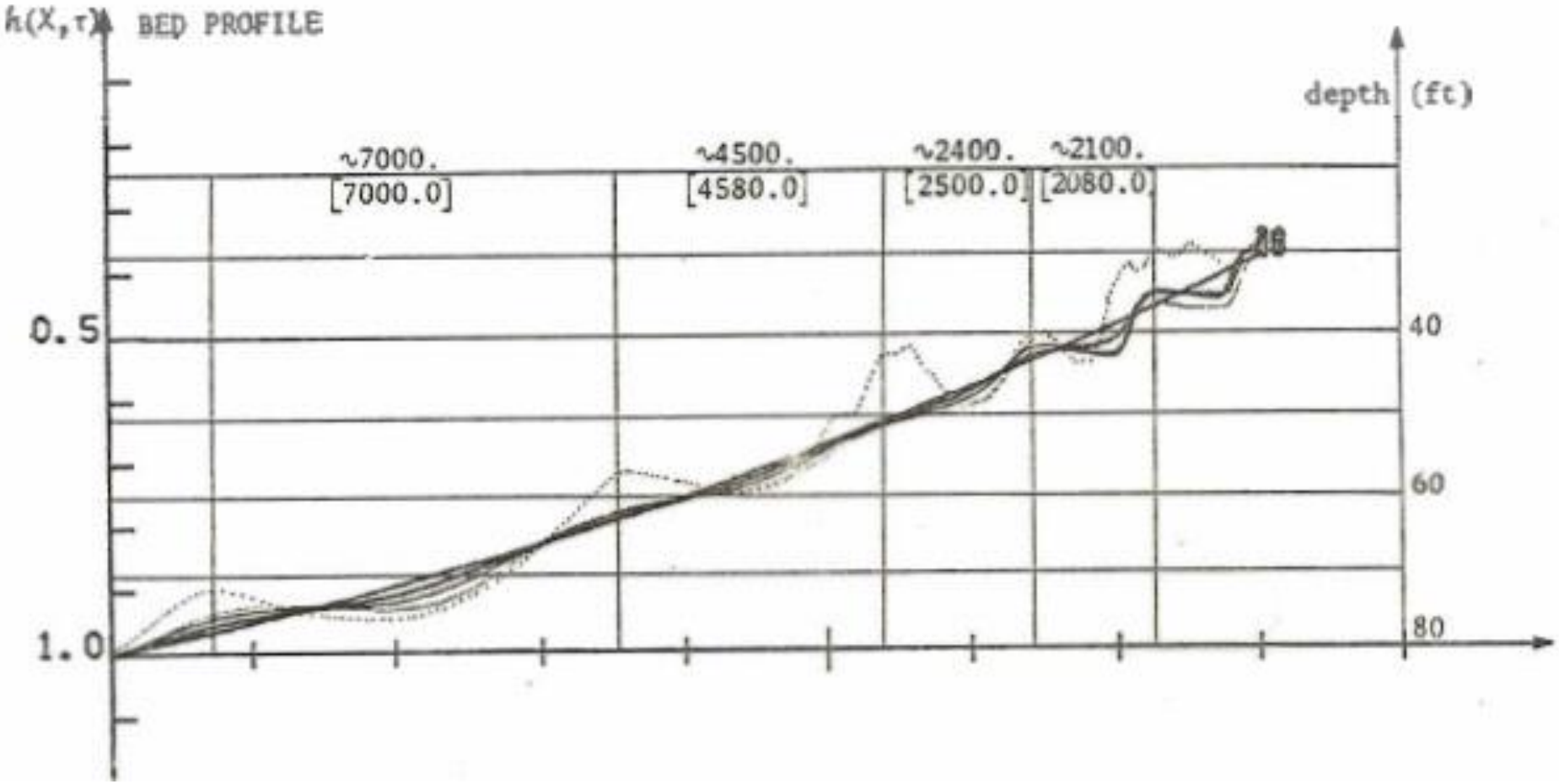

OCEAN CITY-.004

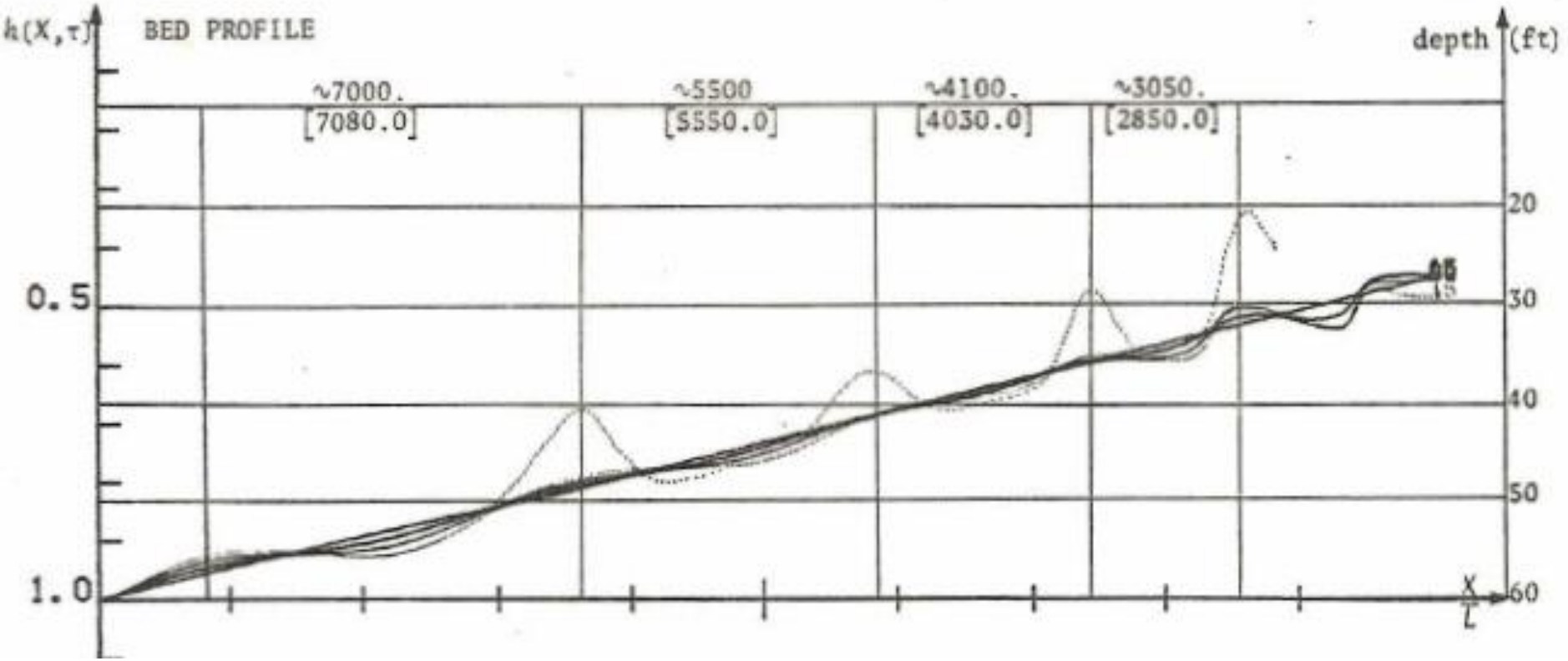

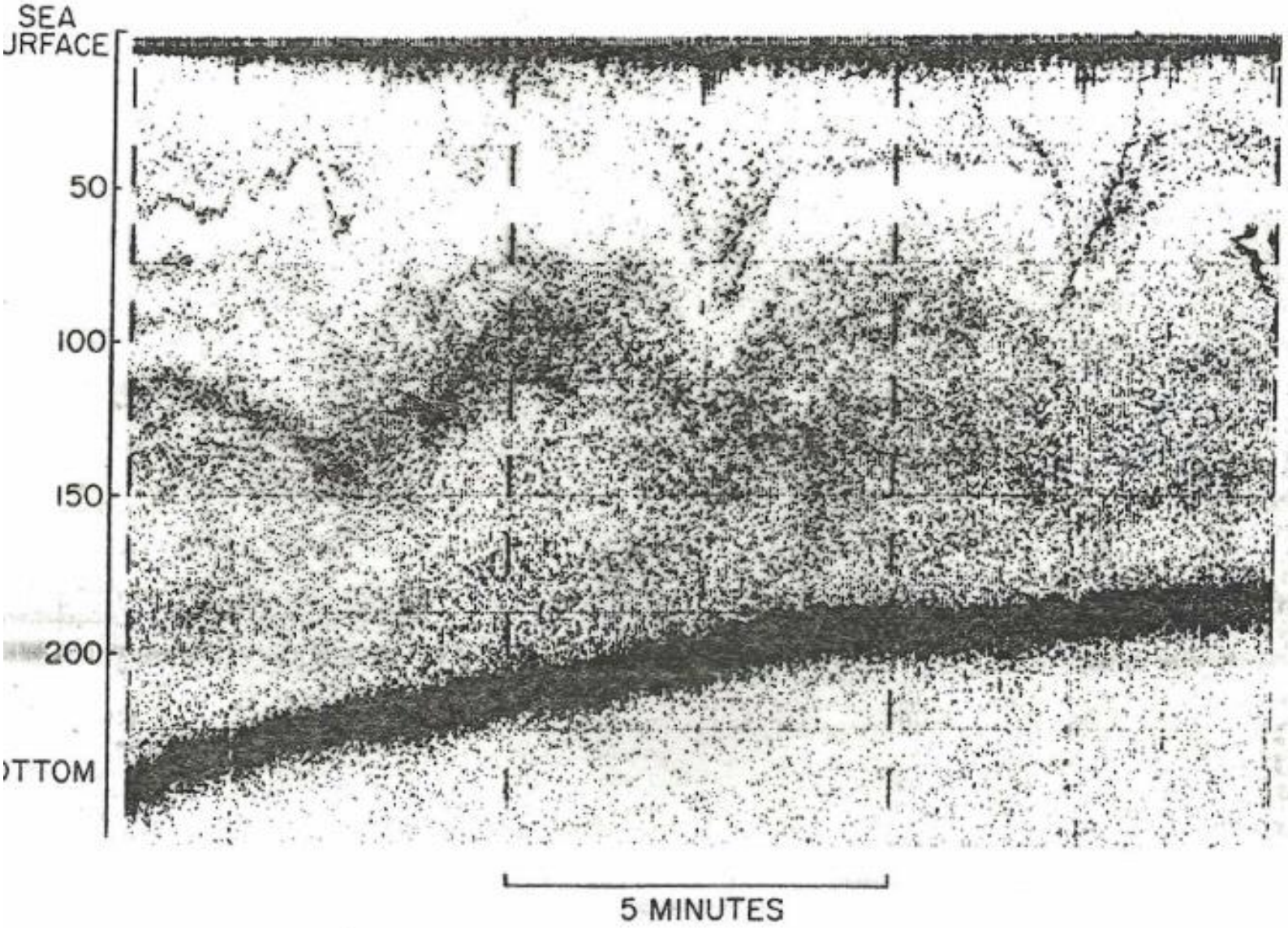

Fig. 2. Twelve-kHz sounder record near the shelf break showing two internal solitons (prominently visible around 50 m depth) inshore of an internal depression. Ship is traveling at 4.2 ms^{-1}.

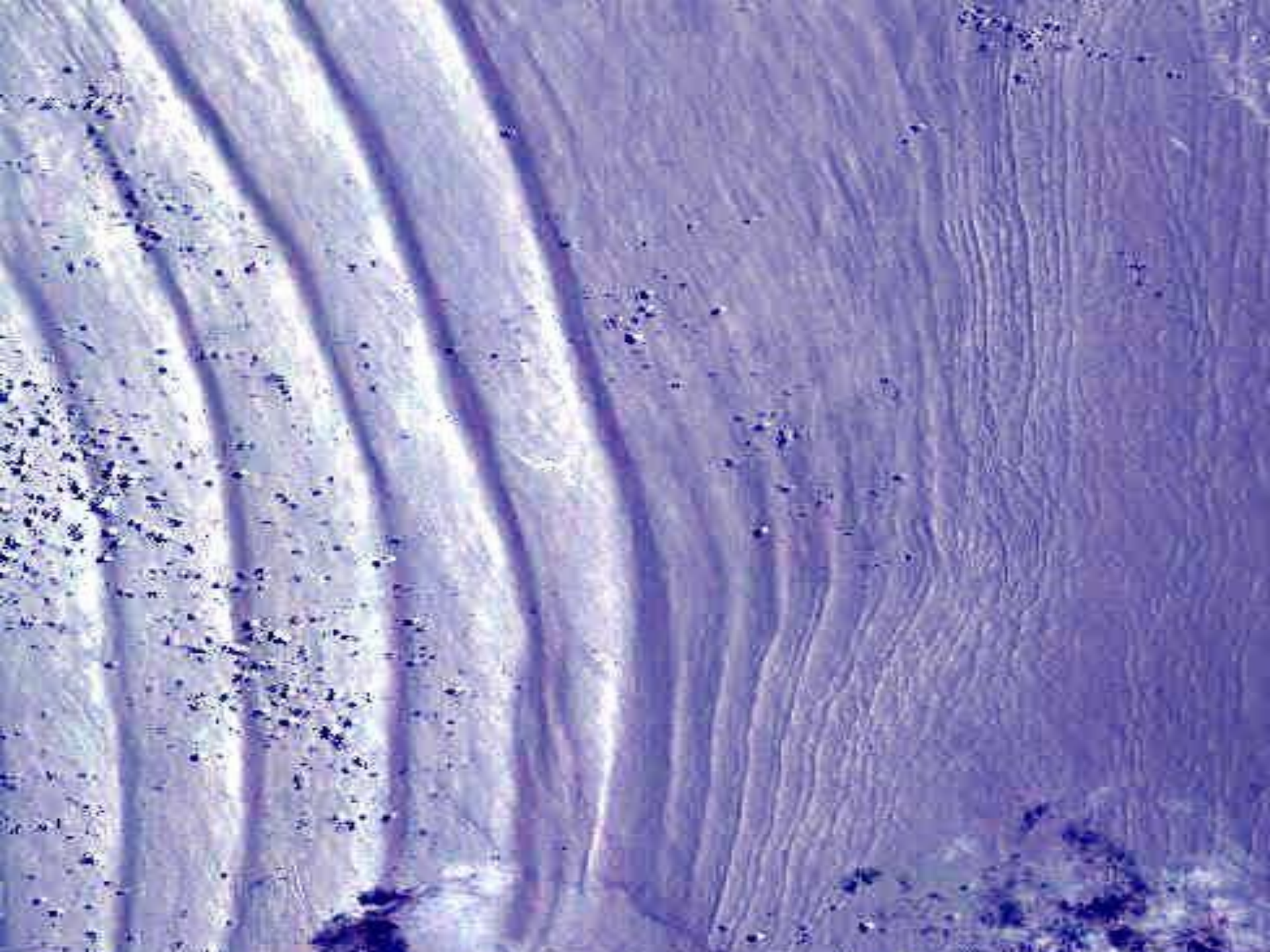

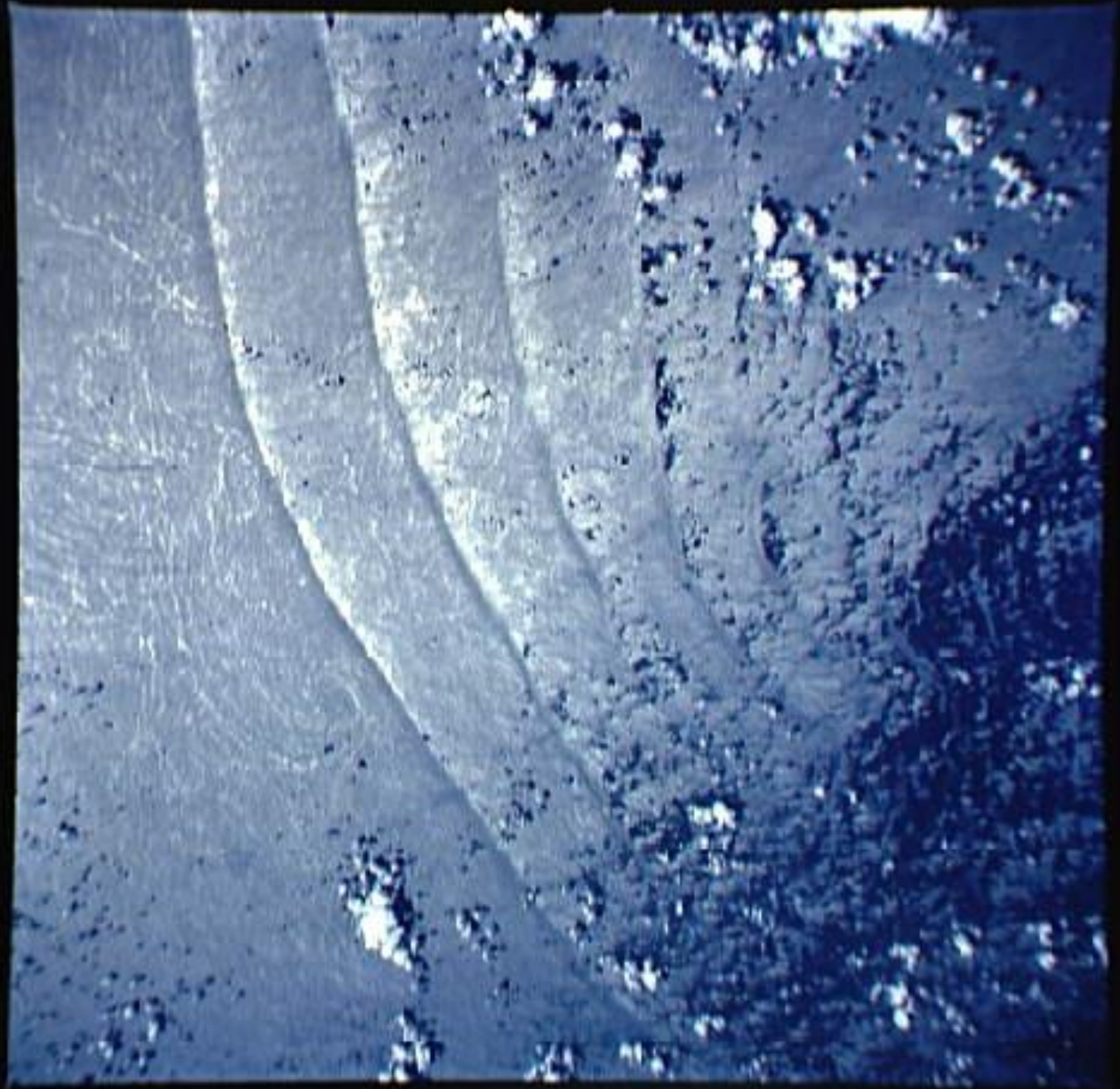

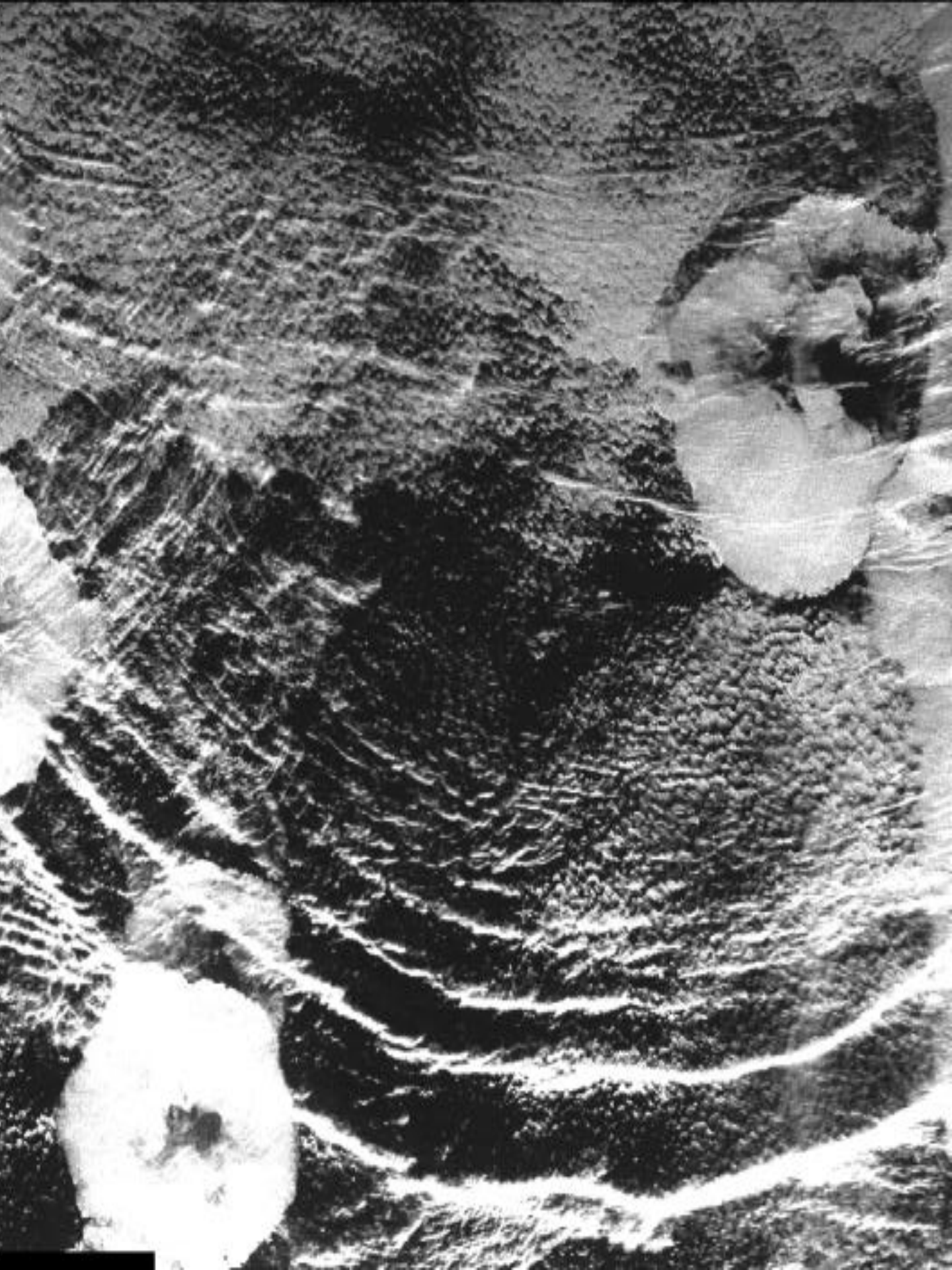

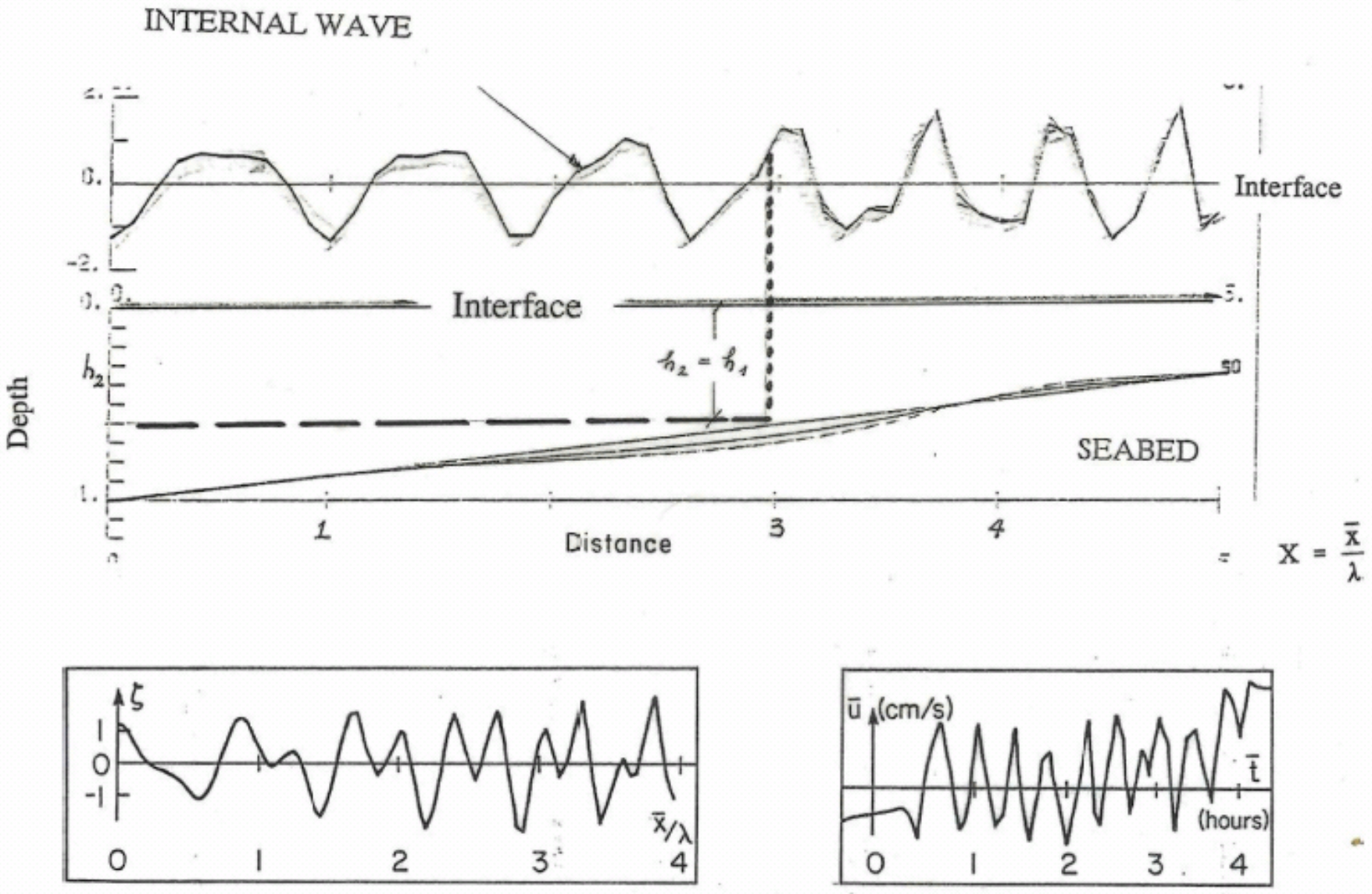
INTERNAL WAVE
Interface
Interface
$h_2 = h_1$
SEABED
Depth
Distance
1
3
4
$X = \frac{\bar{x}}{\lambda}$
ζ
1
0
-1
$\bar{x}/\lambda$
0
1
2
3
4
$\bar{u}$ (cm/s)
$\bar{t}$
(hours)
0
1
2
3
4

SABLE ISLAND

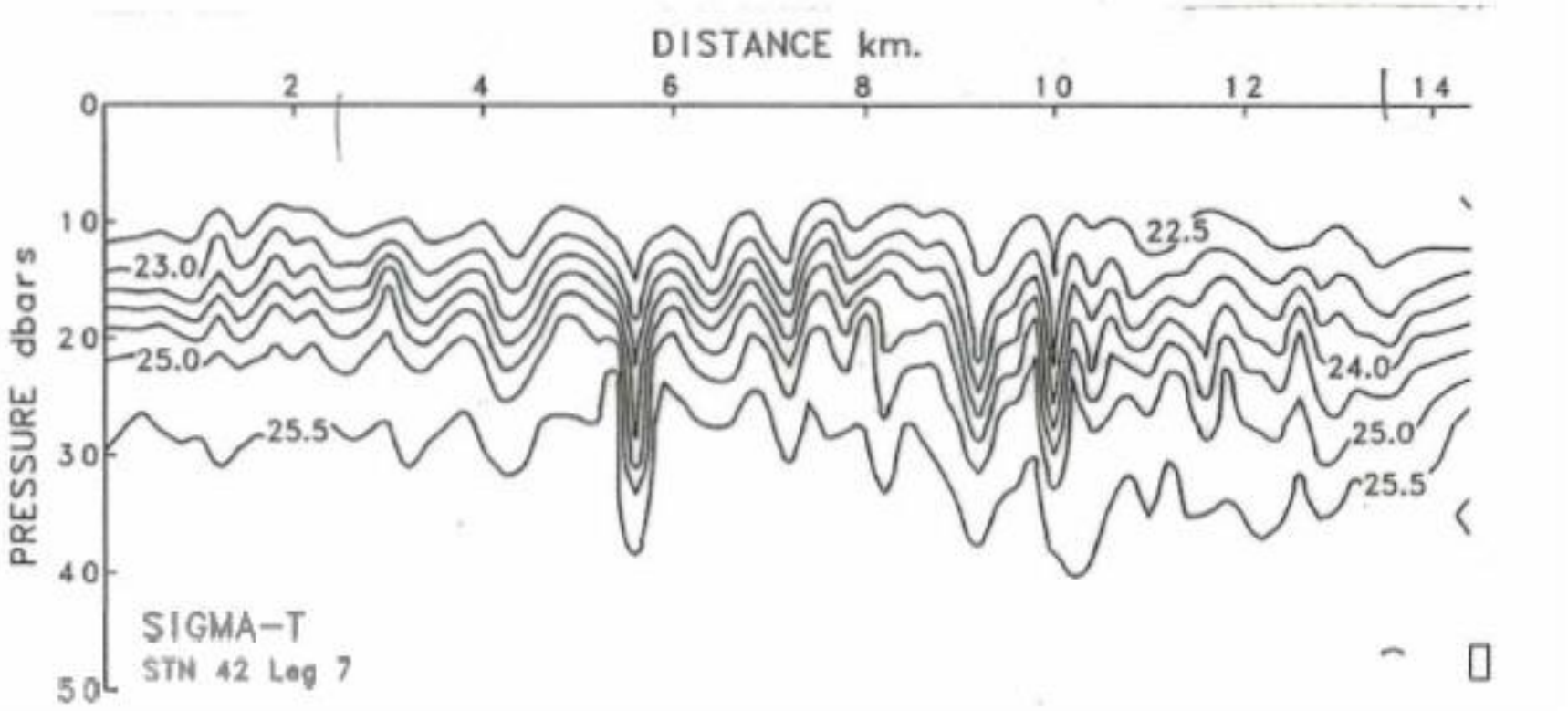

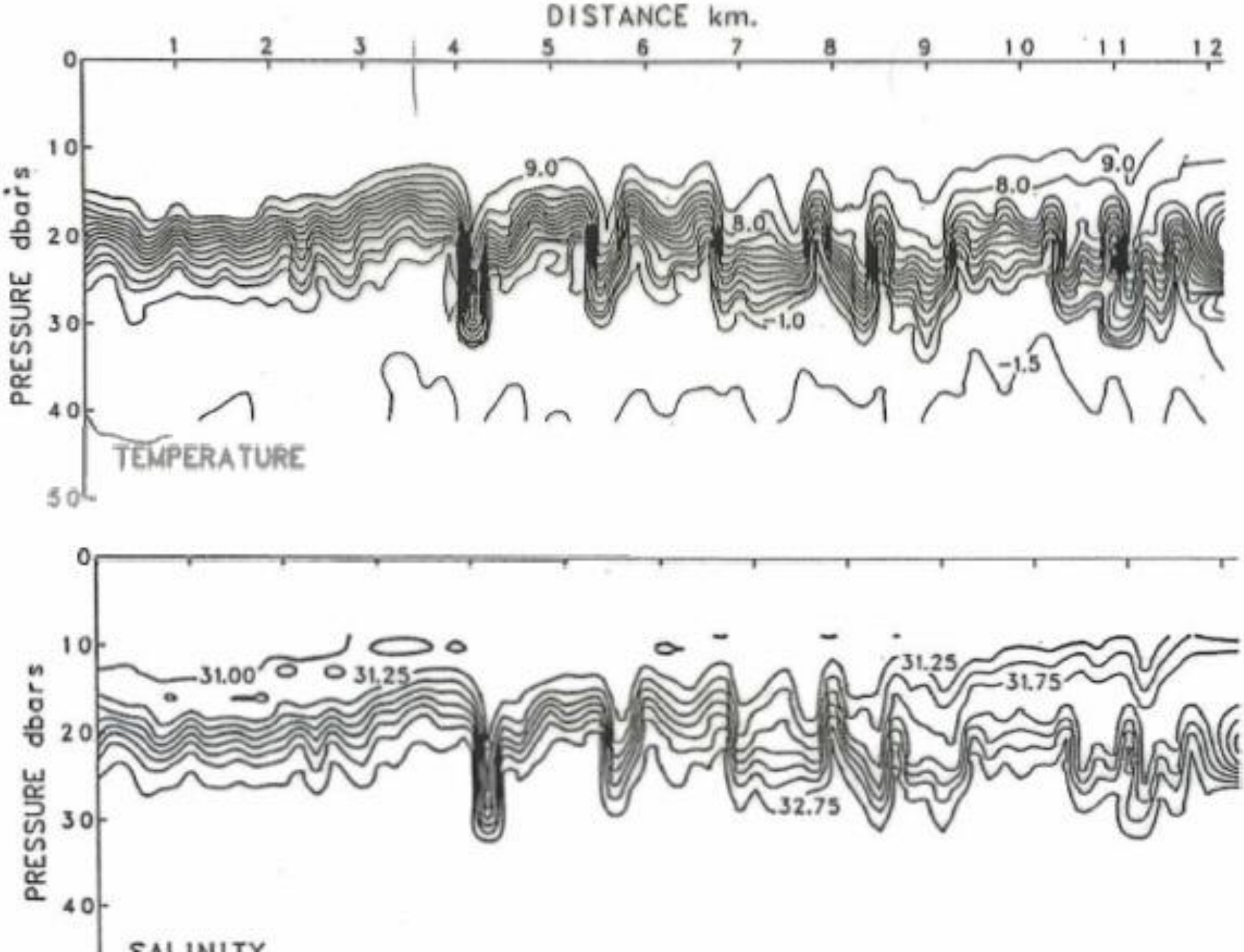
DISTANCE km.
1
2
3
4
5
6
7
8
9
10
11
12
0
10
20
30
40
50
PRESSURE dbars
9.0
8.0
9.0
8.0
1.0
1.5
TEMPERATURE
0
10
20
30
40
PRESSURE dbars
31.00
31.25
31.25
31.75
32.75
SALINITY

ORMATION OF SAND RIDGES : SABLE ISLAND

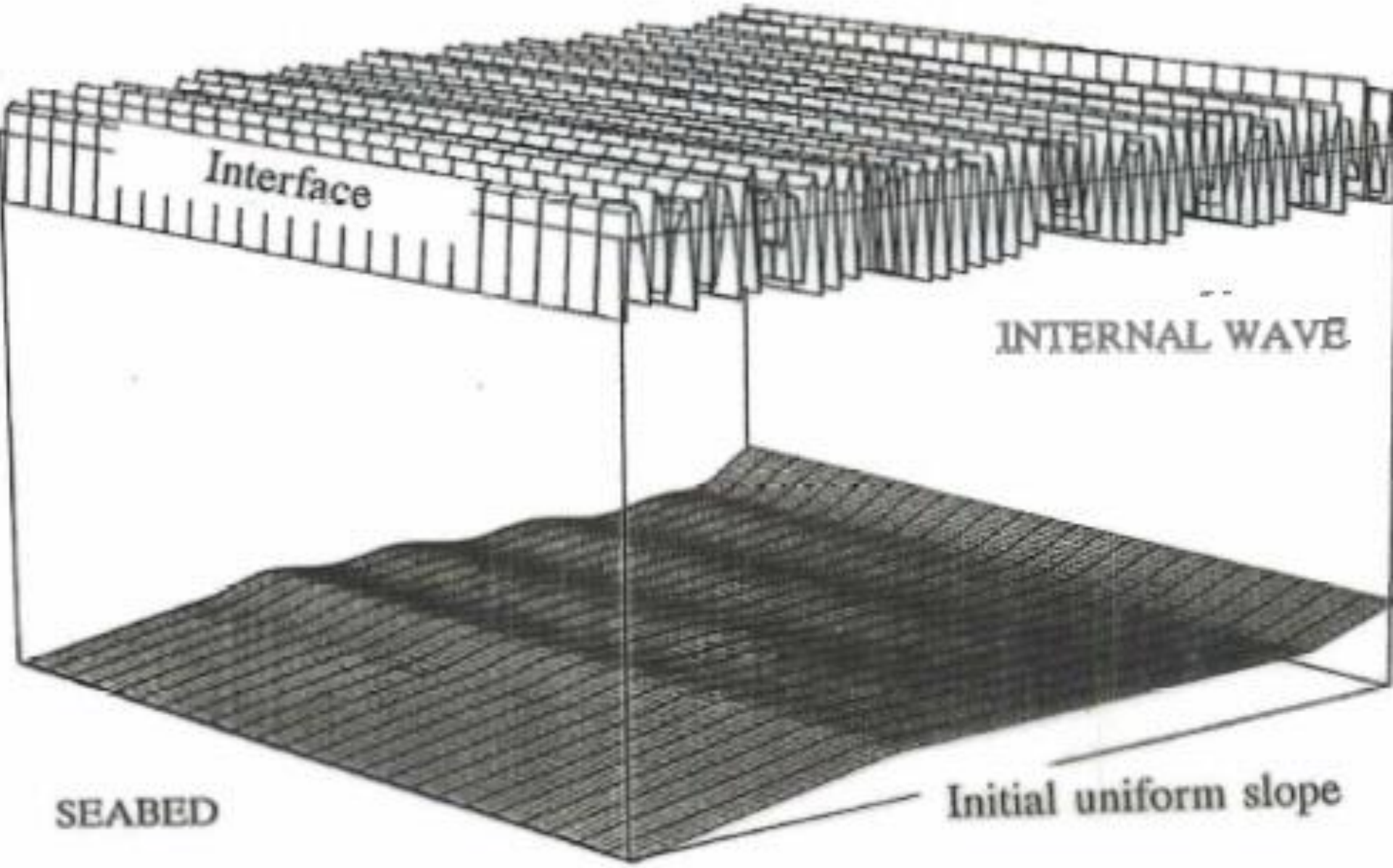

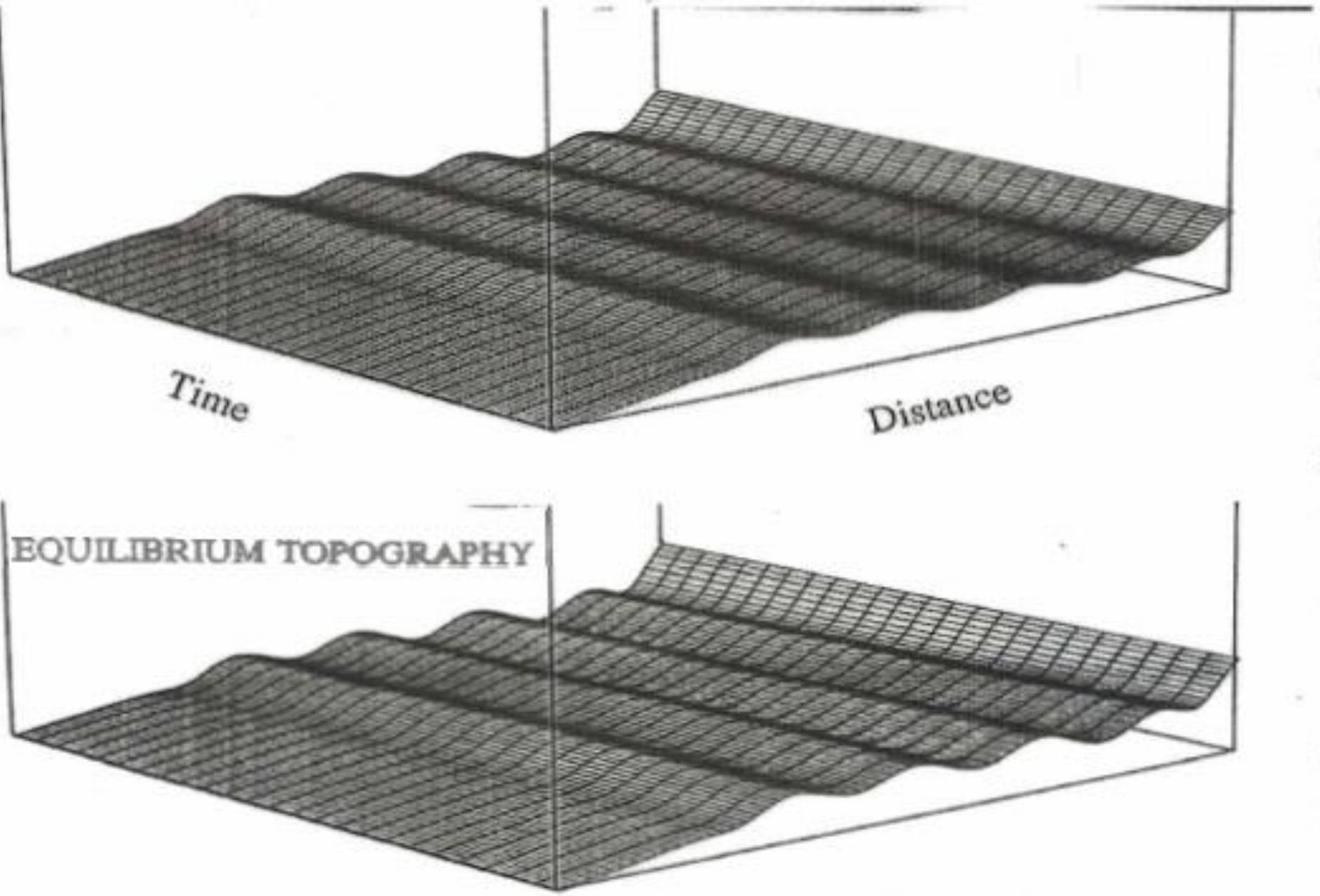
Time
Distance
EQUILIBRIUM TOPOGRAPHY

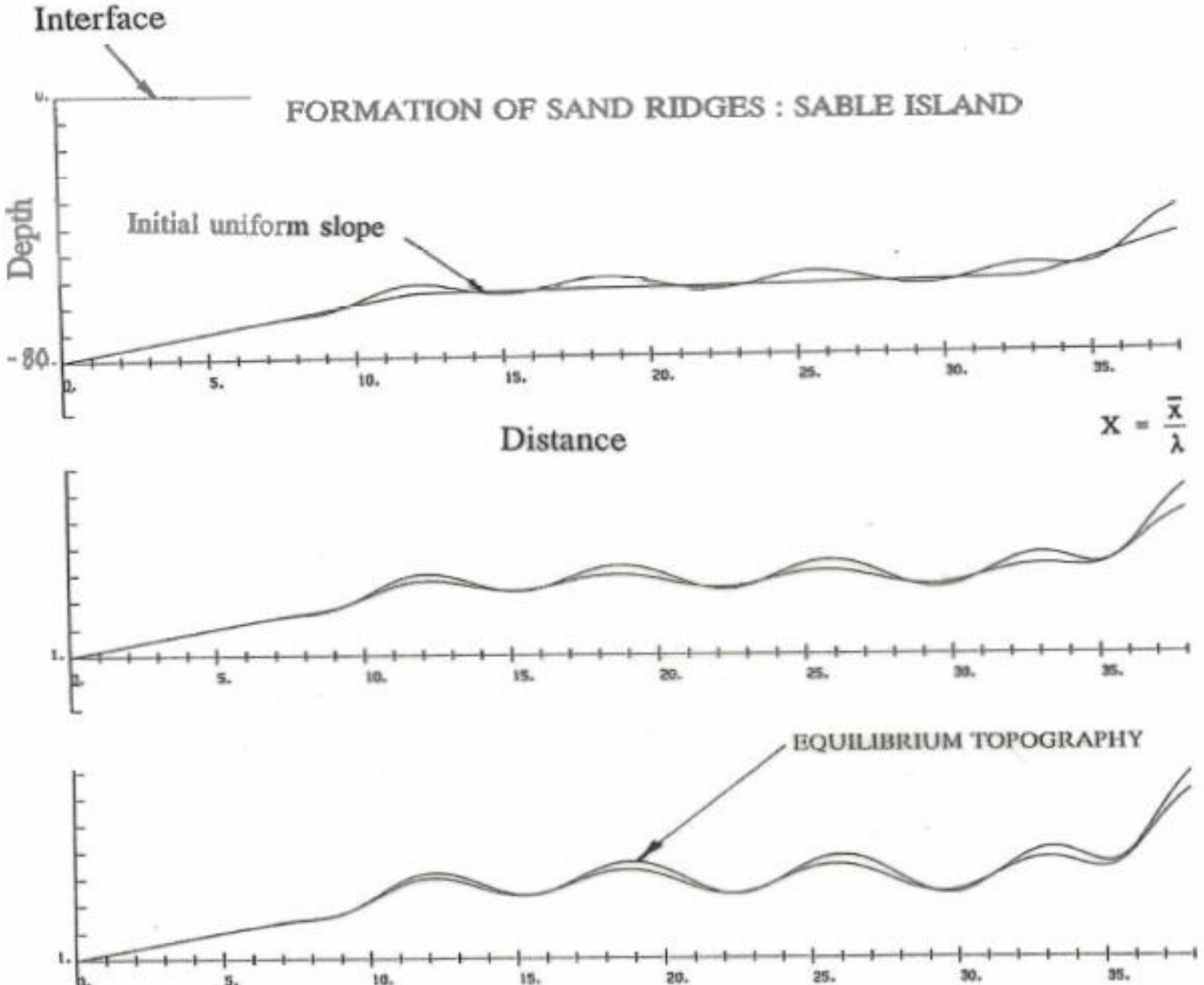
Interface
FORMATION OF SAND RIDGES : SABLE ISLAND
Depth
Initial uniform slope
-80.
0.
5.
10.
15.
20.
25.
30.
35.
Distance
X = x̄/λ
1.
EQUILIBRIUM TOPOGRAPHY

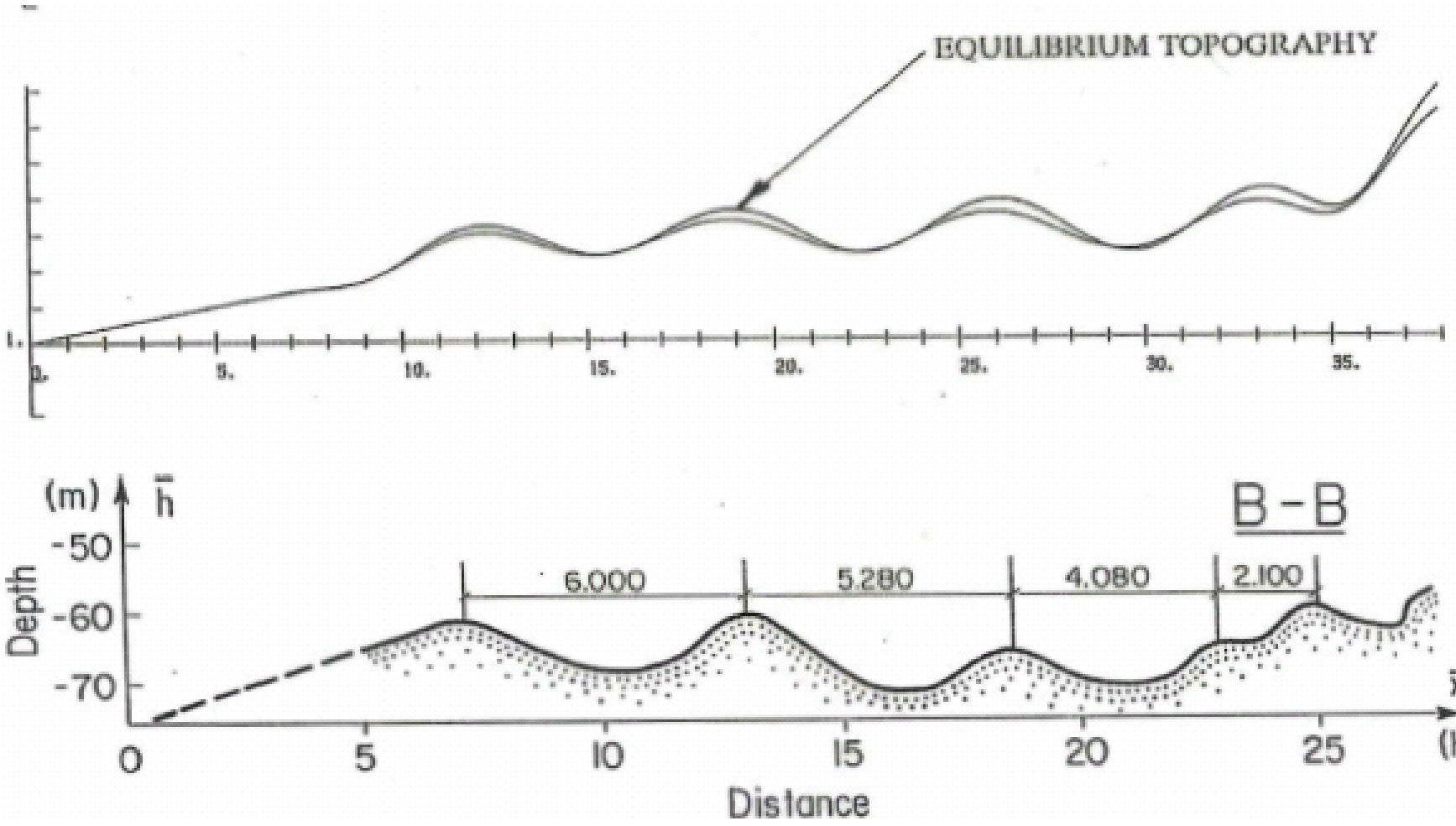
EQUILIBRIUM TOPOGRAPHY
5.
10.
15.
20.
25.
30.
35.
(m)
h̄
B - B
-50
-60
-70
Depth
6.000
5.280
4.080
2.100
x̄
0
5
10
15
20
25
(Km)
Distance

FORMATION OF SAND RIDGES : GRAND BANKS OF NFL

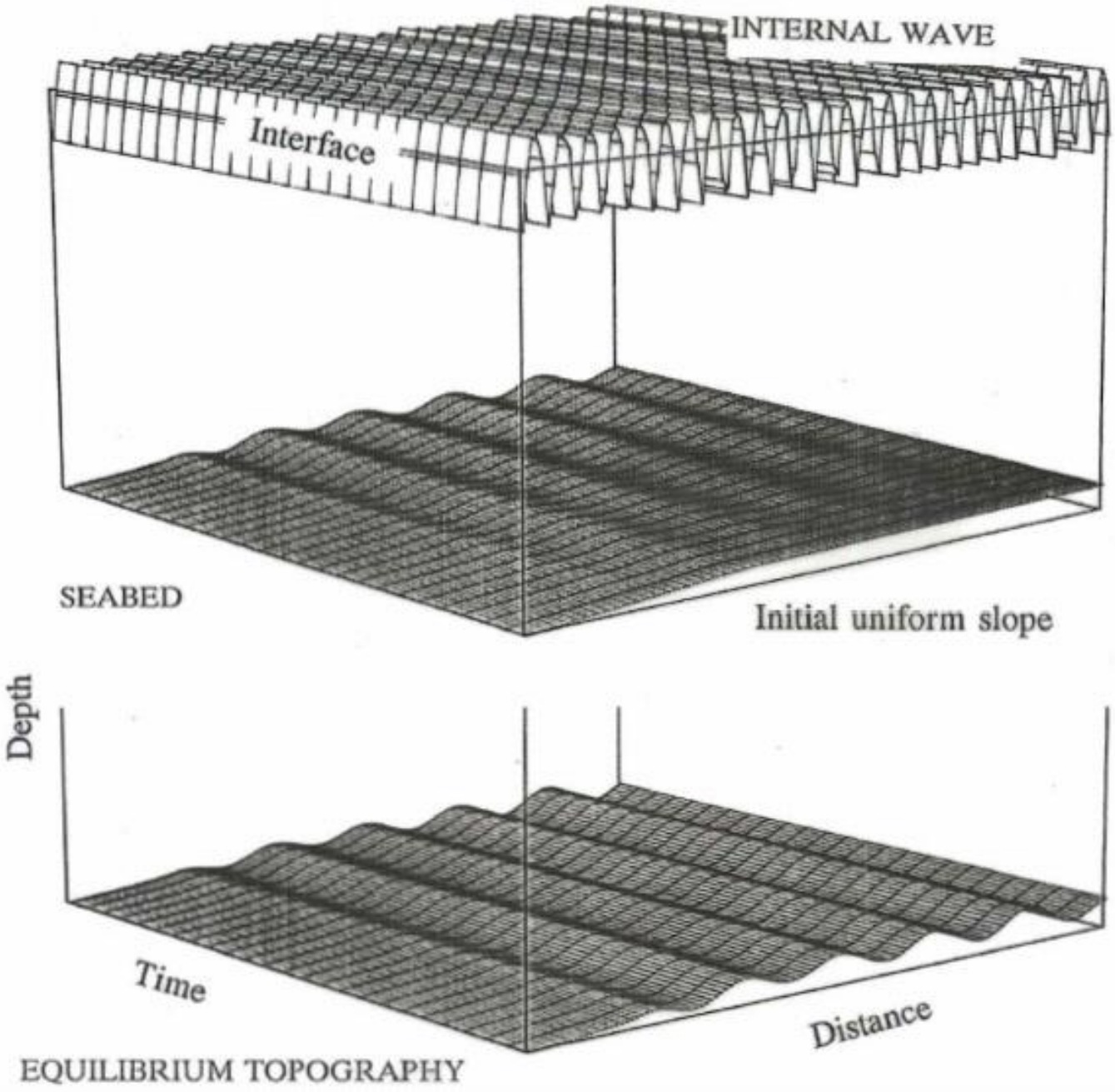

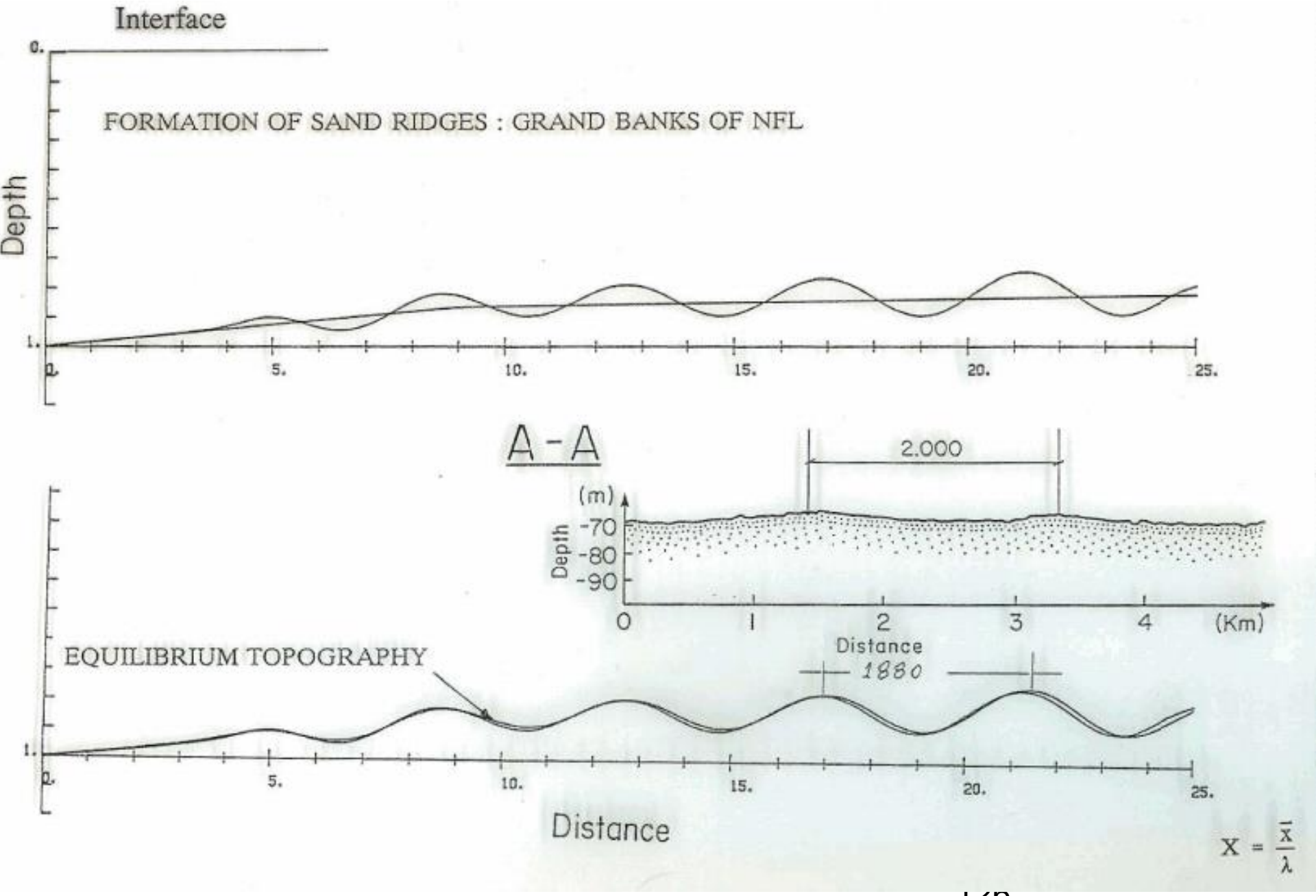
Interface
FORMATION OF SAND RIDGES : GRAND BANKS OF NFL
Depth
0.
1.
0.
5.
10.
15.
20.
25.
A - A
2.000
(m)
-70
-80
-90
Depth
0
1
2
3
4
(Km)
Distance
1880
EQUILIBRIUM TOPOGRAPHY
Distance
X = x̄/λ

FORMATION OF SAND RIDGES : AUSTRALIA - PACIFIC

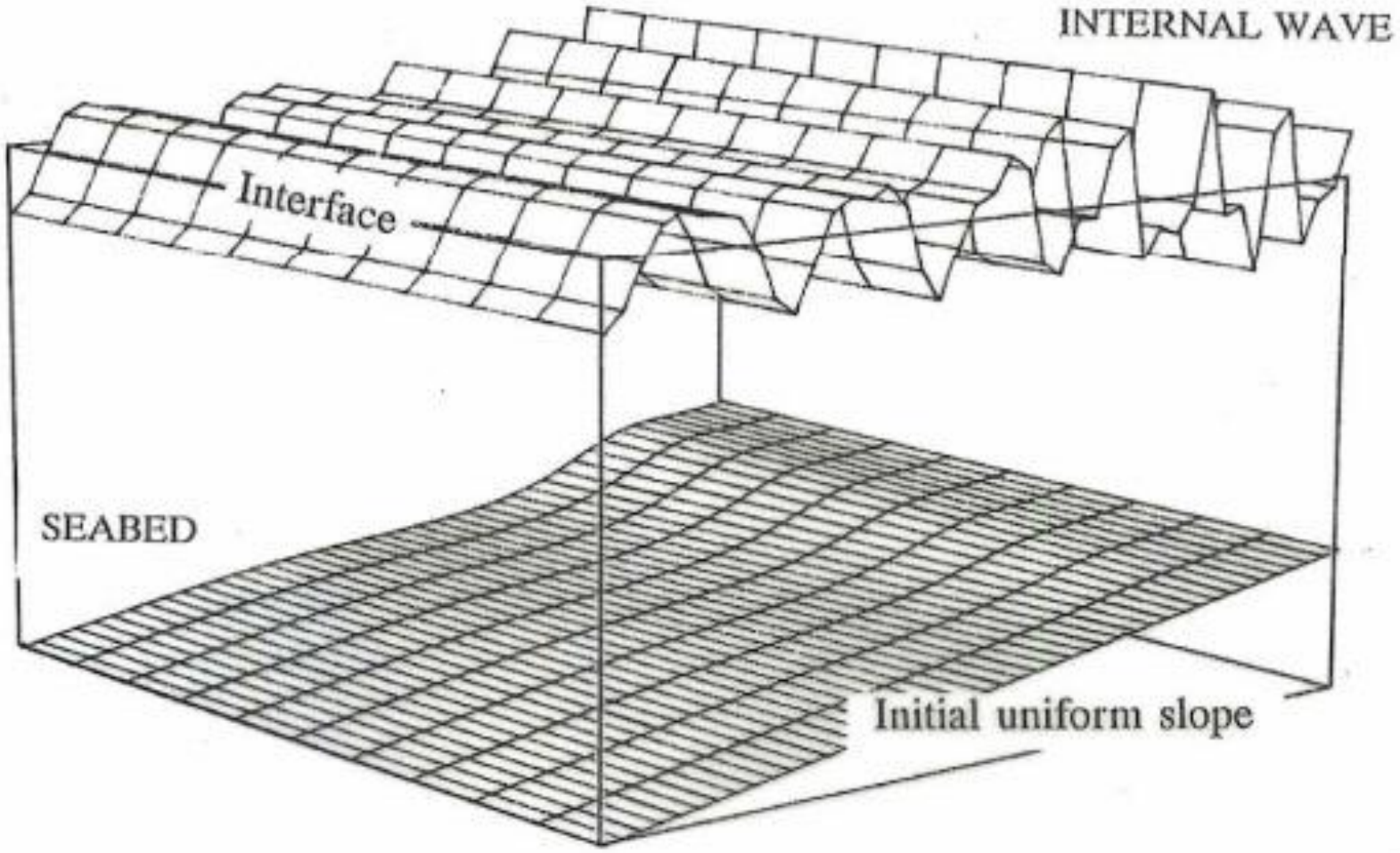

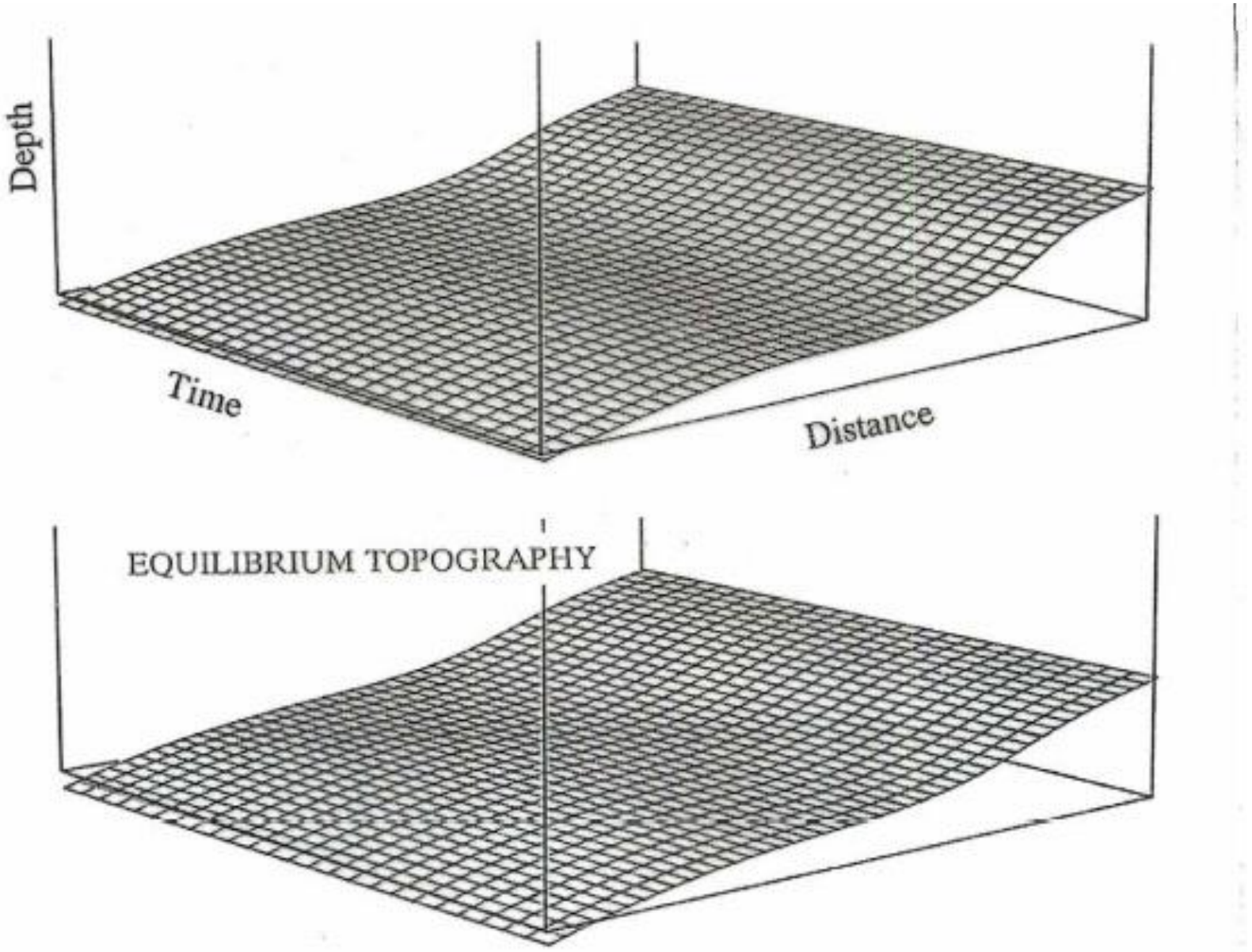
Depth
Time
Distance
EQUILIBRIUM TOPOGRAPHY

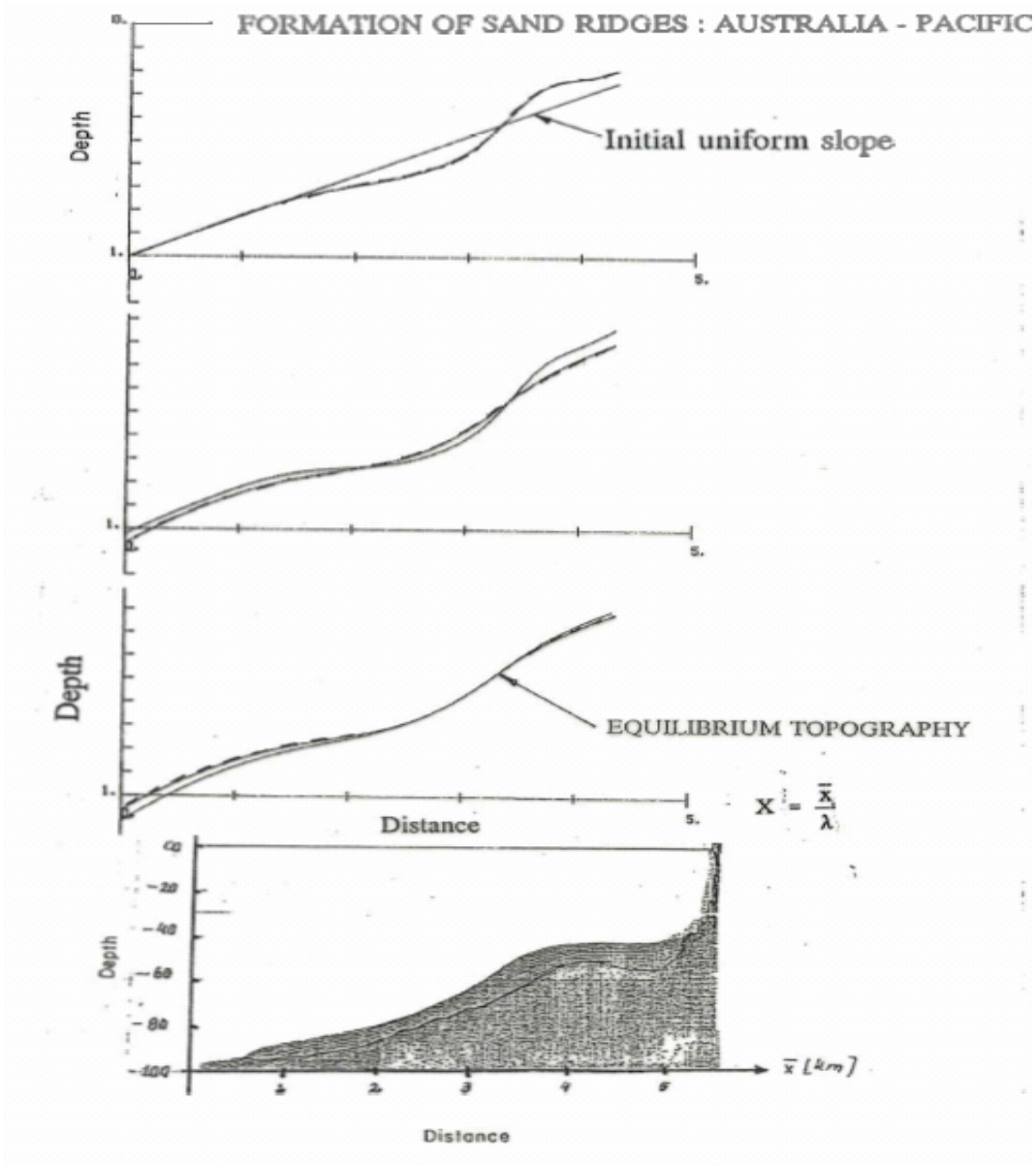
FORMATION OF SAND RIDGES : AUSTRALIA - PACIFIC
Depth
Initial uniform slope
EQUILIBRIUM TOPOGRAPHY
Distance
Depth
Distance

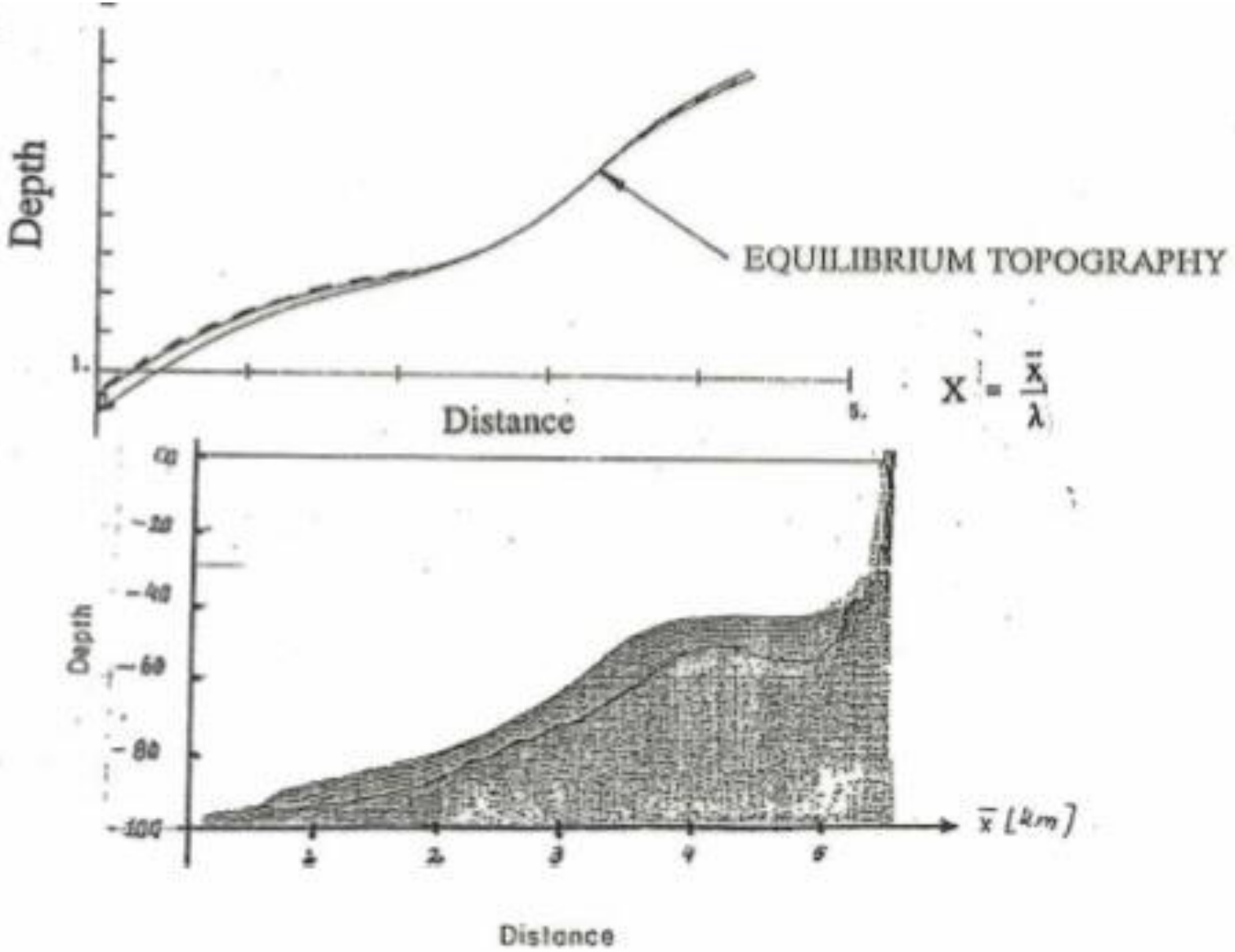
Depth
EQUILIBRIUM TOPOGRAPHY
Distance
$X = \frac{\bar{x}}{\lambda}$
Depth
$\bar{x}$ [km]
Distance

Thank you!
for your attention

Roger!!

Roger!

Comparisons with Experiments

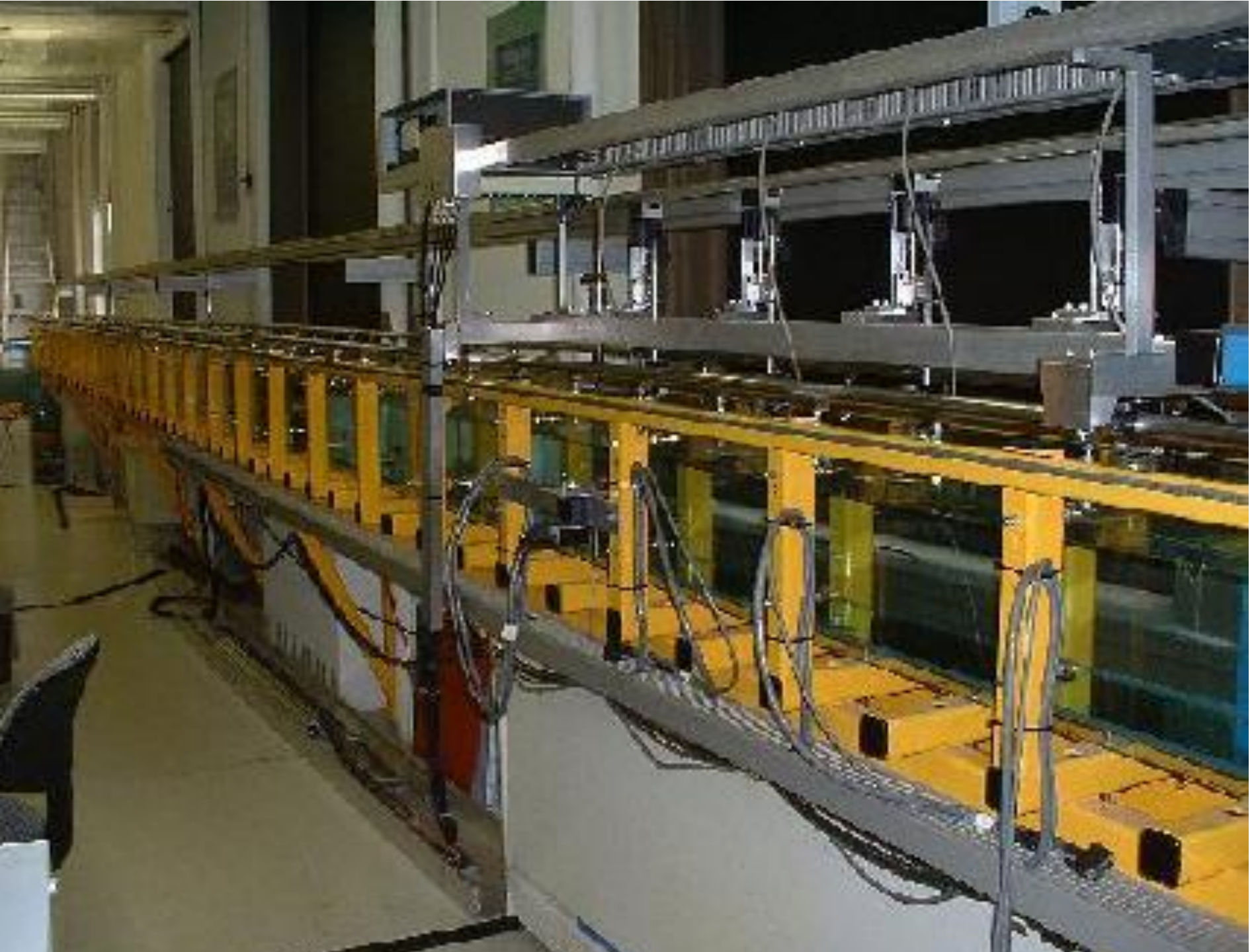

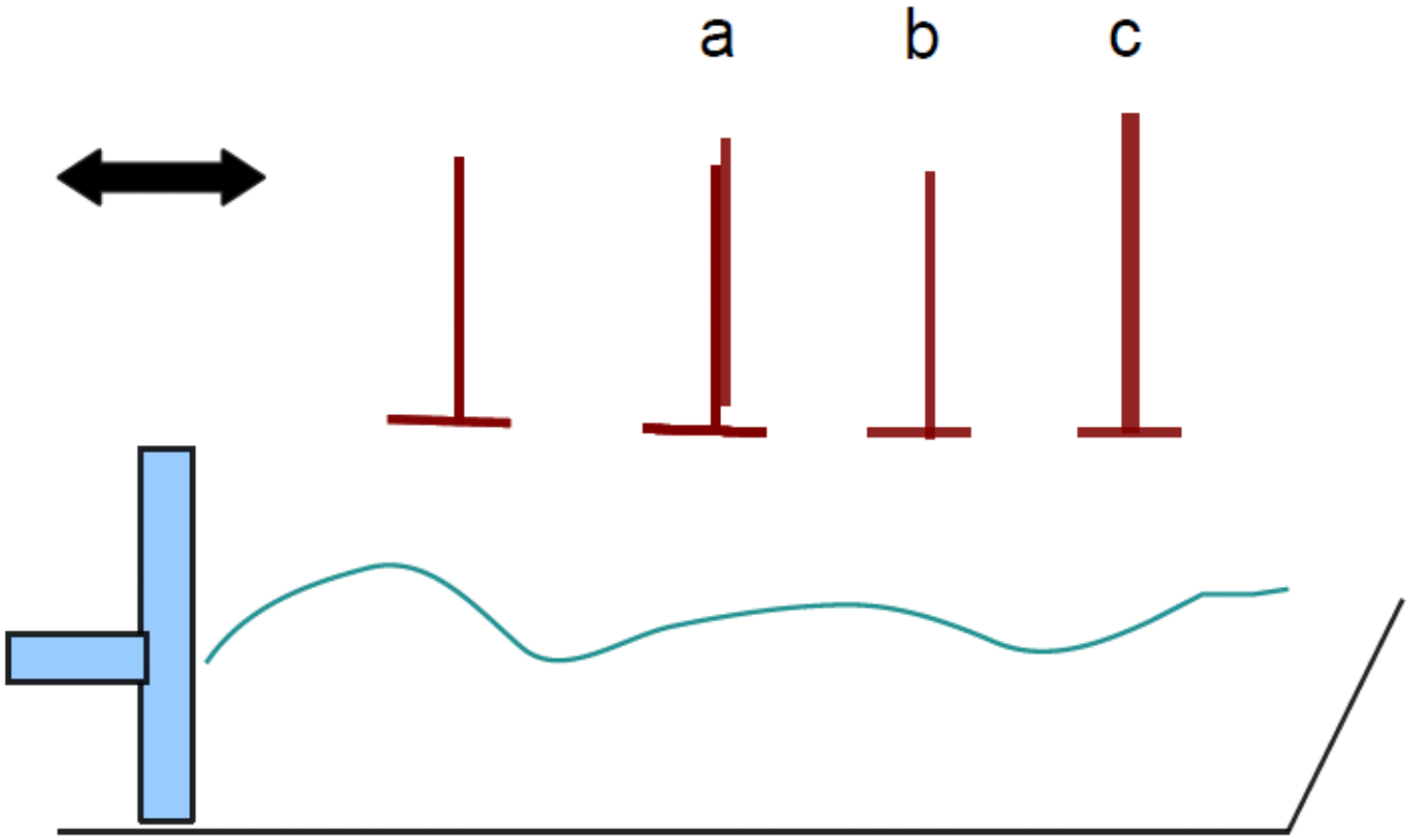
a
b
c

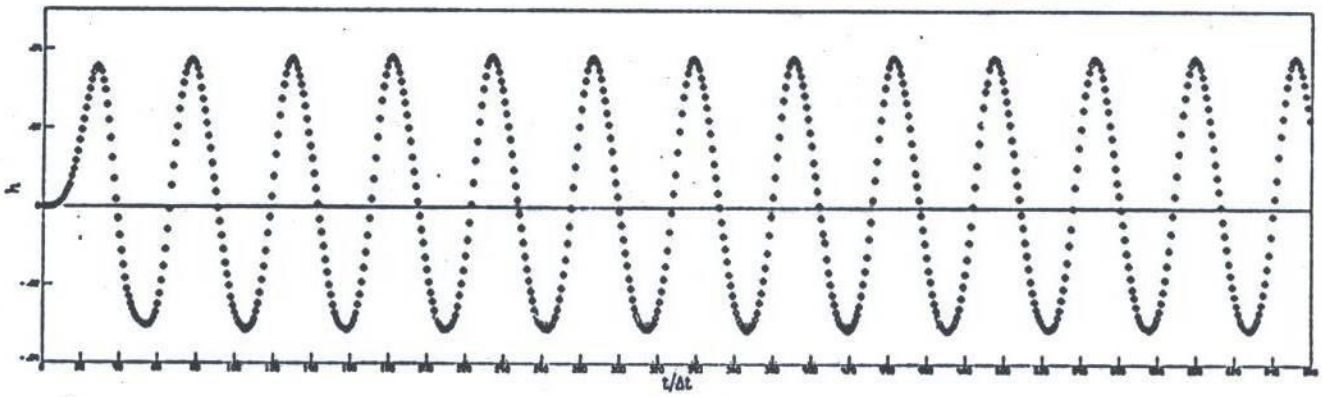

FIGURE 2

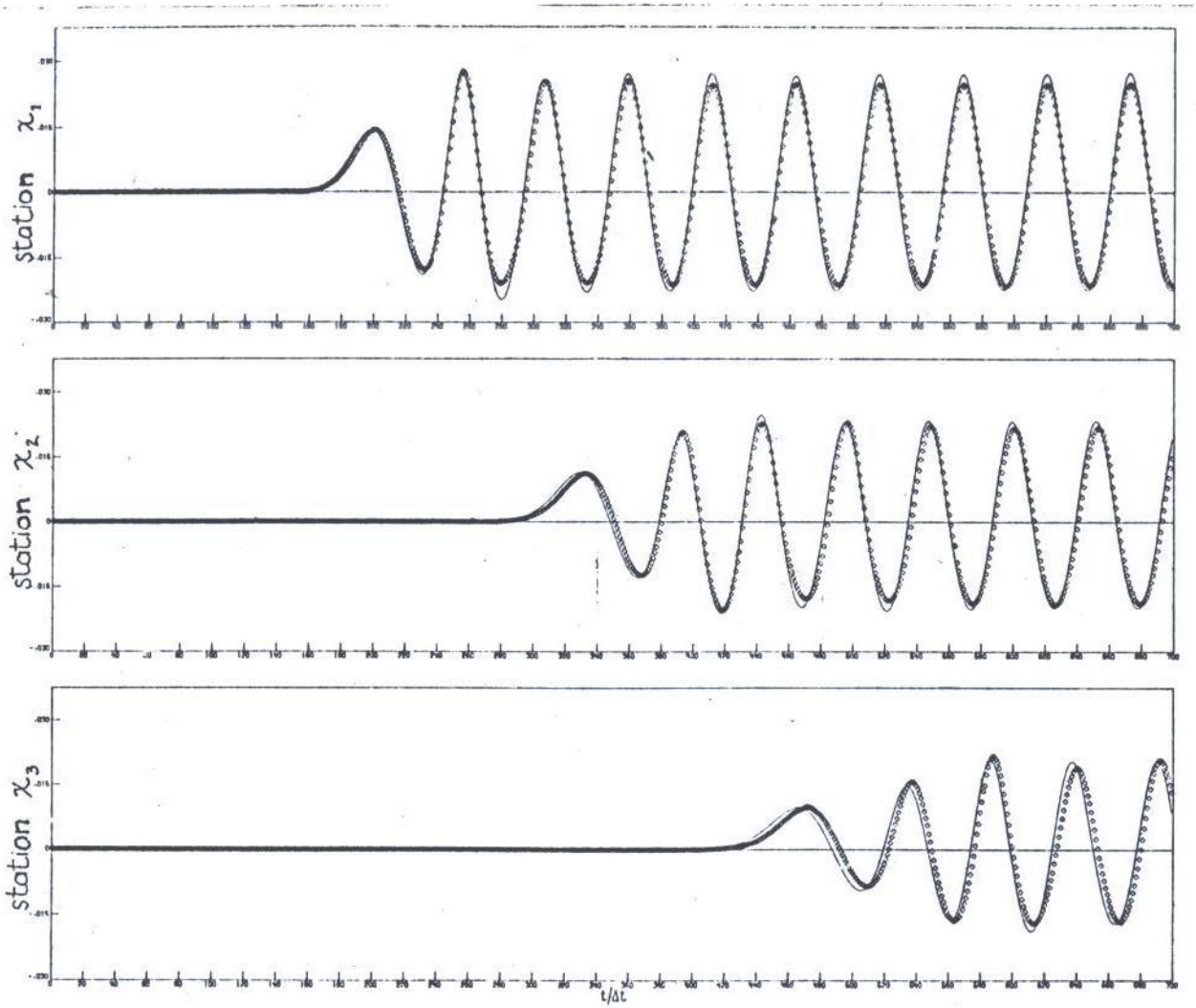

Figure 3. Comparison of experimental data (the ◇'s) and numerical integration of the model (25), for Stokes number 4.5.

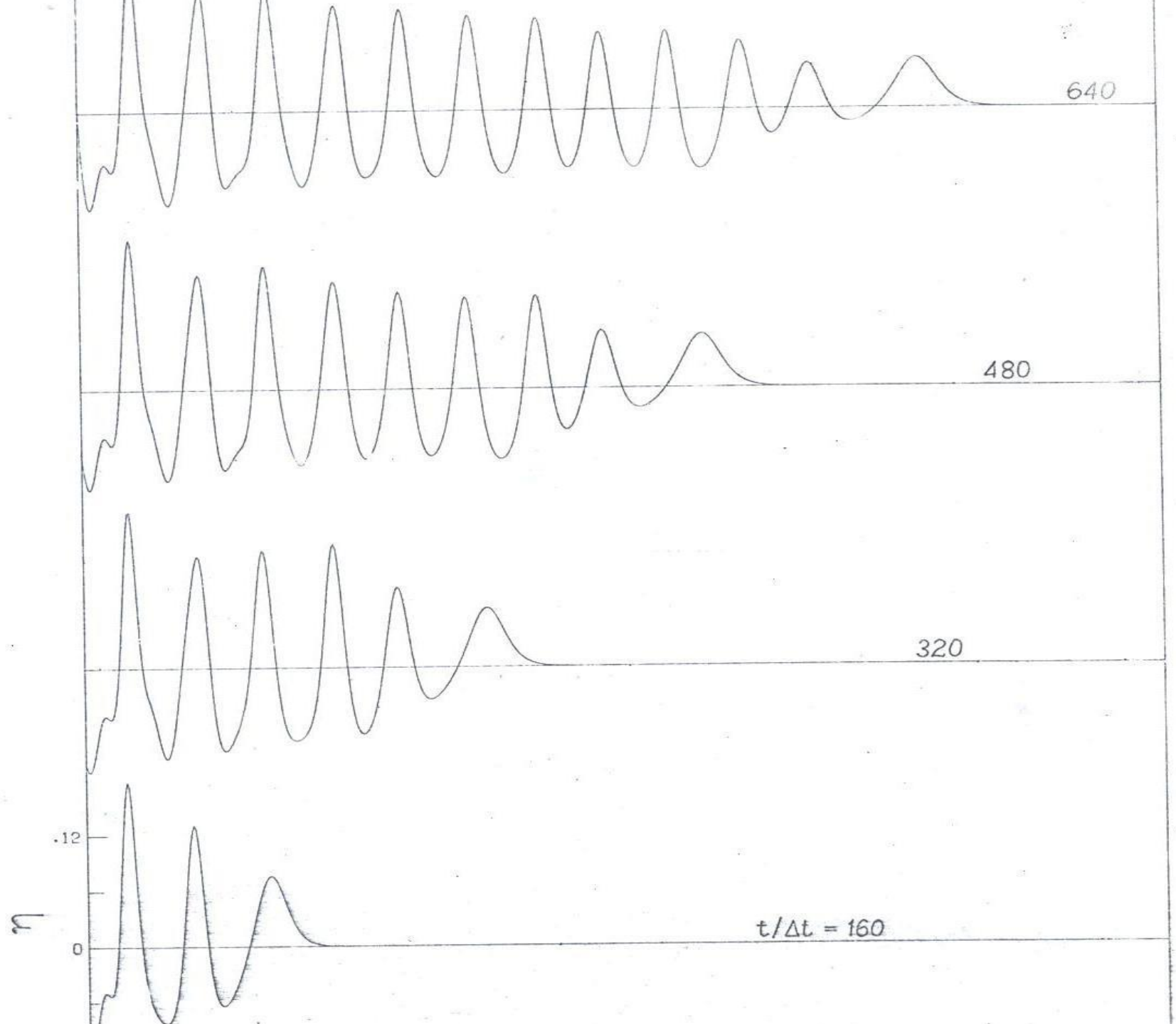
640
480
320
.12
η
0
t/Δt = 160

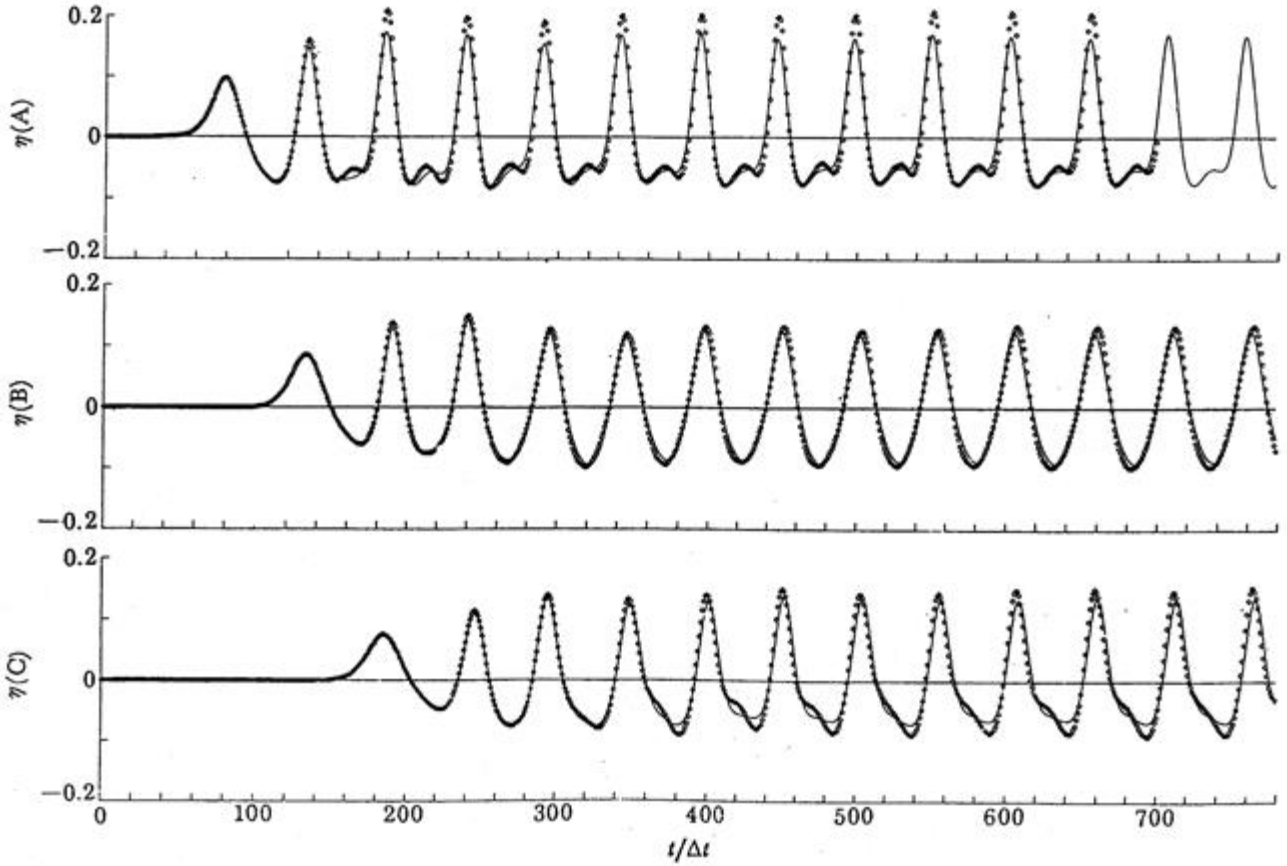

FIGURE 25. The experiment at $S = 26.3$ is compared with (M†) when $\alpha = 0.9898$, $\beta = \frac{3}{2}$, $\nu = 0$, $\mu = 0.014$, $\gamma = 0.1325$.

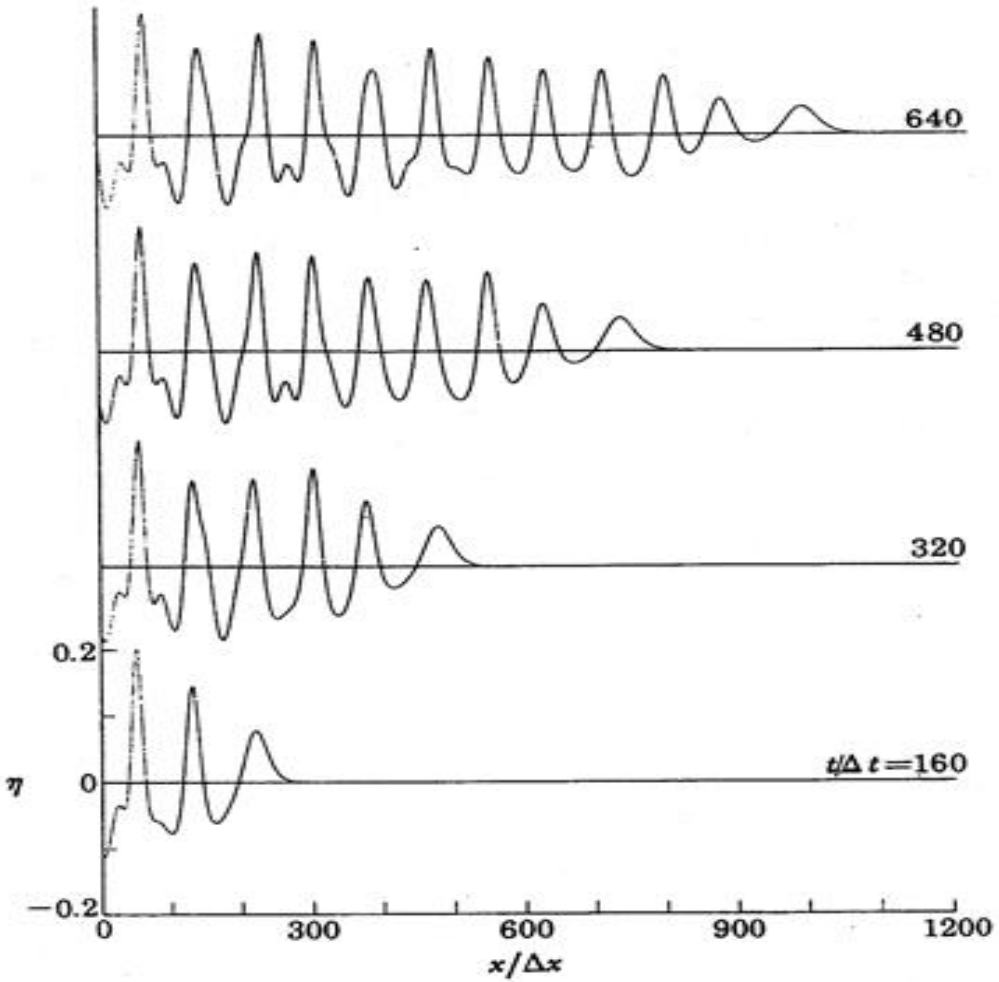
640
480
320
t/Δ t=160
0.2
0
−0.2
η
0
300
600
900
1200
x/Δx

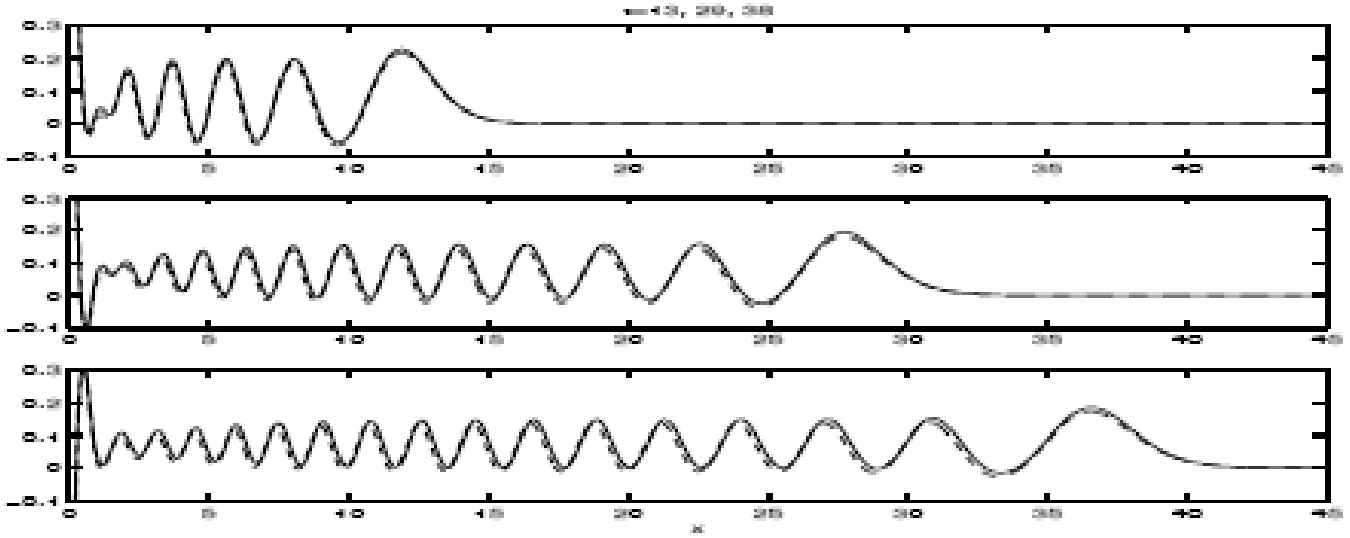

FIGURE 11. Comparison with $\epsilon = 0.2$.

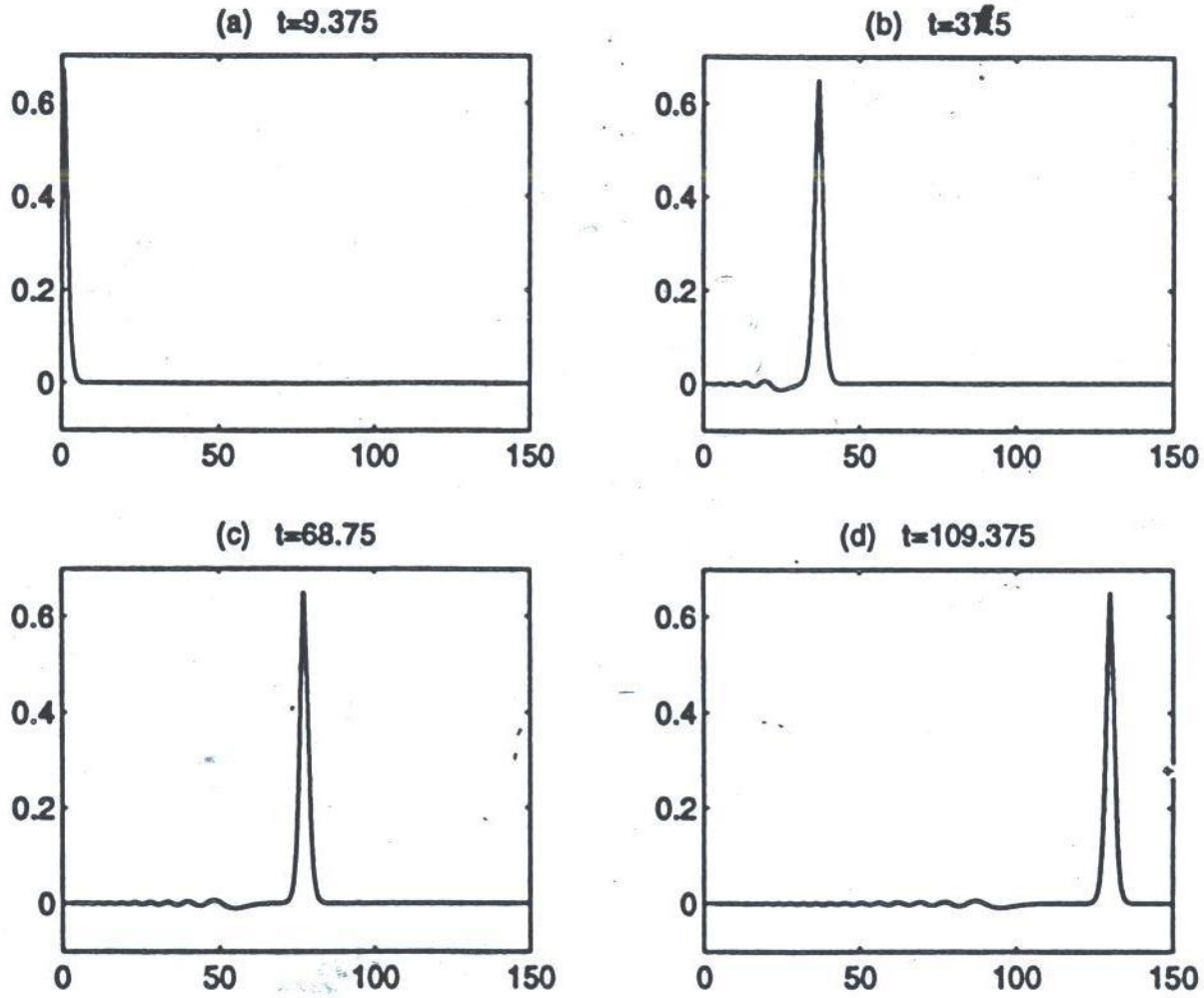

FIGURE 1. A solitary wave followed by a dispersive tail.

Speed versus Amplitude of Solitary Waves

Scott Russell:

$$c = \sqrt{gh}\sqrt{1 + \eta_0/h}$$

Korteweg & de Vries:

$$c = \sqrt{gh}\left(1 + \eta_0/2h\right)$$

Second-order approximation to the full, 2-dimensional Euler equations.

$$c = \sqrt{gh}\left(1 + \eta_0/2h - \frac{3}{20}(\eta_0/h)^2\right)$$

(Fenton; Su & Mariej Temperville)

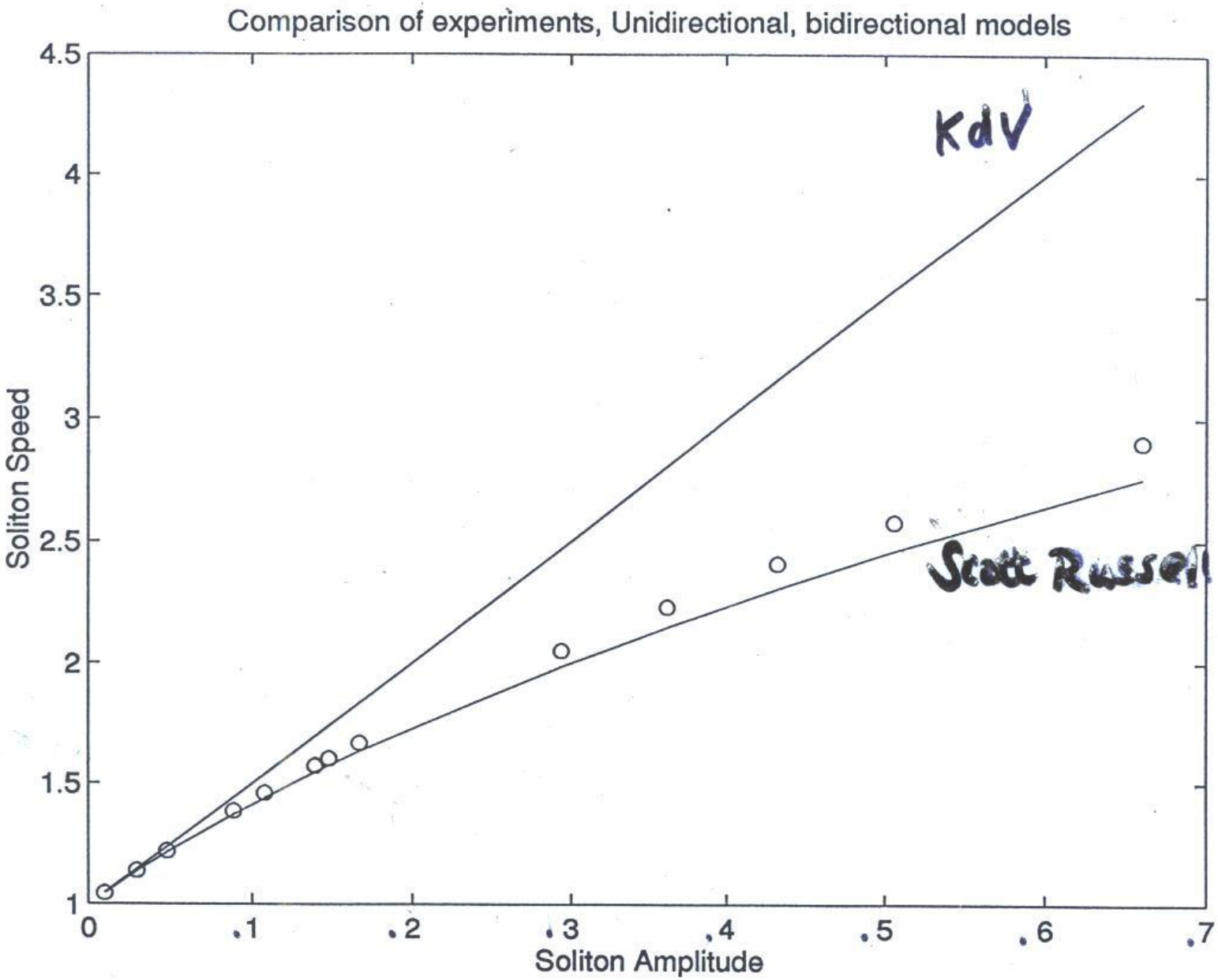
Comparison of experiments, Unidirectional, bidirectional models
KdV
Scott Russell
Soliton Speed
Soliton Amplitude
4.5
4
3.5
3
2.5
2
1.5
1
0
.1
.2
.3
.4
.5
.6
.7